Regulation of Runx2 Accumulation and Its Consequences

Junko Shimazu

Submitted in partial fulfillment of the
requirement for the degree of
Doctor of Philosophy
in the Graduate School of Arts and Sciences

COLUMBIA UNIVERSITY
2016

ABSTRACT

Regulation of Runx2 Accumulation and Its Consequences

Junko Shimazu

Osteoblasts are bone-forming cells and therefore they are responsible of the synthesis of type I collagen, the main component of bone matrix. However, there is an apparent disconnect between the regulation of osteoblast differentiation and bone formation since the synthesis of Type I collagen precedes the expression of *Runx2*, the earliest determinant of osteoblast differentiation. Recently, genetic experiments in the mouse have revealed the existence of an unexpected cross-regulation between bone and other organs. In particular this body of work has highlighted the importance of osteoblasts as endocrine cells to regulate whole-body glucose homeostasis by secretion of a hormone, osteocalcin. However, the fundamental question of why bone regulates glucose homeostasis remained to be answered. Therefore, in my thesis, considering that bone is a metabolically demanding organ that constantly renews itself, I hypothesized that characterizing the connection between the need of glucose as a main nutrient in osteoblasts and bone development will provide a key to deeper understanding of why bone regulates glucose homeostasis.

My work shows here that glucose uptake through GLUT1 in osteoblasts is needed for osteoblast differentiation by suppressing the AMPK-dependent activation by phosphorylation at S148 of Smurf1 that targets Runx2 for degradation. I also uncovered the mechanism of action of Smurf1 in this setting. In a distinct but synergetic way, glucose uptake promotes bone formation by inhibiting a distinct function of AMPK. In turn, Runx2 favors *Glut1* expression, and this feedforward regulation

between Runx2 and *Glut1* determines the onset of osteoblast differentiation during development and the extent of bone formation throughout life.

Furthermore, I also identified that Smurf1 not only regulates osteoblast differentiation by targeting Runx2 for degradation but also contributes to whole-body glucose homeostasis by regulating the activation of osteocalcin by targeting the insulin receptor for degradation in vivo. These results identify Smurf1 as a determinant of osteoblast differentiation during development, of bone formation and glucose homeostasis post-natally. Most importantly, we show that these Smurf1 functions required AMPK-phosphorylation site S148 in vivo.

Altogether, these results revealed the absolute necessity of glucose as a regulator of Runx2 accumulation during osteoblast differentiation and bone formation in vivo and highlight the fundamental importance of the intricate cross-talk between bone and whole-body glucose metabolism.

TABLE OF CONTENTS

LIST OF FIGURES

CHAPTER I Figures

CHAPTER II Figures

CHAPTER III Figures

CHAPTER IV Figures

LIST OF ABBREVIATIONS

1,25(OH)2D- 1,25-dihydroxy vitamin D

ADHR- Autosomal dominant hypophosphatemic rickets

ADP- Adenosine diphosphate

AMP- Adenosine monophosphate

AMPK- 5' AMP-activated protein kinase

ATP- Adenosine triphosphate

BSP- Bone sialoprotein

ECM- Extracellular matrix

ELISA- Enzyme-linked immunoassay

ERK- Extracellular signal-regulated kinase

FGF- Fibroblast growth factor

GAPDH- Glyceraldehyde 3-phosphate dehydrogenase

GLA- Gamma carboxyglutamic acid

GLU- Glutamic acids

GLUT- Glucose transporter

GPCR- G-protein coupled receptor

GSIS- Glucose stimulated insulin secretion test

GTT- Glucose tolerance test

INSR- Insulin Receptor

ITT- Insulin tolerance test

Kb- Kilobases

M-CSF- Macrophage colony stimulating factor

MAPK- Mitogen-activated protein kinase

MEKK2- MAPK/ERK kinase kinase 2

NADPH- Nicotinamide adenine dinucleotide phosphate

OCN- Osteocalcin

OPG- Osteoprotegerin

OST-PTP- Osteoblast testis-specific protein tyrosine phosphatase

RANK- Receptor activator of nuclear factor κ-B

RANKL- Receptor activator of nuclear factor κ-B ligand

Runx2- Runt-related transcription factor 2

SGLT- Sodium-glucose co-transporter

SLC2A- Solute Carrier Family 2

SLC5A- Solute Carrier Family 5

SMURF1- SMAD Specific E3 Ubiquitin Protein Ligase 1

TIO- Tumor-induced osteomalacia

TSC-Tuberous sclerosis complex

WAT- White adipose tissue

c-FMS- Colony-stimulating factor-1 receptor

qPCR- Quantitative polymerase chain reaction

αI(1) collagen- Type 1 alpha I collagen

ACKNOWLEDGEMENTS

First of all, I would like to thank my thesis advisor and my mentor Dr. Gerard Karsenty for his excellent guidance and mentorship throughout my graduate studies. It was a great experience to be part of his lab and I cannot thank him enough for leading me through my graduate school journey. I strongly believe that not only the completion of my thesis work but also my motivation and inspiration as a scientist are gift from the training from Dr. Karsenty. I appreciate all the opportunities Dr. Karsenty has given me to grow as a scientist

I would like to express my gratitude towards every current and past members of the Karsenty lab but especially I would like to thank Dr. Jianwen Wei who contributed largely to my thesis projects for his endless support and encouragement in the laboratory. I also thank the past member of the lab, Dr. Mathieu Ferron and Dr. Frank Oury for their technical assistance and support during my rotation and in the beginning of my doctoral studies. Lori Khrimian is another member of the Karsenty lab who I would like to personally thank for her kindness and encouragement. I cannot imagine how difficult my graduate school life would be if I did not meet her. Thank you so much for being a wonderful friend.

I would also like to extend my gratitude to my qualifying committee and thesis research advisory committee members – Drs. Timothy Bestor, Virginia Papaioannou, Lori Sussel and Eric Schon. I thank them for their comments and advice for the progression of my thesis projects. In addition, most importantly, I thank them for guiding me to make a transition from being a student to a scientist. Thanks to the training from them, I am more confident now to present my research in

progress in seminar and to write a research proposal and summary.

I also would like to thank Dr. Stavoula Kousteni and Dr. Francesco Ramirez for accepting to be part of my thesis defense committee.

In addition, I take this opportunity to express gratitude to all of the members and faculties of Department of Genetics and Development at CUMC for their intellectual inspirations and the training to grow as a scientist. Thanks to the effort of the department, I was able to focus on doing a good science and at the same time I felt at home at CUMC because people in the department are truly supportive. I was fortunate to be part of such a wonderful and inspirational community.

Finally, I must express my profound gratitude to my parents, Hideki and Keiko and to my brother and sister, Hidekazu and Satoko for providing me with continuous support and encouragement throughout my years of graduate school. It was a big decision for me to come to the states from Japan to study and without their encouragement and support, I could not go through all the difficulties that I faced to achieve my goals. Thank you so much for always believing in me.

DEDICATION

This thesis is dedicated to my beloved parents, Hideki and Keiko Shimazu and grandparents, Etsuko Kusajima and Toshiko Shimazu for their endless love, support and encouragement.

In memory of my grandfather, Kazu Kusajima.

CHAPTER I: General Introduction

1. The Basic Principles of Skeletal Cell Biology and Development

The skeleton is one of the latest organs to appear during evolution and this makes vertebrates distinct and unique from other organisms. A key feature of the skeletal biology is that it is composed of two distinctive tissues, bone and cartilage, and contains three specific cell types: osteoblasts and osteoclasts in the bone and chondrocytes in the cartilage. The osteoblasts and chondrocytes originate from mesenchymal cell (Ducy et al., 1997) whereas osteoclasts are multinucleated cells that derive from hematopoietic progenitors in the bone marrow (Bar-Shavit, 2007). Each of these three cell types is responsible for unique functions that are important for the development as well as maintenance of the integrity of the skeleton. The earliest step of the skeletal development is the formation of the mesenchymal condensations at the location of the future skeletal elements. Subsequently, there are two developmentally distinct modes of skeletal development: intramembranous ossification and endochondral ossification. Intramembranous ossification, seen in only a few bones, allows mesenchymal condensations to differentiate directly into osteoblasts without any cartilaginous intermediate steps. In contrast, most skeletal elements are generated through endochondral bone formation that includes a cartilage intermediate stage (Karsenty and Wagner, 2002). Here, the two modes of skeletal development as well as the transcriptional regulation of differentiation and features of the functions of three specific cell types in the skeleton are described.

i. Intramembranous ossification

Intramembranous ossification is the characteristic process of ossification in parts of the skull and

the lateral halves of the clavicles (Yang and Karsenty, 2002). In addition, sutures, the junction between calvarial bones that are responsible for the maintenance of a separation between membranous bones and for regulating the expansive growth of the skull, are the major sites of intramembranous bone (Ornitz and Marie, 2002). The first step of the intramembranous ossification begins with the condensation of neural crest-derived mesenchymal cells at the location of future skeletal elements. During intramembranous ossification, the cells of the mesenchymal condensations differentiate directly into osteoblasts without intermediate processes (Figure 1) (Karsenty and Wagner, 2002).

ii. Structural and functional features of osteoblast

Osteoblasts are bone forming cells. They are responsible for the synthesis of a unique combination of bone extracellular matrix (ECM) proteins and they control the subsequent mineralization of the bone ECM (Ducy et al., 1997; Long, 2012). Histochemical and cytological analysis has shown that, during osteoblast differentiation, there is overall cell enlargement due to the increase in the size of the Golgi element, the accumulation of mitochondria as well as cytoplasmic basophilic materials (Pritchard, 1952). These observations are consistent with the notion that differentiated osteoblasts are metabolically active and engaged in the synthesis and secretion of collagenous and non-collagenous bone ECM proteins including osteocalcin, alkaline phosphatase and a large amount of type I collagen (Long, 2012). The metabolically active nature of osteoblasts is further supported by early studies demonstrating that a significant amount of glucose is consumed and used as a main nutrient by osteoblasts (Borle et al., 1960; Cohn and Forscher, 1962; Esen and Long, 2014).

Yet, despite its metabolically demanding nature, there is limited genetic and molecular studies addressing the fundamental importance of glucose uptake as a main energy source for osteoblast to fulfill its function during development and in postnatal life.

iii. Bone extracellular matrix (ECM) and osteoblasts

The bone extracellular matrix (ECM) contains two types of proteins, collagens and non-collagenous proteins that are mainly secreted by differentiated osteoblasts. The collagens in bone ECM is mainly type I collagen, a heterotrimeric protein made of two α1(I) chains and one α2(I) chain, which are encoded by two different genes (Vuorio and de Crombrugghe, 1990). Since Type I collagen secreted by differentiated osteoblasts, is by far the most abundant protein in the bone ECM, it is often used as a marker for bone formation by osteoblasts. The non-collagenous proteins, such as osteocalcin and alkaline phosphatase that are secreted by osteoblasts, compose 10 to 15% of total bone protein (Clarke, 2008). Approximately 25% of non-collagenous protein is exogenously derived, including serum albumin (Clarke, 2008). The synthesis of bone matrix starts from the deposition of organic matrix rich in type I collagen which is not yet mineralized (Florencio-Silva et al., 2015). Subsequently, mineralization occurs through the accumulation of calcium phosphate in the form of hydroxyapatite crystals, a major mineral crystal present in bone ECM, both within and between collagen fibrils (Florencio-Silva et al., 2015; Long, 2012). Bone mineral provides mechanical rigidity and load-bearing strength to bones, whereas the organic matrix provides elasticity and flexibility (Clarke, 2008).

iv. Transcriptional control of osteoblast differentiation

The earliest and most specific determinant of osteoblast differentiation is Runx2, a transcription factor that belongs to the runt-domain gene family, and is a vertebrate homolog of the *Drosophila* Runt protein (Ducy et al., 1997; Komori et al., 1997a). *Runx2* is expressed in the cells of osteoblastic lineage and regulates osteoblast-specific expression of downstream target genes, such as *Osteocalcin* (*Ocn*)*, Osterix and Bone sialoprotein (Bsp)* (Ducy et al., 1997; Nishio et al., 2006). Genetic studies have shown that Runx2 inactivation results in a complete absence of osteoblast differentiation (Figure 2) and its haplo-insufficiency, in mice and humans, results in cleidocranial dysplasia (CCD) (Komori et al., 1997a; Lee et al., 1997a; Mundlos et al., 1997a; Otto et al., 1997d) (Figure 3). CCD that is caused by delay of osteoblast differentiation in bone forming through intramembranous ossification, is characterized by open fontanelles and short clavicles (Lee et al., 1997a; Mundlos et al., 1997a; Otto et al., 1997d). Conversely, an increase in Runx2 activity, as seen in mice and humans lacking one allele of *Twist*, results in craniosynostosis, characterized by early closure of the sutures, due to a premature osteoblast differentiation in the skull (Bialek et al., 2004) (Figure 4).

Given the absolute necessity of Runx2 in osteoblast differentiation, the genetic regulation of osteoblast differentiation by Runx2 during development has been intensively studied. However, several aspects of Runx2 biology described below are still poorly defined.

a. <u>Contribution of Runx2 to bone formation</u>

It is assumed that Runx2 activity is required for the bone formation by differentiated osteoblasts

because in vitro Runx2 binds to and upregulates the activity of the promoter of *α1(I) collagen*, the main constituent of bone ECM and thus a marker for bone formation (Ducy et al., 1999; Kern et al., 2001). However, in vivo, type I collagen synthesis precedes *Runx2* expression in prospective osteoblasts. Indeed, in mouse, the expression of *α1(I) collagen* is already observed in the mesenchymal condensation at E10.5 whereas *Runx2* expression is not detectable in the cells of mesenchymal condensation before E12.5 (this study) (Figure 5). Therefore both, the contribution of Runx2 to bone formation and the molecular mechanism regulating Type1 collagen synthesis in vivo remain poorly understood. If Runx2 does not regulate the expression of *α1(I) collagen* in vivo, there is an apparent disconnect between differentiation and bone formation by osteoblasts. In other words, how bone formation is initiated once osteoblast differentiation has occurred remains largely unknown.

b. <u>Regulation of Runx2 accumulation by ubiquitination</u>

Another aspect of Runx2 biology that raises several important questions is understanding how its accumulation in osteoblast lineage cells during development is regulated. Since osteoblast differentiation is mainly controlled by Runx2, understanding how Runx2 accumulation is regulated in prospective osteoblasts during development will not only lead to a deeper understanding of the regulation of osteoblast differentiation but also will better delineate the pathological principles of bone diseases that are caused by improper osteoblast differentiation during development, such as CCD and craniosynostosis. For instance, a significant number of CCD patients do not have any detectable mutations in *Runx2* (Puppin et al., 2005; Tessa et al., 2003), thus there might be other mechanisms

that once disrupted causes a delay of osteoblast differentiation and causes CCD.

Recently, it has become apparent that the ubiquitination-proteasome system is involved in the regulation of bone turnover and Runx2 has been shown to be degraded through the ubiquitin-proteasome pathway (Severe et al., 2013; Tintut et al., 1999). Ubiquitin is a cellular signal that labels proteins as a post-translational modification to direct proteins to proteasome degradation (Dikic et al., 2009). The ubiquitination cascade involves the successive actions of three types of enzymes: E1 ubiquitin-activating enzyme, E2 ubiquitin-conjugating enzyme and E3 ubiquitin ligase. The E1 ubiquitin-activating enzyme is responsible for recruiting ubiquitin. The E2 ubiquitin-conjugating enzyme transfers the ubiquitin to the targeted protein. The E3 ubiquitin ligase carries out the final step in the ubiquitination cascade and is acting as a scaffold protein that interacts with the E2 enzyme and transfers ubiquitin to the target protein (Dikic et al., 2009; Severe et al., 2013) (Figure 6). There are two major types of E3 ubiquitin ligase in eukaryotes, defined by the presence of either a HECT or a RING domain (Deshaies and Joazeiro, 2009). The important feature of the E3 ubiquitin ligases is that they confer substrate recognition, thus substrate specificity (Ardley and Robinson, 2005).

Several E3 ubiquitin ligases have been implicated as regulators of bone formation postnatally (Jones et al., 2006; Shu et al., 2013; Yamashita et al., 2005; Zhao et al., 2004). Particularly, Smurf1, the HECT domain family of E3 ubiquitin ligase, is reported to regulate osteoblast differentiation by favoring the degradation of Runx2 in vitro (Zhao et al., 2003). Furthermore, a loss-of-function study showed that *Smurf1-/-* mice exhibited age-dependent increase in bone mineral density by promoting

degradation of the mitogen-activated protein (MAP) kinase, MEKK2, in vivo (Yamashita et al., 2005). Conversely, *Smurf1* transgenic mice exhibited significantly reduced bone formation during postnatal life (Zhao et al., 2004). However, despite the biochemical evidence showing that Smurf1 targets Runx2, no genetic studies have yet addressed the role of Smurf1 as a regulator of osteoblast differentiation by targeting Runx2.

Furthermore, given its involvement in skeletal development, there is a growing interest to better elucidate the mechanisms regulating Smurf1 activation. Smurf1, which is C2-WW-HECT E3 ubiquitin ligase, contains a catalytic HECT domain in the C-terminal, two WW domains (WW1 and WW2) and a phospholipid-binding C2 domain in the N-terminal region (Cao and Zhang, 2013) (Figure 7). The HECT domain interacts with both E2 and ubiquitin molecules during ubiquitination and the C2 domain binds to phospholipid-containing membranes and alters both subcellular localization and function of Smurf1 (Cao and Zhang, 2013). The WW domains play a role to capture substrates which contain the PY motif (Cao and Zhang, 2013). In recent years, it has become apparent that a critical regulatory step for protein ubiquitination is phosphorylation of either substrate proteins or E3 ubiquitin ligases (Gallagher et al., 2006; Hayami et al., 2005; Xing et al., 2010). Indeed, several C2-WW-HECT E3 ligases are regulated by phosphorylation and their E3 ligase activity is enhanced by phosphorylation-induced confirmation changes (Gao et al., 2004; Xing et al., 2010). However, whether phosphorylation of Smurf1 is required for its activation to target Runx2 and/or other Smurf1 targets remain unknown. Although phosphorylation of Runx2 affects its degradation, Smurf1 is not involved in this

phosphorylation-dependent degradation of Runx2 (Shen et al., 2006; Xing et al., 2010). If Smurf1 activation does depend on its phosphorylation**,** the important questions remained to be answered in vivo are: which kinase(s) phosphorylate(s) Smurf1 and which domain(s) if not amino acid(s) in Smurf1 is/are needed to allow degradation of Runx2 degradation by favoring their phosphorylation.

Altogether, rigorous genetic and molecular studies showing the mechanisms whereby regulation of osteoblast differentiation is regulated by E3 ubiquitin ligase will better delineate the molecular mechanism leading to Runx2 accumulation in osteoblast lineage cells during development.

v. Endochondral ossification and chondrocyte differentiation

The majority of bones develop through endochondral ossification, a two-step process involving chondrogenesis and osteognenesis. The first step of the endochondral bone development begins with the condensation of mesenchymal cells at the location of future skeletal elements, a prerequisite for subsequent chondrogenic differentiation (Karsenty and Wagner, 2002). In mouse, the formation of the mesenchymal condensation is observed after embryonic day E9.5. Subsequently, at E11.5, the expression of *α1(I) collagen* observed in the mesenchymal condensation is suppressed in mesenchymal cells that are differentiated into chondrocytes, the first skeleton specific cell type to appear during endochondral development (Dessau et al., 1980; Yang and Karsenty, 2002). The transcription factor Sox9 is a master regulator of the differentiation of mesenchymal cells into chondrocytes (Lefebvre and de Crombrugghe, 1998). The resulting chondrocytes have a characteristic

round-shape and rapidly proliferate and secrete a number of proteins for the cartilage extracellular matrix (ECM) that results in linear enlargement of the skeletal elements (Kronenberg, 2003). Particularly, Sox9 binds to and activates enhancer elements of *aggrecan* and *α1(II) collagen* that are considered as biological markers of the differentiating chondrocytes (Karsenty and Wagner, 2002; Lefebvre et al., 1997; Sekiya et al., 2000). In the cartilage ECM, the large aggregates of hyaluronan-aggrecan allow the tissue to withstand compression and type II collagen fibrils provide the framework for the tissue (Mackie et al., 2011). The undifferentiated mesenchymal cells that continue to express *α1 (I) collagen* remain at the periphery of the skeletal element and form the structure called perichondrium (Figure 8).

Around E13.5, the innermost chondrocytes stop proliferating and become hypertrophic. These cells are called hypertrophic chondrocytes and no longer express *α1(II) collagen*, instead they express *α1(X) collagen*, the main specific marker for hypertrophic chondrocytes. Once chondrocyte hypertrophy is initiated, cells in perichondrium start to differentiate into osteoblasts to form a mineralized bony outer cortex structure around the cartilaginous core (Karsenty and Wagner, 2002; Maes et al., 2010). Eventually, hypertrophy chondrocytes die by apoptosis, allowing vascular invasion from the mineralized bone cortex (Mackie et al., 2008). The cartilage ECM surrounding hypertrophy chondrocytes is degraded by chondroclasts brought by vascular invasion (Vu et al., 1998). Moreover, the osteoclasts that are brought via vascular invasion further assist in the removal of cartilage matrix and this provides a scaffold for precursors of osteoblasts that also invade along with blood vessels to

differentiate and form the bone matrix within the site (Kronenberg, 2003) (Figure 8).

vi. Osteoclast differentiation

Osteoclasts are multinucleated, terminally differentiated cells that originate from mononuclear cells of the hematopoietic stem cell lineage (Florencio-Silva et al., 2015). Osteoclasts are the last cell type of the skeleton to appear during development and are responsible for bone resorption.

The osteoclast differentiation pathway is common to that of macrophages and dendritic cells (Vaananen et al., 2000). The essential factors necessary for osteoclast differentiation are macrophage colony-stimulating factor (M-CSF) and receptor activator of nuclear factor-κB ligand (RANKL) (Boyle et al., 2003; Vaananen et al., 2000). Osteoclast precursors express M-CSF receptor, c-Fms, and RANKL receptor, RANK (Yamashita et al., 2012). In the presence of M-CSF and RANKL that are required to induce expression of gene including the lytic enzymes, *cathepsin K* and *tartrate-resistant acid phosphatase* (*TRAP*), osteoclast precursor cells are differentiated into mature osteoclasts (Boyle et al., 2003).

A breakthrough in the knowledge of the regulation of osteoclast differentiation was the identification of osteoprotegerin (OPG), secreted by osteoblasts and osteogenic stromal stem cell (Boyce and Xing, 2007; Boyle et al., 2003). Secreted OPG acts as a decoy receptor of RANKL to compete with RANK on the surface of osteoclast lineage cells and inhibits osteoclast formation and function (Yamashita et al., 2012). Thus, osteoblasts/stromal cells are involved in osteoclast differentiation as well as functions and OPG/RANKL/RANK regulatory axis is an important determinant

of osteoclast differentiation and thus bone resorption (Boyle et al., 2003).

vii. Osteoclast functions

Bone is the only tissue that contains a cell type, the osteoclast, that destroys the host tissue. Osteoclasts have an efficient machinery for dissolving crystalline hydroxyapatite and degrading organic mineralized bone matrix rich in collagen fibers (Vaananen et al., 2000). The unique structural features of osteoclasts that confer this efficient machinery are two domains that are in contact with the bone matrix: sealing zone and the ruffled border. Bone resorption only occurs when osteoclasts bind to the mineralized bone surface. Therefore, the first step of osteoclast activity is the formation of a tightly sealed bone attachment compartment called sealing zone. The primary adhesion mediating actin-rich structure of osteoclasts is known as podosomes (Luxenburg et al., 2007). Podosomes consist of a core of densely packed actin filaments and F-actin-associated proteins surrounded by integrins and attachment-related proteins (Itzstein et al., 2011). Then, due to intense trafficking of lysosomal and endosomal components, there is a formation of a highly convoluted ruffled border, an exit site to the resorption space (resorption lacunae) for protons and a number of enzymes including lysosomal protease called cathepsin K, that are necessary for the bone resorption (Roodman, 1991) (Figure 9). Particularly, bone resorption depends on a vascuolar-type proton ATPase (V-ATPase), located in the membrane of the ruffled border, and cathepsin K. V-ATPase mediates proton transport into resorption lacunae that acidifies resorption lacunae and dissolves inorganic hydroxyapatite minerals of bone matrix (Blair and Athanasou, 2004). The secretion of protons via V-ATPase by the ruffled border

causes exocytosis of cathepstin K, a cysteine protease, into resorption lacunae. Cathepsin K is responsible for the degradation of a major organic bone matrix, type I collagen (Inui et al., 1997; Wilson et al., 2009). Thus, the sealing zone determines the bone resorption site and the ruffled border serves as the actual bone resorbing organelle.

As in the case of bone formation by osteoblasts, bone resorption is an energy demanding process. Glucose is the principal energy source required for osteoclasts and bone resorption is glucose concentration-dependent (Larsen et al., 2005; Williams et al., 1997).

2. The Basic Principles of Bone Mass Control: Bone (Re) modeling

The structural integrity of the skeleton is absolutely critical for vertebrates to survive because of its importance as a supportive framework of the body, mechanical protection of internal organs such as brain and for a wide range of movements. Furthermore, the bone marrow in the skeleton is the predominant site of hematopoiesis (Morrison and Scadden, 2014) and is essential for homeostatic control of the level of minerals in the blood because the skeleton contains more than 99% of the calcium, 80-90% of the phosphate and two thirds of the sodium in the body (Copp and Shim, 1963).

In order for the skeleton to fulfill these functions throughout adulthood, the skeleton constantly renews itself through a process called bone modeling during childhood and bone remodeling during adulthood. Bone (re)modeling is characterized by bone resorption of pre-existing mineralized bone ECM by osteoclasts followed by de novo bone formation by osteoblasts (Takeda et al., 2003). Bone resorption and bone formation occur not only sequentially but also in a balanced manner to maintain

bone mass constant during adulthood (Wei and Ducy, 2010). Thus, any unbalance between bone resorption and bone formation causes skeletal disorders characterized either by a low or by a high bone mass (Takeda et al., 2003). For example, osteoporosis is the most frequent bone remodeling disease that is characterized by a relative increase in osteoclastic activity leading to a low bone mass and a high risk of fracture (Feng and McDonald, 2011; Takeda et al., 2003)

The noteworthy feature of bone remodeling is that this process occurs constantly and simultaneously throughout the skeleton, that covers a large surface in the body, to insure its complete renewal and to maintain its structural integrity. Therefore, this process requires constantly a large supply of energy, mostly in the form of glucose, to bone cells, osteoblasts and osteoclasts.

3. The Endocrine Functions of Bone

Classically, the skeleton was viewed merely as an inert supportive framework in the body that is necessary for mobility, protection of internal organs, calcium homeostasis and maintenance of the hematopoietic niche. However, thanks to the advance of genetic approaches, knowledge regarding the functions of the skeleton has recently expanded beyond its role in the homeostatic regulation of bone mass. Advancement in genetic approaches allows scientists to systemically decipher the function of a gene of interest in vivo and to reveal hidden crosstalk between organs that influence each other. In other words, the whole-body organism analysis using genetic approach can further strengthen the fundamental principle of physiology: the mutual dependence between organs. Through genetic means, one additional yet unconventional function of the skeleton has been revealed: its endocrine function. It

has been apparent that the skeleton produces at least two hormones, fibroblast growth factor 23 (FGF23) and osteocalcin (Ocn). Here, the several functions of these two hormones secreted by bone beyond the regulations of bone homeostasis are described.

i. FGF23

The first discovery that implicates bone as an endocrine organ has been the identification of FGF23 as a hormone secreted exclusively by osteoblasts and osteocytes, which are osteoblasts embedded in mineralized matrix in bone. FG23 regulates serum phosphate levels by altering levels of active vitamin D ($1,25(OH)_2D$) and the activity of specific phosphate transporters in the kidney (DiGirolamo et al., 2012; Shimada et al., 2004). The serum levels of FGF23 increase and act physiologically to reduce serum phosphate and active vitamin D in response to increased serum levels of these molecules (Liu et al., 2006; Shimada et al., 2004). Accordingly, *fgf23* null mice exhibited significantly high serum phosphate with increased renal phosphate reabsorption (Shimada et al., 2004). They also showed high serum active vitamin D that enhances intestinal phosphate absorption (Shimada et al., 2004). These phenotypes seen in *fgf23-/-* mice are the mirror image of what is seen in human patients with hypophosphatemia disorders caused by a primary increase in the serum levels of FGF23. These disorders includes TIO (Tumor-Induced Osteomalacia) and ADHR (Autosomal Dominant Hypophosphatemic Rickets) in which *fgf23* was identified as responsible gene (Fukumoto and Martin, 2009; Shimada et al., 2001; White et al., 2000).

Altogether, genetic and clinical studies have shown that abnormal levels of the bone derived

hormone FGF23 alter phosphate and vitamin metabolism.

ii. Osteocalcin

A more surprising new dimension of physiological functions of the skeleton was uncovered after the identification of osteocalcin (Ocn), secreted exclusively by osteoblasts, as a multifunctional hormone. Osteocalcin is the most abundant non-collagenous protein in bone ECM and contains 46-50 amino acid residues that undergo post-translational modification of three glutamic acid residues (GLA residues) by vitamin K-dependent γ-carboxylation before its secretion from osteoblasts (Hauschka et al., 1989). This post-translational modification of osteocalcin is essential for calcium and hydroxyapatite binding and allows deposition of osteocalcin in bone ECM (Razzaque, 2011). On the contrary, undercarboxylated osteocalcin, formed as a result of post-translational modification, have a low affinity for hydroxyapatite and is more easily released in to the blood circulation (Razzaque, 2011).

Osteocalcin was thought to play a role solely in bone biology due to its confined expression in osteoblasts. However, surprisingly, *Ocn* deletion resulted in mice in which bone mineralization was normal but that were abnormally docile and fatty. *Ocn-/-* mice also bred poorly. In addition to those unexpected phenotypes seen in *Ocn-/-* mice, there are several clinical and experimental observations that support the hypothesis that the bone is an endocrine organ.

First, as described above, the skeletal biology suggests that bone remodeling is metabolically demanding process. Therefore it has been hypothesized that there is a coordinated regulation of bone mass and energy metabolism (Karsenty, 2006) and clinical observations support this notion. For

instance, when food intake is decreased during childhood, there is an arrest of growth; when this situation develops in adults, there is bone loss (Wei and Karsenty, 2015).

Secondly, clinically, it is well-known that the sex steroid hormones are one of the powerful hormonal regulations of bone remodeling necessary to maintain skeletal integrity (Khosla et al., 2001; Nakamura et al., 2007). Since the fundamental principle of whole-body physiology is mutual dependence of organs, it has been suggested that bone may in turn affect reproductive functions.

Lastly, in another view of skeletal biology, leptin, a hormone secreted primarily by adipocytes and regulating appetite and gonadal function, inhibits bone mass accrual by signaling in brainstem neurons to prevent the synthesis of serotonin (Friedman and Halaas, 1998; Oury et al., 2010; Takeda et al., 2002; Yadav et al., 2009). The identification of the brain as a determinant of bone mass accrual raises the question whether bone in turn signals back to the brain.

Indeed, several extensive genetic studies in mice and humans have proved that osteocalcin once activated as a hormone by undercarboxylation, influences glucose metabolism, male fertility and brain development and functions (Ferron et al., 2010a; Lee et al., 2007; Oury et al., 2013c; Oury et al., 2011) (Figure 10). Specifically, genetic as well as molecular studies have verified that osteocalcin promotes glucose homeostasis by acting on pancreatic β-cells to increase their proliferation as well as insulin secretion and to favor insulin sensitivity in both muscle and white adipose tissues (Ferron et al., 2010a; Lee et al., 2007). Furthermore, osteocalcin also favors testosterone production by the Leydig cells of the testis and thereby regulate male fertility (Oury et al., 2011). Recently, a study has shown that the

spectrum of osteocalcin functions even extends to brain development and cognition. Specifically, osteocalcin enhances postnatal neurogenesis and prevents anxiety as well as depression and also favors memory. Furthermore, maternal osteocalcin favors brain development of the fetus and affects their cognition postnatally (Oury et al., 2013c). These results showed that bone does signal back to brain and shed a light on a crosstalk between bone and brain.

Altogether, the multifunctional role of osteocalcin secreted exclusively by osteoblasts revealed that bone is a true endocrine organ. Yet, all of the functions of osteocalcin as well as its target tissues/cells are not fully discovered and further studies on the impact of osteocalcin signaling on whole-body physiology will further reveal the physiological importance of the skeleton as an endocrine organ.

4. Integration of Bone Remodeling and Glucose Metabolism by Insulin Signaling

An important feature of osteocalcin biology is that, to act as a hormone, osteocalcin needs to be undercarboxylated before reaching the blood stream. In vitro as well as in vivo studies showed that only the undercarboxylated form of osteocalcin (GLU13 is not carboxylated) indeed is the active form of the hormone (Ferron et al., 2008; Ferron et al., 2015; Karsenty and Ferron, 2012; Oury et al., 2011). Given that protein decarboxylation is known to occur only in an acidic pH, it was hypothesized that bone resorption, whose acidification process occurs at a low pH in resorption lacunae (pH4.5), may be involved in the activation of osteocalcin. In other words, the endocrine function of the skeleton may also require the coordinated actions of both osteoblasts and osteoclasts.

In addition, as osteocalcin secreted by osteoblasts as a regulator of insulin secretion, several

observations have led to the hypothesis that insulin signaling in osteoblasts in return regulates the activation of osteocalcin. This hypothesis was raised mainly based on the fact that *Ocn* is not the only gene that affects glucose homeostasis in osteoblasts. Indeed the deletion of *Esp*, a gene encoding osteoblast testis-specific protein tyrosine phosphatase (OST-PTP), results in mice that display a mirror image of what is observed in *Ocn-/-* mice (Lee et al., 2007). Importantly, the mice in which *Esp* was deleted either globally or specifically in osteoblast exhibited the same phenotype. Specifically, they were hypoglycemic, hyperinsulinemic and the serum fraction of undercarboxylated osteocalcin was significantly higher than in control mice (Lee et al., 2007). Given that osteocalcin is not phosphorylated, this raised the question what is the substrate of OST-PTP that influences the activity of osteocalcin. Since OST-PTP is a tyrosine phosphatase, the insulin receptor (InsR) in osteoblasts was hypothesized to be a target of OST-PTP since InsR activity is often inhibited by protein tyrosine phosphatase (Schlessinger, 2000). Furthermore, investigation of insulin signaling in osteoblasts was more relevant since mice lacking the insulin receptor (*InsR*) in two classical insulin target organs, skeletal muscle and white adipose tissue (WAT), did not display glucose intolerance thus implicating that insulin must act in additional tissue to achieve glucose homeostasis (Bluher et al., 2002; Bruning et al., 1998).

Here, the contribution of osteoclasts to the endocrine function of the bone and the importance of insulin signaling in osteoblasts to integrate bone remodeling and glucose metabolism by promoting activation of osteocalcin are described.

i. Insulin signaling in osteoblasts integrates bone remodeling and glucose homeostasis

The insulin Receptor (InsR) is a tyrosine kinase that can be activated by its conformational changes upon insulin binding that induces auto-phosphorylation required for the kinase activity and inactivated by phosphotyrosine-specific phosphatases (Kasuga et al., 1983; Siddle, 2011; Wilden et al., 1992). Molecular and genetic studies have identified that a tyrosine phosphatase OST-PTP encoded by a gene named *Esp* dephosphorylates and inactivates the InsR in osteoblasts (Ferron et al., 2010a). Genetic studies further confirmed that insulin signaling in osteoblasts indeed is necessary for the regulation of glucose homeostasis. Specifically, the metabolic phenotype of the mice lacking the *InsR* ($InsR_{osb}$-/-) in osteoblasts was similar to the one of *Ocn-/-* mice. They were glucose intolerant and insulin insensitive and had significantly less active osteocalcin in serum. Accordingly, double heterozygous compounds for *InsR* and *Ocn* ($InsR_{osb}$+/-;*Ocn*+/-) displayed metabolic abnormalities similar with *Ocn-/-* mice. In contrast, removing one allele of *InsR* from *Esp-/-* mice ($InsR_{osb}$+/-;*Esp-/-*) normalized the metabolic abnormalities of the *Esp-/-* mice. Thus, these genetic studies verified that insulin signaling in osteoblasts is a determinant of osteocalcin bioactivity (Ferron et al., 2010a; Lee et al., 2007). The important question was how insulin signaling acts in osteoblasts to favor activation of osteocalcin and regulate whole-body glucose homeostasis. It was revealed that insulin signaling takes advantage of the osteoblast ability to promote bone resorption by decreasing the expression of *Opg*, an inhibitor of osteoclast differentiation. The decrease in *Opg* expression in osteoblasts promotes bone resorption resulting in an acidification of bone ECM (pH 4.5) that activates osteocalcin by

decarboxyation of one glutamic residue GLU13 (Ferron et al., 2010a; Karsenty and Ferron, 2012) (Figure 11). Altogether, these observations showed that there is a feed-forward regulation between insulin and osteocalcin and that insulin signaling integrates bone remodeling to maintain glucose homeostasis by favoring the activation of osteocalcin.

ii. Insulin signaling in osteoblasts and osteocalcin activity in Human

Recent clinical investigations support the notion that osteocalcin is also involved in the regulation of glucose homeostasis in humans. For example, serum osteocalcin concentration is inversely associated with blood markers of abnormal metabolic phenotype and the active form of osteocalcin stimulates insulin production and promotes β-cell mass and function in human subjects in most studies (Hwang et al., 2009; Kanazawa et al., 2009; Pittas et al., 2009; Sabek et al., 2015). The importance of osteocalcin signaling in human is further confirmed by the fact that two individuals with the missense mutation in GPRC6A, a receptor mediates osteocalcin signaling in β-cells as well as in the Leydig cells, displayed glucose intolerance (Oury et al., 2013a). In addition, studies have identified that PTP1B, tyrosine phosphatase in human osteoblasts, fulfills the same functions as OST-PTP in mouse osteoblasts. As seen in mouse studies, insulin signaling in human osteoblasts is regulated by PTP1B and favors bone resorption by regulating the expression of *Opg* and this notion is further implied in osteopetrotic patients and mice showed the increase in osteocalcin carboxylation and decrease in insulin blood levels (Ferron et al., 2010a). Altogether, these studies confirmed that osteocalcin activity indeed is associated with glucose homeostasis and is in part determined by bone

resorption regulated by insulin signaling in osteoblasts in human.

iii. Pathogenic contribution of insulin resistance in bone to glucose homeostasis

The question raised by the contribution of insulin signaling in osteoblasts to whole-body glucose homeostasis in mice fed a normal diet was whether bone contributes to the insulin resistance that develops in mice fed a high-fat diet (HFD). Indeed, in mice fed a HFD, the circulating levels of the active form of osteocalcin are significantly lower than in control mice. This leads to a decrease in insulin secretion and sensitivity (Wei et al., 2014a; Wei and Karsenty, 2015). Biochemical studies have revealed that insulin resistance develops in bone as a result of an increase in circulating levels of free saturated fatty acids that enhances the E3 ubiquitin ligase Smurf1-mediated loss of InsR accumulation in osteoblasts. Specifically in osteoblasts, the increase in circulating level of free saturated fatty acids upregulates *Smurf1* expression that favors the degradation of the InsR. This molecular mechanism explained how insulin resistance in bone affects whole-body glucose homeostasis. However, despite its significant role in regulating InsR accumulation in osteoblasts, the metabolic phenotype of *Smurf1-/-* mice has never been investigated in vivo. Thus, the functions of Smurf1 in osteoblasts may extend beyond osteoblast differentiation and bone formation since by favoring the degradation of the InsR in osteoblasts, Smurf1 could be a regulator of circulating osteocalcin levels in vivo.

Overall, these genetic and biochemical observations suggest that insulin resistance in bone develops as a result of loss of InsR mediated by Smurf1 upon increase in the circulating level of free saturated fatty acids. Clinically, along with the importance of osteocalcin and insulin signaling in

osteoblasts for glucose homeostasis in human, they further suggest in a pathological situation that bone contributes to whole-body glucose homeostasis (Oury et al., 2013a; Wei et al., 2014a).

5. Glucose Uptake in Bone Cells

The identification of the crosstalk between insulin signaling and bone to regulate glucose homeostasis (Ferron et al., 2010a) raised a fundamental question: why does bone regulate whole-body glucose homeostasis in the first place? It can be hypothesized that glucose may be important for bone remodeling and particularly that the development and functions of osteoblasts and osteoclasts characterizing bone remodeling is intimately linked to glucose homeostasis.

Glucose indeed is the major source of energy in most living cells for development and growth. Most mammalian cells, including osteoblasts and osteoclasts, are dependent on a continuous supply of glucose, as a source for adenosine 5' triphosphate (ATP) synthesis, ribose 5 phosphate for nucleic acid synthesis and NADPH for reductive biosynthetic process. Furthermore, there is an emerging concept suggesting that glucose is not only a source of energy but also acts as signaling molecules and exerts transcriptional control in the cells (Mobasheri, 2012). Yet, the crosstalk between metabolic pathways and bone development and functions is largely unexplored.

In mammalian cells, glucose is not freely permeable across the lipid bilayer. Glucose enters across mammalian cells through members of the GLUT/*SLC2A* family of facilitative sugar transporters and the SGLT/*SLC5A* family of Na+ dependent active sugar transporters (Gould and Holman, 1993; Wood and Trayhurn, 2003). SGLT has a limited tissue expression and the Na+ dependent active transportation of

glucose (and galactose) by SGLT is found to be taking place across the luminal membrane of cells lining the small intestine and the proximal tubules of the kidney (Wood and Trayhurn, 2003). On the other hand, GLUTs encoded by the *SLC2* genes are found in various tissues and cell types (Mueckler and Thorens, 2013). Despite the importance of glucose transport into cells and the knowledge that bone remodeling is a metabolically demanding process, there is limited published information which GLUT transporter(s) play(s) a major role in glucose uptake occurs in bone cells.

Here, the basic knowledge of structural feature of GLUT family is discussed.

i. The GLUT family

GLUT proteins are facilitative transporters utilize the diffusion gradient of glucose across plasma membranes (Wood and Trayhurn, 2003). The GLUT family can be divided into three classes: Class I (GLUTs 1-4), Class II (GLUTs 5,7,9 and 11) and Class III (GLUTs 6,8,10,12 and HMIT (H+-coupled myo-inositol transporter))(Joost et al., 2002) (Figure 12). The class I facilitative transporters are the best characterized glucose transports and they can be distinguished on the basis of their specific tissue expression. For instance, GLUT1 is ubiquitously expressed with particularly high levels in erythrocytes and in the endothelial cells lining the blood vessels of the brain. GLUT2 is a low-affinity glucose transporter in liver, intestine, kidney and pancreatic beta cells. GLUT3 is expressed in neurons. GLUT1 and GLUT3 allow glucose to cross the blood brain barrier and enter neurons. Importantly, GLUT4 is only insulin-sensitive transporter and is found in heart, skeletal muscle and adipose tissues (Joost et al., 2002; Thorens and Mueckler, 2010). Class II is comprised of the fructose-specific

transporters and Class III is characterized by the lack of glycosylation site in the first extracellular linker domain (Joost et al., 2002).

Despites the extensive characterization of GLUTs, it still remains unclear how glucose uptake occurs in bone cells and what cellular functions will be affected upon disruption of glucose uptake during development and in postnatal life. Yet, there are a few studies indicating the involvement of GLUT1 in human and rodent osteoblastic cell lines (Thomas et al., 1996; Zoidis et al., 2011). Clinically, the importance of glucose uptake in bone development is also suggested since children chronically fed a ketogenic diet experience poor longitudinal growth (Groesbeck et al., 2006). Thus, answering these questions would be critical to improve our knowledge of the biological importance of the proper inflow of glucose as a main nutrient to bone cells to link bone remodeling and glucose metabolism.

6. AMPK and Osteoblasts

Given the possible link between glucose metabolism and bone development described above, bone cells must have a mechanism to regulate their cellular activity when faced with nutrient fluctuations in the extracellular environment. In general, although ATP is mainly generated from ADP by the mitochondrial ATP synthase, all eukaryotic cells contain adenylate kinase, which produces AMP and ATP from 2 ADP (2ADP→ AMP+ATP) (Hardie et al., 2012). Thus, when ATP is consumed, the relative increase in AMP concentration is much greater than that of ADP. Therefore, a key signal of nutrient fluctuations in the extracellular environment is changes in the concentration of AMP. Based on this fact, it seems logical that cells have a means to monitor AMP/ATP ratio. Indeed, AMP-activated

protein kinase (AMPK) is known to be the principal energy sensor in most cells and acts as a guardian of maintenance cellular energy homeostasis (Hardie, 2007; Hardie et al., 2012). Here, the structural and functional features of AMPK and its putative role in bone cells are described.

i. Structural and functional features of AMPK

AMPK exists as heterotrimeric complexes comprising a catalytic α subunit and regulatory β and γ subunits (Hardie et al., 2012). AMPK is activated by energy stress causing depletion of ATP and elevated cellular level of AMP or ADP (Hardie et al., 2012). Once activated, AMPK maintains energy homeostasis by phosphorylating downstream targets at Ser/Thr residues within a characteristic sequence motif. This results in activation of catabolism to generate ATP and inhibition of a number of energy consuming pathways including protein, carbohydrate and lipid biosynthesis as well as cell growth and proliferation (Hardie, 2007; Hardie et al., 2012) (Figure 13).

Here, among a number of regulatory mechanisms that AMPK exerts, particularly, regulation of protein synthesis through AMPK regulation of mTORC1 is described.

ii. Regulation of protein synthesis by mTORC1 and AMPK

The mammalian target of rapamycin complex 1 (mTORC1) signaling pathway integrates both intracellular and variety of extracellular signals and serves as a central regulator of mRNA translation, and therefore protein synthesis (Mahoney et al., 2009). mTORC1 has five components: mTOR, which is the catalytic subunit of the complex; regulatory-associated protein of mTOR (Raptor); mammalian

lethal with Sec13 protein 8 (mLST8); proline rich AKT substrate 40 kDa (PRAS40); and DEP-domain-containing mTOR-interacting protein (Deptor) (Laplante and Sabatini, 2009; Peterson et al., 2009). mTORC1 positively controls protein translation by phosphorylating downstream targets, eukaryotic initiation factor 4E (elF4E)-binding protein 1 (4E-BP1) and the p70 ribosomal S6 kinase (S6K) that mediates protein translation (Schmelzle and Hall, 2000). One of the associated proteins in mTORC1 complex, the Raptor, acts as a scaffold to recruit 4E-BP1 and S6K to the mTORC1 (Gwinn et al., 2008). It is also known that tuberous sclerosis complex (TSC) tumor suppressors, TSC1 and TSC2, are critical upstream inhibitors of the phosphorylation of S6K and 4EBP1, thus of mTORC1 complex (Gwinn et al., 2008; Inoki et al., 2003).

Nutrient status, is signaled to mTORC1 through AMPK-mediated regulation (Laplante and Sabatini, 2009). Specifically, there are two modes of AMPK mediated inhibition of mTORC1 activity. First, TSC2 is regulated by AMPK-dependent phosphorylation and plays an essential role in regulating mTOC1 activity in response to the cellular energy status (Inoki et al., 2003). Specifically, TSC2 contains a GTPase activation protein (GAP) domain that inactivates the Rheb GTPase that directly activates the mTORC1 complex in vitro (Sancak et al., 2007). Upon energy stress, AMPK is activated and phosphorylates TSC2 which increases the GAP activity of TSC2 towards Rheb and reduces mTORC1 activity (Inoki et al., 2003). Additionally, AMPK can reduce mTORC1 activity in response to energy depletion by directly phosphorylating Raptor on two well-conserved serine residues (Gwinn et al., 2008). Thus, mTORC1-mediated protein synthesis is regulated in response to the nutrient status by

AMPK.

iii. Perspective: The role of AMPK in osteoblast differentiation and functions

AMPK, which is a major mediator of energy sensing mechanisms, is expressed ubiquitously. However, even though some studies have implicated the involvement of AMPK in bone, how AMPK exerts its effect on bone cells during development and in postnatal life is poorly defined. In addition, mice lacking AMPK specifically in osteoblasts or osteoclasts have not yet been generated and analyzed. Thus, it is critical to study the physiology of mice lacking AMPK specifically in bone cells to determine the functions of AMPK in vivo during development and in postnatal life. Investigating how AMPK regulates osteoblasts and/or osteoclasts function upon energy stress requires the identification of the downstream targets of AMPK in bone cells that provide a significant insight into the link between metabolic pathways and development and functions of bone cells.

Figures

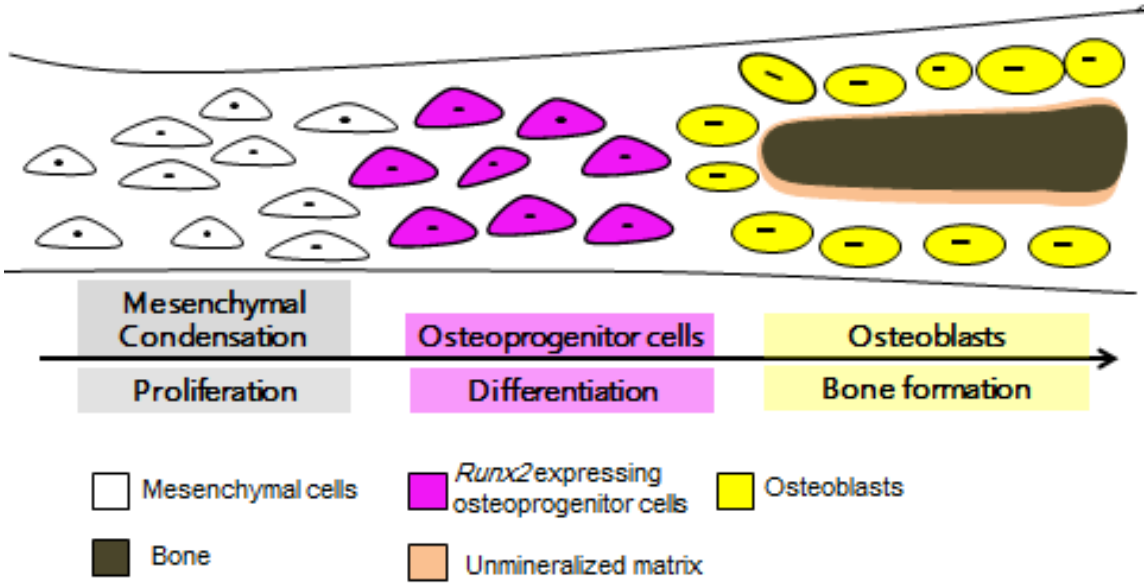

Figure 1. Intramembranous ossification.

Schematic illustration of intramembranous ossification during development. The cells of the mesenchymal condensations differentiate directly into bone-forming osteoblasts. Modified from (Ornitz and Marie, 2002).

Figure 2. Alcian blue/alizarin red staining of WT and *Runx2-/-* embryos at embryonic day (E) 16.5.

Alcian blue stains cartilage (blue) and alizarin red stains mineralized bone (red). The mineralized bone is completely absent in *Runx2-/-* embryo (b) even though the mineralized bone is present in WT embryo (a) at E16.5.

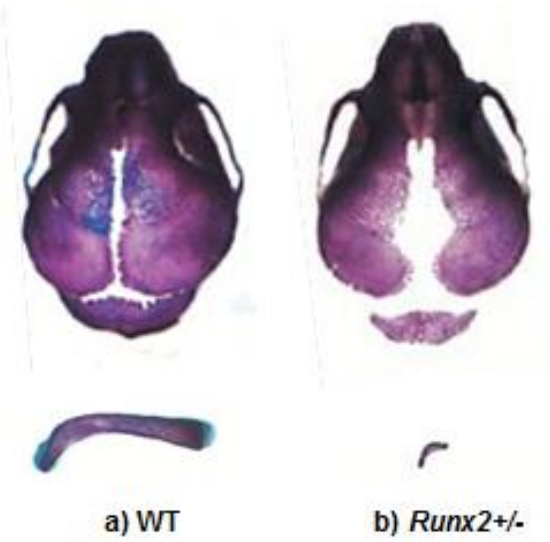

Figure 3. Alcian blue/alizarin red staining of newborn WT and *Runx2+/-* mice.

Alcian blue/alizarin red staining of clavicles and skulls of WT (a) and *Runx2+/-* (b) newborn mice. *Runx2+/-* mouse displays cleidocranial dysplasia characterized by open fontanelles and short clavicles. Modified from (Bialek et al., 2004).

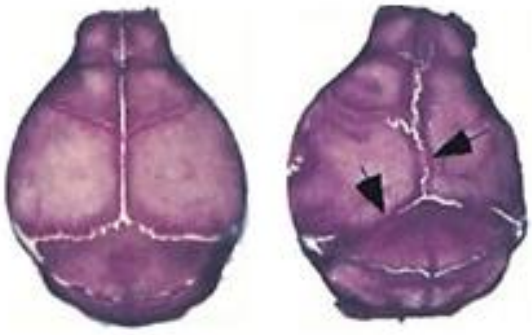

Figure 4. Alcian blue/alizarin red staining of 10-day-old WT and *Twist-1* +/- mice.

Alcian blue/alizarin red staining of skulls of 10-day-old WT (a) and *Twist-1*+/- (b) mice. *Twist-1*+/- mouse displays craniosynostosis characterized by fusion of sutures (arrows). Modified from (Bialek et al., 2004).

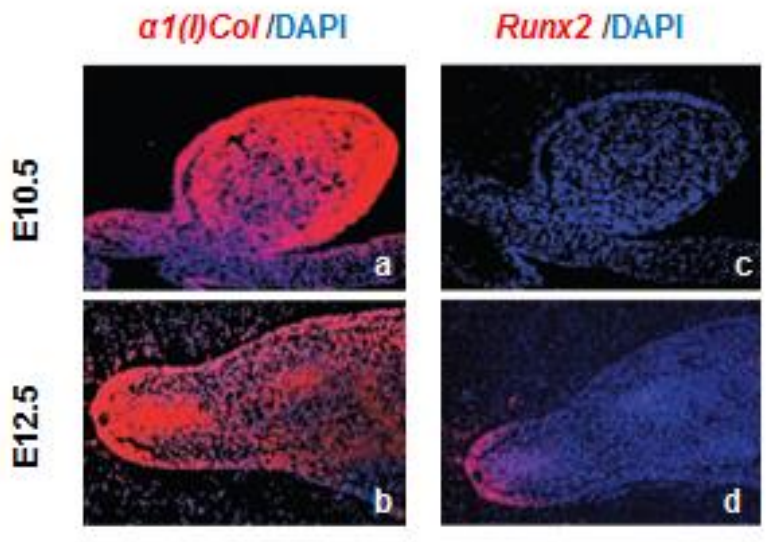

Figure 5. Spatial and temporal expression of *α1(I) Collagen* and *Runx2* in hind limbs during development.

In situ hybridization analysis of *α1(I)Collagen* (a-b), *Runx2* (c-d) in hind limbs at E10.5 and E12.5.

Modified from (Wei et al., 2015a).

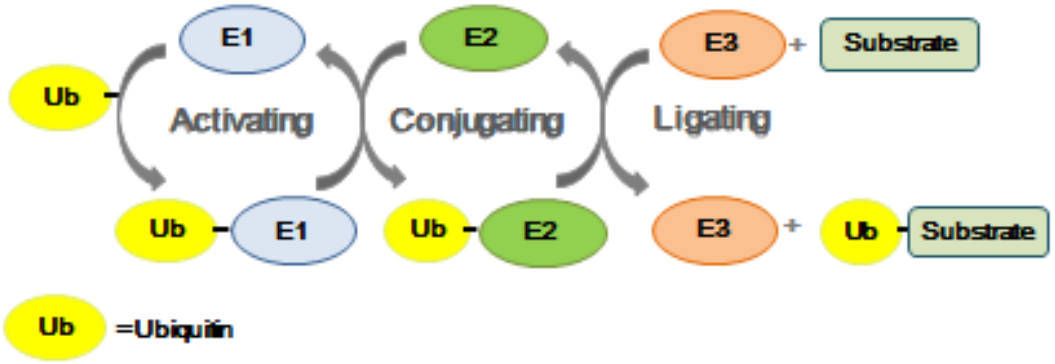

Figure 6. Enzymatic cascade for protein ubiquitination.

The ubiquitination cascade involves the successive actions of three types of enzymes: E1 ubiquitin-activating enzymes that recruits ubiquitin (Ub), E2 ubiquitin-conjugating enzymes that transfers the ubiquitin to the targeted protein via E3 ubiquitin ligases that recognize substrate protein. Ub: Ubiquitin. Modified from (Dikic et al., 2009).

Figure 7. Domain architectures of Smurf1.

Smurf1 contains a catalytic HECT domain in the C-terminal, two WW domains (WW1 and WW2) and a phospholipid-binding C2 domain in the N-terminal region. Modified from (Cao and Zhang, 2013).

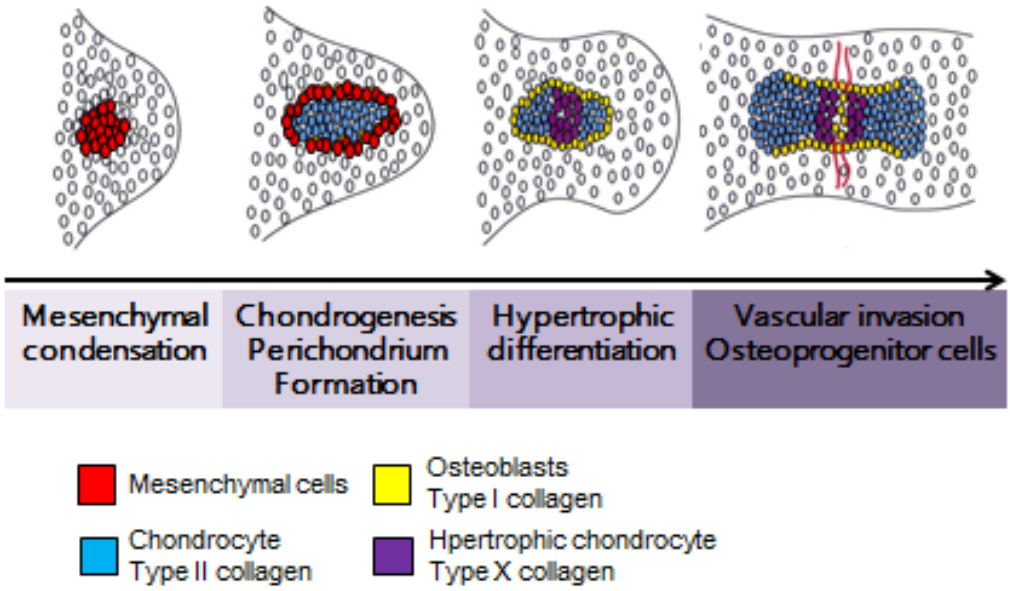

Figure 8. Endochondral ossification.

Schematic illustration of endochondral ossification during development. The cells of mesenchymal condensation (red) are differentiated into chondrocytes expressing type II collagen (blue). Then, the innermost chondrocytes become hypertrophic and express *α1(X) collagen* (purple). Once chondrocyte hypertrophy is initiated, cells in perichondrium start to differentiate into osteoblasts (yellow). The final step is vascular invasion and the formation of a center of ossification containing type I collagen-expressing osteoblasts. Modified from (Ornitz and Marie, 2002).

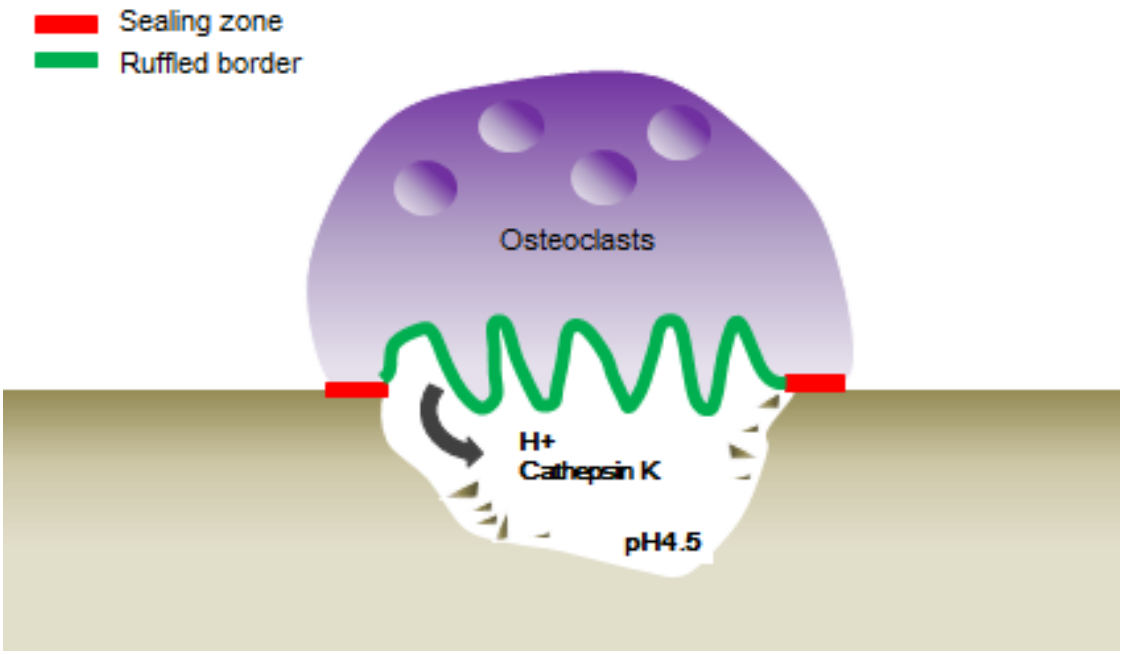

Figure 9. The structural features of osteoclasts.

Schematic view of a bone-resorbing osteoclast. Two domains of osteoclasts, sealing zone (red) and ruffle border (green), are in contact with the bone matrix. Acidification of bone ECM by secretion of proton (H+) results in the activation of cathepsin K, that is responsible for the degradation of a major organic bone matrix, type I collagen (Boyle et al., 2003; Vaananen et al., 2000). Modified from (Boyle et al., 2003; Vaananen et al., 2000)

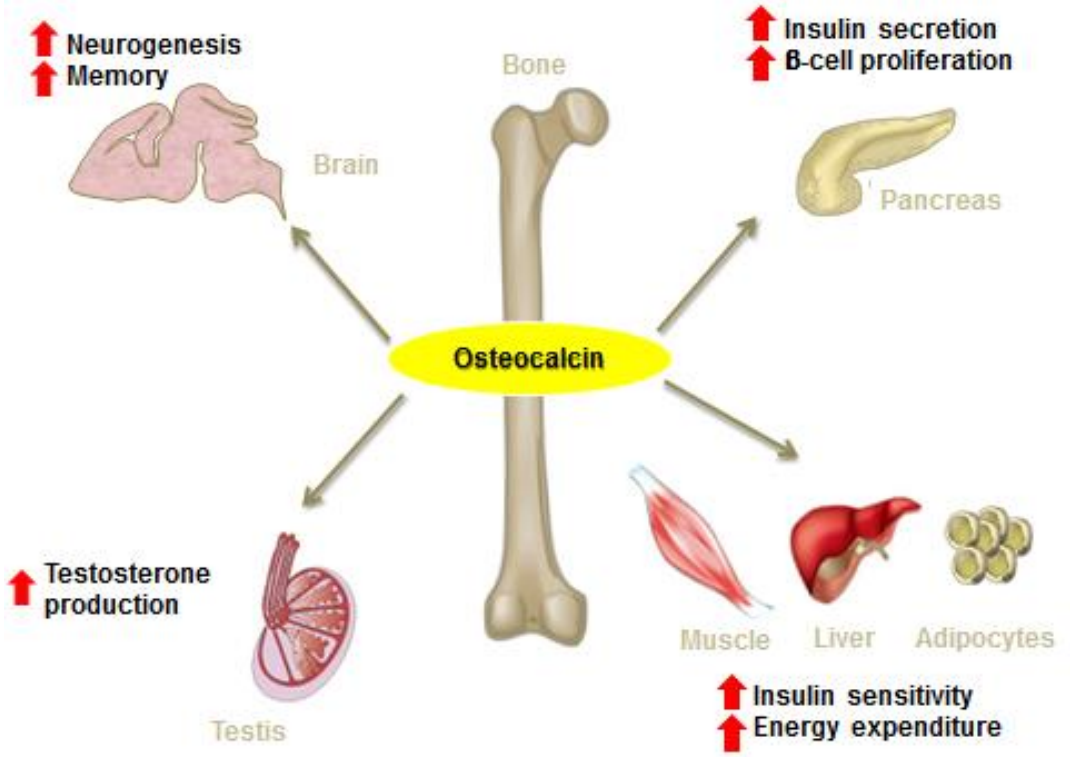

Figure 10. Bone-derived hormone osteocalcin regulates several organs.

Schematic illustration of the multifunctional roles of osteocalcin. Undercarboxylated (active) osteocalcin favors insulin secretion and β-cell proliferation in the pancreas, energy expenditure and insulin sensitivity in muscle, liver and white adipose tissue (WAT), male fertility by stimulating testosterone synthesis and brain development and memory. Modified from (Karsenty and Ferron, 2012; Karsenty and Oury, 2012).

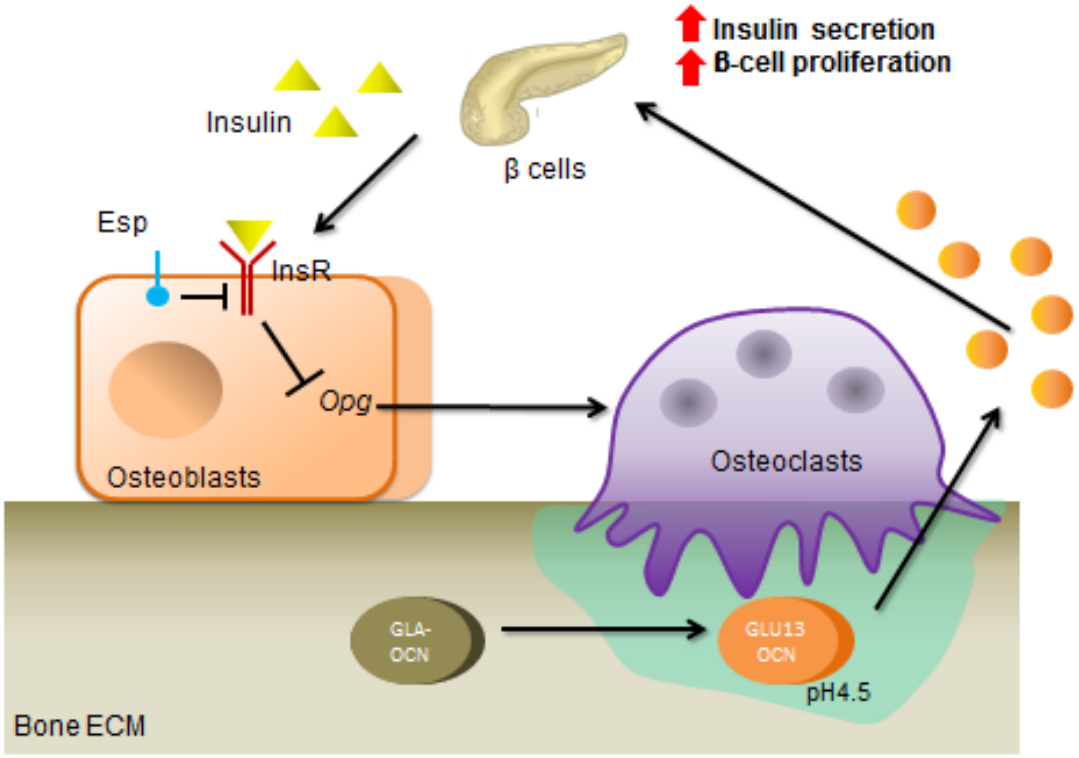

Figure 11. Insulin signaling in osteoblasts regulates of osteocalcin activation via bone resorption

Insulin signaling in osteoblasts is regulated by Esp and promotes bone resorption by decreasing the expression of *Opg*, an inhibitor of osteoclast differentiation. The acidification of bone ECM (pH 4.5) activates osteocalcin by decarboxyation. As a result, the active form of osteocalcin promotes insulin secretion, β-cell proliferation and insulin sensitivity. Modified from (Karsenty and Ferron, 2012).

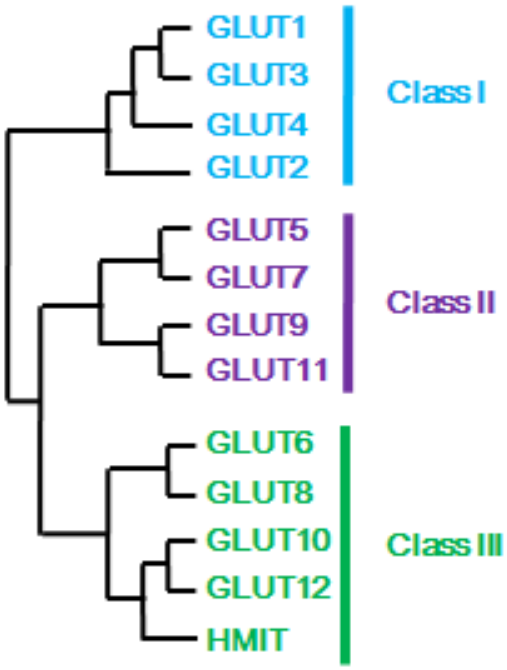

Figure 12. Dendrogram of the glucose transporter GLUT family.

The GLUT family can be divided into three classes depicting sequence similarities: Class I, Class II and Class III that are shown as blue, purple and green color respectively. Modified from (Joost et al., 2002).

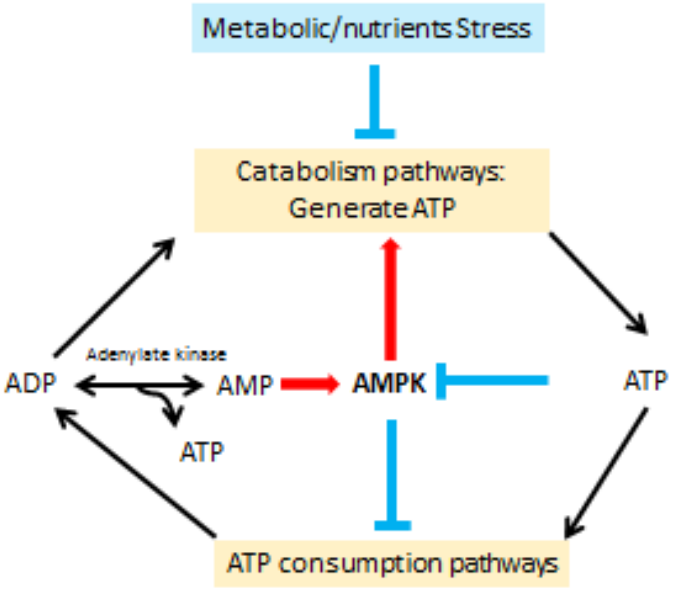

Figure 13. Regulation of energy metabolism by AMPK

AMPK is activated by elevated cellular level of AMP and/or ADP. Once activated, AMPK maintains energy homeostasis by activation of catabolic pathways to generate more ATP and by inhibition of a number of ATP consuming pathways. Modified from (Hardie, 2007).

References

Ardley, H.C., and Robinson, P.A. (2005). E3 ubiquitin ligases. Essays Biochem *41*, 15-30.

Bar-Shavit, Z. (2007). The osteoclast: a multinucleated, hematopoietic-origin, bone-resorbing osteoimmune cell. J Cell Biochem *102*, 1130-1139.

Bialek, P., Kern, B., Yang, X., Schrock, M., Sosic, D., Hong, N., Wu, H., Yu, K., Ornitz, D.M., Olson, E.N.*, et al.* (2004). A twist code determines the onset of osteoblast differentiation. Dev Cell *6*, 423-435.

Blair, H.C., and Athanasou, N.A. (2004). Recent advances in osteoclast biology and pathological bone resorption. Histol Histopathol *19*, 189-199.

Bluher, M., Michael, M.D., Peroni, O.D., Ueki, K., Carter, N., Kahn, B.B., and Kahn, C.R. (2002). Adipose tissue selective insulin receptor knockout protects against obesity and obesity-related glucose intolerance. Dev Cell *3*, 25-38.

Borle, A.B., Nichols, N., and Nichols, G., Jr. (1960). Metabolic studies of bone in vitro. I. Normal bone. The Journal of biological chemistry *235*, 1206-1210.

Boyce, B.F., and Xing, L. (2007). The RANKL/RANK/OPG pathway. Curr Osteoporos Rep *5*, 98-104.

Boyle, W.J., Simonet, W.S., and Lacey, D.L. (2003). Osteoclast differentiation and activation. Nature *423*, 337-342.

Bruning, J.C., Michael, M.D., Winnay, J.N., Hayashi, T., Horsch, D., Accili, D., Goodyear, L.J., and Kahn, C.R. (1998). A muscle-specific insulin receptor knockout exhibits features of the metabolic syndrome of NIDDM without altering glucose tolerance. Mol Cell *2*, 559-569.

Cao, Y., and Zhang, L. (2013). A Smurf1 tale: function and regulation of an ubiquitin ligase in multiple cellular networks. Cell Mol Life Sci *70*, 2305-2317.

Clarke, B. (2008). Normal bone anatomy and physiology. Clin J Am Soc Nephrol *3 Suppl 3*, S131-139.

Cohn, D.V., and Forscher, B.K. (1962). Aerobic metabolism of glucose by bone. The Journal of biological chemistry *237*, 615-618.

Copp, D.H., and Shim, S.S. (1963). The homeostatic function of bone as a mineral reservoir. Oral Surgery, Oral Medicine, Oral Pathology *16*, 738-744.

Deshaies, R.J., and Joazeiro, C.A. (2009). RING domain E3 ubiquitin ligases. Annu Rev Biochem *78*, 399-434.

Dessau, W., von der Mark, H., von der Mark, K., and Fischer, S. (1980). Changes in the patterns of collagens and fibronectin during limb-bud chondrogenesis. J Embryol Exp Morphol *57*, 51-60.

DiGirolamo, D.J., Clemens, T.L., and Kousteni, S. (2012). The skeleton as an endocrine organ. Nat Rev Rheumatol *8*, 674-683.

Dikic, I., Wakatsuki, S., and Walters, K.J. (2009). Ubiquitin-binding domains - from structures to functions. Nat Rev Mol Cell Biol *10*, 659-671.

Ducy, P., Starbuck, M., Priemel, M., Shen, J., Pinero, G., Geoffroy, V., Amling, M., and Karsenty, G. (1999). A Cbfa1-dependent genetic pathway controls bone formation beyond embryonic development. Genes Dev *13*, 1025-1036.

Ducy, P., Zhang, R., Geoffroy, V., Ridall, A.L., and Karsenty, G. (1997). Osf2/Cbfa1: a transcriptional

activator of osteoblast differentiation. Cell *89*, 747-754.

Esen, E., and Long, F. (2014). Aerobic glycolysis in osteoblasts. Curr Osteoporos Rep *12*, 433-438.

Feng, X., and McDonald, J.M. (2011). Disorders of bone remodeling. Annu Rev Pathol *6*, 121-145.

Ferron, M., Hinoi, E., Karsenty, G., and Ducy, P. (2008). Osteocalcin differentially regulates beta cell and adipocyte gene expression and affects the development of metabolic diseases in wild-type mice. Proc Natl Acad Sci U S A *105*, 5266-5270.

Ferron, M., Lacombe, J., Germain, A., Oury, F., and Karsenty, G. (2015). GGCX and VKORC1 inhibit osteocalcin endocrine functions. J Cell Biol *208*, 761-776.

Ferron, M., Wei, J., Yoshizawa, T., Del Fattore, A., DePinho, R.A., Teti, A., Ducy, P., and Karsenty, G. (2010). Insulin signaling in osteoblasts integrates bone remodeling and energy metabolism. Cell *142*, 296-308.

Florencio-Silva, R., Sasso, G.R., Sasso-Cerri, E., Simoes, M.J., and Cerri, P.S. (2015). Biology of Bone Tissue: Structure, Function, and Factors That Influence Bone Cells. Biomed Res Int *2015*, 421746.

Friedman, J.M., and Halaas, J.L. (1998). Leptin and the regulation of body weight in mammals. Nature *395*, 763-770.

Fukumoto, S., and Martin, T.J. (2009). Bone as an endocrine organ. Trends Endocrinol Metab *20*, 230-236.

Gallagher, E., Gao, M., Liu, Y.C., and Karin, M. (2006). Activation of the E3 ubiquitin ligase Itch through a phosphorylation-induced conformational change. Proc Natl Acad Sci U S A *103*, 1717-1722.

Gao, M., Labuda, T., Xia, Y., Gallagher, E., Fang, D., Liu, Y.C., and Karin, M. (2004). Jun turnover is controlled through JNK-dependent phosphorylation of the E3 ligase Itch. Science *306*, 271-275.

Gould, G.W., and Holman, G.D. (1993). The glucose transporter family: structure, function and tissue-specific expression. Biochem J *295 (Pt 2)*, 329-341.

Groesbeck, D.K., Bluml, R.M., and Kossoff, E.H. (2006). Long-term use of the ketogenic diet in the treatment of epilepsy. Dev Med Child Neurol *48*, 978-981.

Gwinn, D.M., Shackelford, D.B., Egan, D.F., Mihaylova, M.M., Mery, A., Vasquez, D.S., Turk, B.E., and Shaw, R.J. (2008). AMPK phosphorylation of raptor mediates a metabolic checkpoint. Mol Cell *30*, 214-226.

Hardie, D.G. (2007). AMP-activated/SNF1 protein kinases: conserved guardians of cellular energy. Nat Rev Mol Cell Biol *8*, 774-785.

Hardie, D.G., Ross, F.A., and Hawley, S.A. (2012). AMPK: a nutrient and energy sensor that maintains energy homeostasis. Nat Rev Mol Cell Biol *13*, 251-262.

Hauschka, P.V., Lian, J.B., Cole, D.E., and Gundberg, C.M. (1989). Osteocalcin and matrix Gla protein: vitamin K-dependent proteins in bone. Physiological Reviews *69*, 990-1047.

Hayami, R., Sato, K., Wu, W., Nishikawa, T., Hiroi, J., Ohtani-Kaneko, R., Fukuda, M., and Ohta, T. (2005). Down-regulation of BRCA1-BARD1 ubiquitin ligase by CDK2. Cancer Res *65*, 6-10.

Hwang, Y.C., Jeong, I.K., Ahn, K.J., and Chung, H.Y. (2009). The uncarboxylated form of osteocalcin is associated with improved glucose tolerance and enhanced beta-cell function in middle-aged male

subjects. Diabetes Metab Res Rev *25*, 768-772.

Inoki, K., Zhu, T., and Guan, K.L. (2003). TSC2 mediates cellular energy response to control cell growth and survival. Cell *115*, 577-590.

Inui, T., Ishibashi, O., Inaoka, T., Origane, Y., Kumegawa, M., Kokubo, T., and Yamamura, T. (1997). Cathepsin K antisense oligodeoxynucleotide inhibits osteoclastic bone resorption. The Journal of biological chemistry *272*, 8109-8112.

Itzstein, C., Coxon, F.P., and Rogers, M.J. (2011). The regulation of osteoclast function and bone resorption by small GTPases. Small GTPases *2*, 117-130.

Jones, D.C., Wein, M.N., Oukka, M., Hofstaetter, J.G., Glimcher, M.J., and Glimcher, L.H. (2006). Regulation of adult bone mass by the zinc finger adapter protein Schnurri-3. Science *312*, 1223-1227.

Joost, H.G., Bell, G.I., Best, J.D., Birnbaum, M.J., Charron, M.J., Chen, Y.T., Doege, H., James, D.E., Lodish, H.F., Moley, K.H.*, et al.* (2002). Nomenclature of the GLUT/SLC2A family of sugar/polyol transport facilitators. Am J Physiol Endocrinol Metab *282*, E974-976.

Kanazawa, I., Yamaguchi, T., Yamamoto, M., Yamauchi, M., Kurioka, S., Yano, S., and Sugimoto, T. (2009). Serum osteocalcin level is associated with glucose metabolism and atherosclerosis parameters in type 2 diabetes mellitus. J Clin Endocrinol Metab *94*, 45-49.

Karsenty, G. (2006). Convergence between bone and energy homeostases: leptin regulation of bone mass. Cell Metab *4*, 341-348.

Karsenty, G., and Ferron, M. (2012). The contribution of bone to whole-organism physiology. Nature *481*, 314-320.

Karsenty, G., and Oury, F. (2012). Biology without walls: the novel endocrinology of bone. Annu Rev Physiol *74*, 87-105.

Karsenty, G., and Wagner, E.F. (2002). Reaching a genetic and molecular understanding of skeletal development. Dev Cell *2*, 389-406.

Kasuga, M., Fujita-Yamaguchi, Y., Blithe, D.L., White, M.F., and Kahn, C.R. (1983). Characterization of the insulin receptor kinase purified from human placental membranes. The Journal of biological chemistry *258*, 10973-10980.

Kern, B., Shen, J., Starbuck, M., and Karsenty, G. (2001). Cbfa1 contributes to the osteoblast-specific expression of type I collagen genes. The Journal of biological chemistry *276*, 7101-7107.

Khosla, S., Melton, L.J., 3rd, Atkinson, E.J., and O'Fallon, W.M. (2001). Relationship of serum sex steroid levels to longitudinal changes in bone density in young versus elderly men. J Clin Endocrinol Metab *86*, 3555-3561.

Komori, T., Yagi, H., Nomura, S., Yamaguchi, A., Sasaki, K., Deguchi, K., Shimizu, Y., Bronson, R.T., Gao, Y.H., Inada, M.*, et al.* (1997). Targeted disruption of Cbfa1 results in a complete lack of bone formation owing to maturational arrest of osteoblasts. Cell *89*, 755-764.

Kronenberg, H.M. (2003). Developmental regulation of the growth plate. Nature *423*, 332-336.

Laplante, M., and Sabatini, D.M. (2009). mTOR signaling at a glance. J Cell Sci *122*, 3589-3594.

Larsen, K.I., Falany, M., Wang, W., and Williams, J.P. (2005). Glucose is a key metabolic regulator of

osteoclasts; glucose stimulated increases in ATP/ADP ratio and calmodulin kinase II activity. Biochem Cell Biol *83*, 667-673.

Lee, B., Thirunavukkarasu, K., Zhou, L., Pastore, L., Baldini, A., Hecht, J., Geoffroy, V., Ducy, P., and Karsenty, G. (1997). Missense mutations abolishing DNA binding of the osteoblast-specific transcription factor OSF2/CBFA1 in cleidocranial dysplasia. Nature genetics *16*, 307-310.

Lee, N.K., Sowa, H., Hinoi, E., Ferron, M., Ahn, J.D., Confavreux, C., Dacquin, R., Mee, P.J., McKee, M.D., Jung, D.Y*., et al.* (2007). Endocrine regulation of energy metabolism by the skeleton. Cell *130*, 456-469.

Lefebvre, V., and de Crombrugghe, B. (1998). Toward understanding SOX9 function in chondrocyte differentiation. Matrix Biol *16*, 529-540.

Lefebvre, V., Huang, W., Harley, V.R., Goodfellow, P.N., and de Crombrugghe, B. (1997). SOX9 is a potent activator of the chondrocyte-specific enhancer of the pro alpha1(II) collagen gene. Mol Cell Biol *17*, 2336-2346.

Liu, S., Tang, W., Zhou, J., Stubbs, J.R., Luo, Q., Pi, M., and Quarles, L.D. (2006). Fibroblast growth factor 23 is a counter-regulatory phosphaturic hormone for vitamin D. J Am Soc Nephrol *17*, 1305-1315.

Long, F. (2012). Building strong bones: molecular regulation of the osteoblast lineage. Nat Rev Mol Cell Biol *13*, 27-38.

Luxenburg, C., Geblinger, D., Klein, E., Anderson, K., Hanein, D., Geiger, B., and Addadi, L. (2007). The architecture of the adhesive apparatus of cultured osteoclasts: from podosome formation to sealing zone assembly. PLoS One *2*, e179.

Mackie, E.J., Ahmed, Y.A., Tatarczuch, L., Chen, K.S., and Mirams, M. (2008). Endochondral ossification: how cartilage is converted into bone in the developing skeleton. Int J Biochem Cell Biol *40*, 46-62.

Mackie, E.J., Tatarczuch, L., and Mirams, M. (2011). The skeleton: a multi-functional complex organ: the growth plate chondrocyte and endochondral ossification. J Endocrinol *211*, 109-121.

Maes, C., Kobayashi, T., Selig, M.K., Torrekens, S., Roth, S.I., Mackem, S., Carmeliet, G., and Kronenberg, H.M. (2010). Osteoblast precursors, but not mature osteoblasts, move into developing and fractured bones along with invading blood vessels. Dev Cell *19*, 329-344.

Mahoney, S.J., Dempsey, J.M., and Blenis, J. (2009). Cell signaling in protein synthesis ribosome biogenesis and translation initiation and elongation. Prog Mol Biol Transl Sci *90*, 53-107.

Mobasheri, A. (2012). Glucose: an energy currency and structural precursor in articular cartilage and bone with emerging roles as an extracellular signaling molecule and metabolic regulator. Front Endocrinol (Lausanne) *3*, 153.

Morrison, S.J., and Scadden, D.T. (2014). The bone marrow niche for haematopoietic stem cells. Nature *505*, 327-334.

Mueckler, M., and Thorens, B. (2013). The SLC2 (GLUT) family of membrane transporters. Mol Aspects Med *34*, 121-138.

Mundlos, S., Otto, F., Mundlos, C., Mulliken, J.B., Aylsworth, A.S., Albright, S., Lindhout, D., Cole, W.G., Henn, W., Knoll, J.H.*, et al.* (1997). Mutations involving the transcription factor CBFA1 cause cleidocranial dysplasia. Cell *89*, 773-779.

Nakamura, T., Imai, Y., Matsumoto, T., Sato, S., Takeuchi, K., Igarashi, K., Harada, Y., Azuma, Y., Krust, A., Yamamoto, Y.*, et al.* (2007). Estrogen prevents bone loss via estrogen receptor alpha and induction of Fas ligand in osteoclasts. Cell *130*, 811-823.

Nishio, Y., Dong, Y., Paris, M., O'Keefe, R.J., Schwarz, E.M., and Drissi, H. (2006). Runx2-mediated regulation of the zinc finger Osterix/Sp7 gene. Gene *372*, 62-70.

Ornitz, D.M., and Marie, P.J. (2002). FGF signaling pathways in endochondral and intramembranous bone development and human genetic disease. Genes Dev *16*, 1446-1465.

Otto, F., Thornell, A.P., Crompton, T., Denzel, A., Gilmour, K.C., Rosewell, I.R., Stamp, G.W., Beddington, R.S., Mundlos, S., Olsen, B.R.*, et al.* (1997). Cbfa1, a candidate gene for cleidocranial dysplasia syndrome, is essential for osteoblast differentiation and bone development. Cell *89*, 765-771.

Oury, F., Ferron, M., Huizhen, W., Confavreux, C., Xu, L., Lacombe, J., Srinivas, P., Chamouni, A., Lugani, F., Lejeune, H.*, et al.* (2013a). Osteocalcin regulates murine and human fertility through a pancreas-bone-testis axis. J Clin Invest *123*, 2421-2433.

Oury, F., Khrimian, L., Denny, C.A., Gardin, A., Chamouni, A., Goeden, N., Huang, Y.Y., Lee, H., Srinivas, P., Gao, X.B.*, et al.* (2013c). Maternal and offspring pools of osteocalcin influence brain development and functions. Cell *155*, 228-241.

Oury, F., Sumara, G., Sumara, O., Ferron, M., Chang, H., Smith, C.E., Hermo, L., Suarez, S., Roth, B.L., Ducy, P.*, et al.* (2011). Endocrine regulation of male fertility by the skeleton. Cell *144*, 796-809.

Oury, F., Yadav, V.K., Wang, Y., Zhou, B., Liu, X.S., Guo, X.E., Tecott, L.H., Schutz, G., Means, A.R., and Karsenty, G. (2010). CREB mediates brain serotonin regulation of bone mass through its expression in ventromedial hypothalamic neurons. Genes Dev *24*, 2330-2342.

Peterson, T.R., Laplante, M., Thoreen, C.C., Sancak, Y., Kang, S.A., Kuehl, W.M., Gray, N.S., and Sabatini, D.M. (2009). DEPTOR is an mTOR inhibitor frequently overexpressed in multiple myeloma cells and required for their survival. Cell *137*, 873-886.

Pittas, A.G., Harris, S.S., Eliades, M., Stark, P., and Dawson-Hughes, B. (2009). Association between serum osteocalcin and markers of metabolic phenotype. J Clin Endocrinol Metab *94*, 827-832.

Pritchard, J.J. (1952). A cytological and histochemical study of bone and cartilage formation in the rat. J Anat *86*, 259-277.

Puppin, C., Pellizzari, L., Fabbro, D., Fogolari, F., Tell, G., Tessa, A., Santorelli, F.M., and Damante, G. (2005). Functional analysis of a novel RUNX2 missense mutation found in a family with cleidocranial dysplasia. J Hum Genet *50*, 679-683.

Razzaque, M.S. (2011). Osteocalcin: a pivotal mediator or an innocent bystander in energy metabolism? Nephrology Dialysis Transplantation *26*, 42-45.

Roodman, G.D. (1991). Osteoclast differentiation. Crit Rev Oral Biol Med *2*, 389-409.

Sabek, O.M., Nishimoto, S.K., Fraga, D., Tejpal, N., Ricordi, C., and Gaber, A.O. (2015). Osteocalcin Effect on Human beta-Cells Mass and Function. Endocrinology *156*, 3137-3146.

Sancak, Y., Thoreen, C.C., Peterson, T.R., Lindquist, R.A., Kang, S.A., Spooner, E., Carr, S.A., and Sabatini, D.M. (2007). PRAS40 is an insulin-regulated inhibitor of the mTORC1 protein kinase. Mol Cell *25*, 903-915.

Schlessinger, J. (2000). Cell signaling by receptor tyrosine kinases. Cell *103*, 211-225.

Schmelzle, T., and Hall, M.N. (2000). TOR, a central controller of cell growth. Cell *103*, 253-262.

Sekiya, I., Tsuji, K., Koopman, P., Watanabe, H., Yamada, Y., Shinomiya, K., Nifuji, A., and Noda, M. (2000). SOX9 Enhances Aggrecan Gene Promoter/Enhancer Activity and Is Up-regulated by Retinoic Acid in a Cartilage-derived Cell Line, TC6. Journal of Biological Chemistry *275*, 10738-10744.

Severe, N., Dieudonne, F.X., and Marie, P.J. (2013). E3 ubiquitin ligase-mediated regulation of bone formation and tumorigenesis. Cell Death Dis *4*, e463.

Shen, R., Wang, X., Drissi, H., Liu, F., O'Keefe, R.J., and Chen, D. (2006). Cyclin D1-cdk4 induce runx2 ubiquitination and degradation. The Journal of biological chemistry *281*, 16347-16353.

Shimada, T., Kakitani, M., Yamazaki, Y., Hasegawa, H., Takeuchi, Y., Fujita, T., Fukumoto, S., Tomizuka, K., and Yamashita, T. (2004). Targeted ablation of Fgf23 demonstrates an essential physiological role of FGF23 in phosphate and vitamin D metabolism. J Clin Invest *113*, 561-568.

Shimada, T., Mizutani, S., Muto, T., Yoneya, T., Hino, R., Takeda, S., Takeuchi, Y., Fujita, T., Fukumoto, S., and Yamashita, T. (2001). Cloning and characterization of FGF23 as a causative factor of tumor-induced osteomalacia. Proceedings of the National Academy of Sciences of the United States of America *98*, 6500-6505.

Shu, L., Zhang, H., Boyce, B.F., and Xing, L. (2013). Ubiquitin E3 ligase Wwp1 negatively regulates osteoblast function by inhibiting osteoblast differentiation and migration. J Bone Miner Res *28*, 1925-1935.

Siddle, K. (2011). Signalling by insulin and IGF receptors: supporting acts and new players. J Mol Endocrinol *47*, R1-10.

Takeda, S., Elefteriou, F., and Karsenty, G. (2003). Common endocrine control of body weight, reproduction, and bone mass. Annu Rev Nutr *23*, 403-411.

Takeda, S., Elefteriou, F., Levasseur, R., Liu, X., Zhao, L., Parker, K.L., Armstrong, D., Ducy, P., and Karsenty, G. (2002). Leptin regulates bone formation via the sympathetic nervous system. Cell *111*, 305-317.

Tessa, A., Salvi, S., Casali, C., Garavelli, L., Digilio, M.C., Dotti, M.T., Di Giandomenico, S., Valoppi, M., Grieco, G.S., Comanducci, G.*, et al.* (2003). Six novel mutations of the RUNX2 gene in Italian patients with cleidocranial dysplasia. Hum Mutat *22*, 104.

Thomas, D.M., Rogers, S.D., Ng, K.W., and Best, J.D. (1996). Dexamethasone modulates insulin receptor expression and subcellular distribution of the glucose transporter GLUT 1 in UMR 106-01, a clonal osteogenic sarcoma cell line. J Mol Endocrinol *17*, 7-17.

Thorens, B., and Mueckler, M. (2010). Glucose transporters in the 21st Century. Am J Physiol

Endocrinol Metab *298*, E141-145.

Tintut, Y., Parhami, F., Le, V., Karsenty, G., and Demer, L.L. (1999). Inhibition of osteoblast-specific transcription factor Cbfa1 by the cAMP pathway in osteoblastic cells. Ubiquitin/proteasome-dependent regulation. The Journal of biological chemistry *274*, 28875-28879.

Vaananen, H.K., Zhao, H., Mulari, M., and Halleen, J.M. (2000). The cell biology of osteoclast function. J Cell Sci *113 (Pt 3)*, 377-381.

Vu, T.H., Shipley, J.M., Bergers, G., Berger, J.E., Helms, J.A., Hanahan, D., Shapiro, S.D., Senior, R.M., and Werb, Z. (1998). MMP-9/gelatinase B is a key regulator of growth plate angiogenesis and apoptosis of hypertrophic chondrocytes. Cell *93*, 411-422.

Vuorio, E., and de Crombrugghe, B. (1990). The family of collagen genes. Annu Rev Biochem *59*, 837-872.

Wei, J., and Ducy, P. (2010). Co-dependence of bone and energy metabolisms. Arch Biochem Biophys *503*, 35-40.

Wei, J., Ferron, M., Clarke, C.J., Hannun, Y.A., Jiang, H., Blaner, W.S., and Karsenty, G. (2014). Bone-specific insulin resistance disrupts whole-body glucose homeostasis via decreased osteocalcin activation. J Clin Invest *124*, 1-13.

Wei, J., and Karsenty, G. (2015). An overview of the metabolic functions of osteocalcin. Rev Endocr Metab Disord *16*, 93-98.

Wei, J., Shimazu, J., Makinistoglu, M.P., Maurizi, A., Kajimura, D., Zong, H., Takarada, T., Iezaki, T., Pessin, J.E., Hinoi, E.*, et al.* (2015). Glucose Uptake and Runx2 Synergize to Orchestrate Osteoblast Differentiation and Bone Formation. Cell *161*, 1576-1591.

White, K.E., Evans, W.E., O'Riordan, J.L.H., Speer, M.C., Econs, M.J., Lorenz-Depiereux, B., Grabowski, M., Meitinger, T., and Strom, T.M. (2000). Autosomal dominant hypophosphataemic rickets is associated with mutations in FGF23. Nature genetics *26*, 345-348.

Wilden, P.A., Siddle, K., Haring, E., Backer, J.M., White, M.F., and Kahn, C.R. (1992). The role of insulin receptor kinase domain autophosphorylation in receptor-mediated activities. Analysis with insulin and anti-receptor antibodies. The Journal of biological chemistry *267*, 13719-13727.

Williams, J.P., Blair, H.C., McDonald, J.M., McKenna, M.A., Jordan, S.E., Williford, J., and Hardy, R.W. (1997). Regulation of osteoclastic bone resorption by glucose. Biochem Biophys Res Commun *235*, 646-651.

Wilson, S.R., Peters, C., Saftig, P., and Bromme, D. (2009). Cathepsin K activity-dependent regulation of osteoclast actin ring formation and bone resorption. The Journal of biological chemistry *284*, 2584-2592.

Wood, I.S., and Trayhurn, P. (2003). Glucose transporters (GLUT and SGLT): expanded families of sugar transport proteins. Br J Nutr *89*, 3-9.

Xing, L., Zhang, M., and Chen, D. (2010). Smurf control in bone cells. J Cell Biochem *110*, 554-563.

Yadav, V.K., Oury, F., Suda, N., Liu, Z.W., Gao, X.B., Confavreux, C., Klemenhagen, K.C., Tanaka, K.F., Gingrich, J.A., Guo, X.E.*, et al.* (2009). A serotonin-dependent mechanism explains the leptin

regulation of bone mass, appetite, and energy expenditure. Cell *138*, 976-989.

Yamashita, M., Ying, S.X., Zhang, G.M., Li, C., Cheng, S.Y., Deng, C.X., and Zhang, Y.E. (2005). Ubiquitin ligase Smurf1 controls osteoblast activity and bone homeostasis by targeting MEKK2 for degradation. Cell *121*, 101-113.

Yamashita, T., Takahashi, N., and Udagawa, N. (2012). New roles of osteoblasts involved in osteoclast differentiation. World J Orthop *3*, 175-181.

Yang, X., and Karsenty, G. (2002). Transcription factors in bone: developmental and pathological aspects. Trends Mol Med *8*, 340-345.

Zhao, M., Qiao, M., Harris, S.E., Oyajobi, B.O., Mundy, G.R., and Chen, D. (2004). Smurf1 inhibits osteoblast differentiation and bone formation in vitro and in vivo. The Journal of biological chemistry *279*, 12854-12859.

Zhao, M., Qiao, M., Oyajobi, B.O., Mundy, G.R., and Chen, D. (2003). E3 ubiquitin ligase Smurf1 mediates core-binding factor alpha1/Runx2 degradation and plays a specific role in osteoblast differentiation. The Journal of biological chemistry *278*, 27939-27944.

Zoidis, E., Ghirlanda-Keller, C., and Schmid, C. (2011). Stimulation of glucose transport in osteoblastic cells by parathyroid hormone and insulin-like growth factor I. Mol Cell Biochem *348*, 33-42.

CHAPTER II: Glucose uptake and Runx2 synergize to orchestrate osteoblast differentiation and bone formation

Jianwen Wei, Junko Shimazu, Munevver Parla Makinistoglu, Antonio Maurizi, Haihong Zong, Takeshi Takarada, Takashi lezaki, Jae-Hyuck Shim, Laurie H. Glimcher, Jeffrey E. Pessin, Eiichi Hinoi and Gerard Karsenty. *Cell*. 161(7):1576-91 (2015)

Preface

The completion of this work is owed to the contribution of the people represented on the authorship list and with generous help of others listed below. *Smurf1*+/- mice were provided by Dr. Jeffrey Wrana. *Glut1fl/fl* mice were generated by Dr. Munevver Parla Makinistoglu. Dr. Eiichi Hinoi and his group generated and provided *Runx2fl/fl* osteoblasts. Dr. Jeffrey E. Pessin and Dr. Haihong Zong assisted to conduct clamp analysis. Dr. Patricia Ducy critically read this manuscript. Under the mentorship of Dr. Gerard Karsenty, in collaboration with Dr. Jianwen Wei who made an equal contribution to this work, I performed the rest of described work. Specifically, I was responsible for the investigations of temporal and spatial gene expression patterns, embryonic skeletal and adult metabolic analyses, histological analyses of bones from embryos, AMPK phosphorylation and ubiquitination assays, mass spectrometry analysis, luciferase assay, western blot and qPCR analyses and a part of skeletal analysis of STZ treated embryos. Dr. Wei, on the other hand, was responsible for measurements of glucose uptake and adenosine levels, adult metabolic and adult skeletal analyses, analyses of STZ treated embryos, western blot, siRNA and qPCR analysis, analyses of α1(I)collagen synthesis and accumulation, luciferase assay and chromatin immunoprecipitation assay. The manuscript was conceptualized, written and edited by Dr. Karsenty, Dr. Wei and I. This work was supported by NIH grant R01AR045548 (G.K.), Columbia University Mandl Connective Tissue Research Fellowship (J.W.) and Honjo International Scholarship (J.S.). The training program in Genetics and Development (J.S.) is supported by an NIH T32 training grant from the National Institute of General Medical Science.

Glucose uptake and Runx2 synergize to orchestrate osteoblast differentiation and bone formation

Jianwen Wei[1a], Junko Shimazu[1a], Munevver Parla Makinistoglu[1], Antonio Maurizi[1], Haihong Zong[3], Takeshi Takarada[2], Takashi Iezaki[2], Jae-Hyuck Shim[4], Laurie H. Glimcher[5], Jeffrey E. Pessin[3], Eiichi Hinoi[2] and Gerard Karsenty[1]*

[1] Department of Genetics & Development, College of Physicians and Surgeons, Columbia University, New York, NY 10032, USA

[2] Laboratory of Molecular Pharmacology, Faculty of Pharmacy, Institute of Medical, Pharmaceutical and Health Sciences, Kanazawa University, Kanazawa, Ishikawa 920-1192, Japan.

[3] Department of Medicine and Molecular Pharmacology, The Albert Einstein College of Medicine, Bronx, New York, NY 10461, USA

[4] Department of Pathology and Laboratory Medicine, Weill Cornell Medical College, New York, NY 10063, USA

[5] Department of Medicine, Weill Cornell Medical College, New York, NY 10063, USA

[a] These authors have equal contribution to this paper.

Summary

The synthesis of Type I collagen, the main component of the bone matrix, precedes the expression of *Runx2*, the earliest determinant of osteoblast differentiation. We hypothesized that the osteoblasts' energetic needs might explain this apparent paradox. We show here that glucose, the main nutrient of osteoblasts, is transported in these cells through *Glut1* whose expression precedes that of *Runx2.* Glucose uptake favors osteoblast differentiation by suppressing the AMPK-dependent proteasomal degradation of RUNX2 and promotes bone formation by inhibiting another function of AMPK. While RUNX2 cannot induce osteoblast differentiation when glucose uptake is compromised, raising blood glucose levels restores collagen synthesis in *Runx2*-null osteoblasts and initiates bone formation in *Runx2*-deficient embryos. Moreover, RUNX2 favors *Glut1* expression, and this feed-forward regulation between RUNX2 and *Glut1* determines the onset of osteoblast differentiation during development and the extent of bone formation throughout life. These results reveal an unexpected intricacy between bone and glucose metabolism.

Introduction

The transcription factor RUNX2 is a master determinant of osteoblast differentiation (Karsenty et al., 2009; Long, 2012). Its expression in prospective osteoblasts precedes osteoblast differentiation, its inactivation prevents osteoblast differentiation and its haplo-insufficiency causes a skeletal dysplasia called cleidocranial dysplasia (CCD) that is characterized by a delay in osteoblast differentiation leading to hypoplastic clavicles and open fontanelles. Several aspects of RUNX2 biology remain however poorly understood. For example, the nature of the molecular events leading to RUNX2 accumulation in cells of the osteoblast lineage is largely unknown. A second question is to determine if and how RUNX2 contributes to bone formation by differentiated osteoblasts. A peculiar feature of osteoblast biology raises this latter issue.

Type I collagen is by far the most abundant protein of the bone extracellular matrix (ECM) and its synthesis by osteoblasts is often considered a biomarker of bone formation. Type I collagen is a heterotrimeric protein made of two *α*1(I) chains and one *α*2(I)chain that are encoded by two different genes (Vuorio and de Crombrugghe, 1990). In vitro, RUNX2 can bind to and up-regulate the activity of a *α1(I) Collagen* promoter fragment (Kern et al., 2001). In vivo, however, Type I collagen synthesis precedes *Runx2* expression in prospective osteoblasts. Thus, the regulation of Type I collagen synthesis in osteoblasts is not fully understood, and by extension since the bone ECM is mainly made of Type I collagen, it is also unclear how bone formation by osteoblasts is regulated.

Besides being responsible of bone formation, the osteoblast is an endocrine cell that secretes a hormone, osteocalcin that favors glucose homeostasis (Lee et al., 2007). Notwithstanding the

molecular complexity of this emerging regulation, the identification of bone as a regulator of glucose metabolism raises a fundamental question: why would bone have this role? A prerequisite to answering this question is to define the functions of glucose in osteoblasts.

Here we asked if the energetic needs of the osteoblast might explain how osteoblast differentiation and bone formation occurs in vivo. We found that glucose is the main nutrient of osteoblasts and it is transported in these cells in an insulin-independent manner through the facilitative *Glut1* glucose transporter whose expression precedes that of *Runx2* during skeletogenesis. By inhibiting one activity of AMPK, glucose is necessary for RUNX2 accumulation and osteoblast differentiation; through the inhibition of another AMPK function glucose is necessary for collagen synthesis and bone formation. Moreover, by promoting RUNX2 accumulation, glucose uptake in osteoblasts favors *Osteocalcin* expression and whole-body glucose homeostasis. We further show that RUNX2 is not sufficient for timely osteoblast differentiation and proper bone formation if glucose uptake is compromised whereas raising blood glucose levels induces collagen synthesis and bone formation in the absence of *Runx2*. The relationship between RUNX2 and glucose uptake is even more elaborate since RUNX2 is needed for *Glut1* expression in osteoblasts. This crosstalk between RUNX2 and glucose uptake acts as an amplification mechanism allowing osteoblast differentiation and bone formation to be coordinated throughout life. This study provides a bone-centric illustration of the importance of the crosstalk between bone and glucose metabolism.

Materials and Methods

Mice generation

To generate *Glut1fl/+* mice, a targeting vector harboring 2 LoxP sites flanking exon 3-10 of *Glut1* was electroporated into ES cells (CSL3,129/SvEvTac) (Figure S2A). Targeted ES cells were detected by southern blots and injected in 129Sv/EV blastocysts to generate chimeric mice. Chimeric mice were crossed with Gt(ROSA)26Sor$^{tm1(FLP1)Dym}$ mice to remove the *Neomycin* resistance cassette and to generate *Glut1fl/+* mice. *Glut1fl/+* mice were then crossed with *Dermo1-Cre(Yu et al., 2003), Osterix-Cre* (Rodda and McMahon, 2006*) or Ocn-Cre* mice (Zhang et al., 2002) to generate *Glut1*$_{osb}$*+/-* mice, whose progenies were intercrossed to obtain *Glut1*$_{dermo1}$*−/−, Glut1*$_{osx}$*−/−* and *Glut1*$_{ocn}$*−/−* mice, respectively. To generate *α1(I)Col-Glut1* transgenic mice, a cDNA fragment of the mouse *Glut1* was cloned into a plasmid containing a 2.3-kb *α1(I)* collagen promoter and microinjected using standard protocol. *Ampka1fl/fl* mice were obtained from The Jackson Laboratory (Nakada et al., 2010). *Runx2fl/fl* mice were generated as previously described (Takarada et al., 2013). *Shn3+/-* and *Smurf1+/-* mice were generous gifts of Dr. L. Glimcher (Weill Cornell Medical College) and Dr. J. Wrana (U of Toronto, Canada) respectively (Jones et al., 2006; Narimatsu et al., 2009). Except for *α1(I)Col-Glut1* mice, which had been backcrossed to C57 background 5 times, all other mice analyzed were maintained on a C57/129 mixed background. Control littermates were analyzed in all experiments. All procedures involving animals were approved by CUMC IACUC and conform to the relevant regulatory standards.

Cell culture

Mouse calvaria osteoblasts were isolated and cultured as described previously (Ducy and Karsenty, 1995). Osteoclast precursors (monocytes) were isolated by culturing bone marrow cells with αMEM/10% FBS containing M-CSF (10 ng/mL) for 6 days and then treated with RANKL (30 ng/mL) and M-CSF (10 ng/mL) for 7 days. C2C12 myoblasts (ATCC), mHippoE-14 embryonic mouse hippocampal hypothalamic cell Line (Cellutions biosystems) and COS-7 cells were cultured in DMEM/10% FBS. *Glut1-/-, Raptor-/-*, *Runx2-/-, Glut1-/-;Ampka1+/-, Glut1-/-;Ampka1-/-, Ampka1+/-* and *Ampka1-/-* calvaria osteoblasts were generated by infecting *Glut1fl/fl*, *Raptorfl/fl, Runx2fl/fl, Glut1fl/fl;Ampka1fl/+, Glut1fl/fl;Ampka1fl/fl, Ampka1fl/+ or Ampka1fl/fl* osteoblasts with either empty vector or *Cre*-expressing adenovirus (1:800 MOI) (University of Iowa). SiRNAs against *Tsc1* and *Tsc2* (Dharmacon) were transfected to primary osteoblasts according to manufacturer's protocol.

Oxygen consumption rate measurements

Cells were seeded in XF96 plates at 20,000 cells/well. The next day, the cells were incubated with 1X KHB buffer (111mM NaCl, 4.7mM KCl, 2mM MgSO4 and 1.2mM Na2HPO4) supplemented with vehicle, 10 mM glucose, 2mM Glutamine or 100μM palmitate and further incubated in CO_2-free incubator at 37°C for 2 hour. Oxygen consumption rate was then analyzed using XF24 Extracellular Flux Analyzer (Seahorse^{TM} bioscience) and normalized to DNA concentrations.

Euglycemic clamps

Euglycemic clamps were conducted in conscious mice following a 12hrs fasting with a continuous

infusion of isotonic saline or human insulin (2.5 mU/kg/min) and a variable infusion of 25% glucose to maintain glucose at 150 mg/dl. To assess tissue-specific glucose uptake, 2-deoxy-*d*-[1-^{14}C]glucose (PerkinElmer Life Sciences) was administered as a bolus (30 μCi, 287mCi/mmol) 75 minutes after the start of the clamp (Zong et al., 2009). In details, at 4~5 days before clamping experiments, mice will be implanted with catheters into the jugular vein and carotid artery using aseptic technique. Following overnight fast (14-hour), D-[3-^{3}H]glucose (0.05 μCi/min) will be infused using microdialysis pumps through the intravenous catheter in the animal for 2 hours to assess basal rate of whole-body glucose turnover. A blood sample (60 μl) will be collected at the end for the measurement of plasma glucose, insulin, and [^{3}H]glucose concentrations (basal parameters). For each blood sample taken, an equal volume of mouse blood will be infused to prevent stress from volume depletion. Following the basal period, a 2-hr euglycemic clamp will be conducted with continuous infusion of either 1xPBS (basal condition without insulin) or human insulin at a rate of 4mU/kg/min (Hyperinsulinemic condition). Blood samples (20 μl) will be collected at 10~20 min intervals for the immediate measurement of plasma glucose (20, 40, 60, 80, 90, 100, 110 and 120 min of clamps). A 20% glucose solution will be infused at variable rates to maintain basal glucose levels (~5 mM). Insulin-stimulated whole-body glucose metabolism will be estimated with a continuous infusion of [^{3}H]glucose throughout the clamps (0.1 μCi/min). To estimate glucose uptake in individual organs, 2-[1-^{14}C]deoxy-D-glucose (2-[^{14}C]DG) will be administered as a bolus (30 μCi/ 287mCi/mmol) at 75 min after the start of clamp. Blood samples (20 μl) will be taken at 80, 85, 90, 100, 110, and 120 min of clamp for the measurement of plasma

[^{3}H]glucose, $^{3}H_2O$, and 2-[^{14}C]DG concentrations. Additional blood samples (50 µl) will be taken at 120 min to measure plasma insulin concentrations (clamp parameters). At the end of clamp, mice will be anesthetized and tissue samples (gastrocnemius, tibialis anterior, and quadriceps from both hindlimbs, epididymal white adipose tissue, liver, tibia and femurs of both legs) isolated for measuring 2-[^{14}C]DG content and molecular analysis.

Glucose consumption and uptake assay

For glucose consumption measurements, following 16-hr incubation with osteoblasts, glucose concentration in the culture medium was assayed with Glucose Assay Kit (Biovision). Glucose uptake was determined by the uptake rate of 2-[U-^{14}C] deoxyglucose (2-DG) in cells. Following 1hr fast in glucose free KRH buffer (50mM HEPES pH7.4, 136mM NaCl, 4.7mM KCl, 1.25mM MgSO4, 1.25mM CaCl2 and 0.1% BSA), cells were cultured in KRH buffer containing 100µM 2-deoxyglucose and 0.5µCi/ml 2-^{14}C-DG (287mCi/mmol, Perkin Elmer, NEC495A) for 1hr. For glucose uptake in bones, 10µCi of 2-^{14}C-DG were IP injected in mice at random feed state for 1h calvariae were then collected for analysis. The amount of 2-^{14}C-DG in total cell or bone lyses was quantified by liquid scintillation counter (WALLAC 1409) and normalized to protein content (Bio-Rad).

Molecular biology and biochemistry

For quantifying gene expression, RNA samples were extracted using TRIZOL reagent (Invitrogen).

One to 2 μg of total RNA was converted into cDNA using M-MLV reverse transcriptase (Invitrogen). QPCR analyses were performed using CFX-Connect realtime PCR system (Bio-Rad). Relative expression levels of each gene were normalized to the levels of 18S ribosomal RNA or *β-actin*. Western blot analyses were carried out using standard protocol. All antibodies were obtained from Cell Signaling Technology, except the anti-GLUT1 (EMD Millipore), anti-COL1A1, anti-RUNX2, anti-SMURF1 (Santa Cruz), anti-Phospho-Ser148 SMURF1 (Genescript) and anti-β-ACTIN (Sigma). Quantification of Western blots was performed using Image J. Protein levels were quantified and normalized to ACTIN or GADPH levels. Relative protein levels were calculated with respect to control samples. All western blot experiments were repeated at least three times, with different samples.

Glycogen assay

After cultured in differentiation medium for 14 days, osteoblasts were homogenized in dH_2O and incubated in boiling water for 5 mins to inactive enzymes. Fifty microliter of lyses was used for glycogen assay (BioVision Inc,) according to manufacturer's protocol. Glycogen content was then normalized to protein concentration.

Skeleton preparation, Bone histology and in situ hybridization

Skeleton preparations and Alcian blue/alizarin red staining were carried out according to standard protocols (McLeod, 1980). Bone histology analyses including Von Kossa staining and alcian blue

staining were performed with histological sections of femurs or clavicle bones using standard protocols. For all skeletal analyses, at least 3 litters for each embryonic stage and at least 5 embryos for each genotype were examined. Bone histomorphometry analyses were performed on L3 and L4 vertebrae as described previously (Chappard et al., 1987; Parfitt et al., 1987b). Von Kossa/van Gieson Staining, toluidine blue staining and calcein double-labeling were performed to measure mineralized bone volume over the total tissue volume (BV/TV), osteoblast number per tissue area, (N.Ob/T.Ar), mineralization apposition rate (MAR) and bone formation rate per bone surface (BFR/BS). For in situ hybridization, tissues were fixed in 4% paraformaldehyde/PBS overnight at 4°C and then after serial of dehydrations embedded in paraffin and sectioned at 5μm. In situ hybridization was performed using ^{35}S-labeled riboprobe as described (Ducy et al., 1997). The *Runx1*, *Runx3*, *Runx2, α1(I)Col, α1(II)Col, α1(X)Col, Osteocalcin* and *Bsp* probes have been previously described (Takeda et al., 2001b).

The *Glut1* probe is a 500-bp fragment of the *Glut1* 3′ untranslated region (its sequence is described below). Hybridizations were performed overnight at 55°C, and washes were performed at 63°C.

Sequence of *Glut1* probe for in situ hybridization

CTGGACCTATGGCCAAGGACACACTAATACCGAACTCTGAGCTAGGAGGCTTTACCGCTGGAGG

CGGTAGCTGCCACCCACTTCCGCAGGCCTGGACCTCGGCACCATAGGGGTCCGGACTCCATTTT

AGGATTCGCCCATTCCTGTCTCTTCCTACCCAACCACTCAATTAATCTTTCCTTGCCTGAGACCAG

TTGGAAGCACTGGAGTGCAGGGAGGAGAGGGAAGGGCCAGGCTGGGCTGCCAGGTTCTAGTCT

CCTGTGCACTGAGGGCCACACAAACACCATGAGAAGGACCTCGGAGGCTGAGAACTTAACTGCT

GAAGACACGGACACTCCTGCCCTGCTGTGTATAGATGGAAGATATTTATATATTTTTTGGTTGTCAA

TATTAAATACAGACACTAAGTTATAGTATATCTGGACAAACCCACTTGTAAATACACCAACAAACTCC

TGTAACTTTACCTAAGCAGATATAAATGGCTGG

µCT analysis

Trabecular and cortical bone architecture of proximal femur was assessed using a µCT system (VivaCT 40; SCANCO Medical AG). Trabecular bone volume, number of trabeculae, cortical bone midshaft thickness and mineralization density were analyzed using the standard software provided by the manufacturer of the µCT scanner.

Metabolic tests

All experimental mice were performed on 3-month old male mice fed a regular diet (PicoLab Rodent Diet 20 #5053). Glucose stimulated insulin secretion test (GSIS), glucose tolerance test (GTT) and insulin tolerance test (ITT) were performed as described previously (Lee et al., 2007).

Serum biochemistry

ELISAs were used to measure mouse insulin (Ultra Sensitive Mouse Insulin ELISA, Crystalchem), mouse PINP (Rat/mouse PINP EIA, IDS) and total and undercarboxylated forms of mouse osteocalcin

(Ferron et al., 2010m). Both osteocalcin and PINP were measured at random fed state in all mice analyzed.

BrdU incorporation assay

BrdU saline solution was IP injected in P14 mice at dose of 100μg/g 16hrs before sacrifice. Calvaria bones were dissected and fixed in 4%PFA overnight at 4°C, decalcified in 14% EDTA for 3 days, soaked in 30% sucrose in PBS for 1 day, embedded in O.C.T. compound (Tissue-Tek) and sectioned at 5μm. BrdU incorporation was detected by using BrdU detection Kit (Roche). Immunohistofluorescence staining using anti-RUNX2 (Santa Cruz Biotech) was performed with standard protocol in the same section to label osteoblasts. Proliferating osteoblasts were identified as both BrdU and RUNX2 positive cells and quantified using Image J software.

Measurement of adenosine levels

Osteoblasts were homogenized and incubated immediately in 10 volumes boiled Tris-Acetate buffer (0.1M Tris, 2mM EDTA pH7.8) for 90 seconds to extract adenosine. Levels of ATP, ATP+ADP and ADP+AMP were measured in the total cell lyses using a luciferase-based assay (AMP-Glo™ Assay, Promega). Cellular contents of ATP, ADP and AMP were calculated accordingly and normalized to protein content.

mTOR kinase assay

Glut1fl/fl and *Glut1-/-* Osteoblasts were incubated in differentiation medium for 7 days. Five hundred micrograms of total protein lyses were used for immunoprecipitation assay according to a standard protocol (Cell Signaling Technology, Inc.). Activity of mTORC1 complex was assessed by immunoprecipitation of mTOR using anti-mTOR antibody (Emdmillipore), followed by kinase assay using K-LISA™ mTOR Activity Kit (Emdmillipore).

Measurement of collagen synthesis rate

Collagen synthesis rate was determined by ^{3}H-proline incorporation assay as described previously (Webster and Harvey, 1979). Briefly, osteoblasts were cultured in medium containing 2μCi of ^{3}H-labeled-proline (PerkinElmer) for 24hrs. Collagens were extracted by pepsin/acetic acid solution followed by salt precipitation. Incorporation of ^{3}H-proline (Perkin Elmer, NET483001MC) in collagen molecules was measured by liquid scintillation counter (WALLAC 1409) and normalized to DNA content (DNA quantitation kit, Sigma).

Detection of ubiquitination

Osteoblasts were incubated in medium containing 25nM bortezomib for 16 hrs. Five hundred micrograms of total protein lyses were used for immunoprecipitation assay according to a standard protocol (Cell Signaling Technology, Inc.). Ubiquitination of RUNX2 was assessed by

immunoprecipitation of the RUNX2 using anti-RUNX2 antibody (Santa Cruz), followed by immunoblotting using anti-Ubiquitin antibody (Cell Signaling Technology, Inc.).

In vitro AMPK phosphorylation assay

GST-SMURF1 and GST-RUNX2 constructs were generated by subcloning mouse *Smurf1* and *Runx2* cDNAs into pGEX4T3. GST-Smurf1 S148A construct was then generated by mutating serine 148 (TCA) to alanine (**G**CA) using standard site directed PCR mutagenesis protocol. GST-SMURF1, GST-SMURF1 S148A and GST-RUNX2 were expressed in Rosetta 2 (DE3)pLysS (Novagen) and purified as previously described (Ferron et al., 2010a). To assess AMPK phosphorylation of SMURF1, 10μg of purified GST-SMURF1 was incubated with 10ng AMPK (A1/B1/G1) (Promega) for 30min at 30˚C in kinase assay buffer containing 5mM MOPS, pH7.2, 2.5mM glycerol 2-phospate, 5mM $MgCl_2$, 1mM EGTA, 0.4mM EDTA, 0.05mM DTT, 50μM ATP, 5μCi [γ^{32} P] ATP and 0.1mM AMP. The reaction was stopped by the addition of Laemmli buffer, and proteins were resolved on SDS-PAGE gel. Phosphorylation of SMURF1 was detected by exposing the gel to a radiographic film. In the phosphorylation reactions used for mass spectrometry analysis, nonradioactive ATP was used.

LC-MS/MS

A coomassie-stained band corresponding to SMURF1 phosphorylated by AMPK was excised from a SDS-polyacrylamide gel, and subjected to LC-MS/MS at W. M. Keck Foundation Biotechnology Resource Laboratory, Mass Spectrometry & Proteomics Resource (Yale University, school of medicine).

In vitro ubiquitination assay.

In vitro ubiquitination of RUNX2 by Smuf1 was assessed as previously described (Lu et al., 2008) using 10μg of purified GST-RUNX2 and 0.7μg of GST-SMURF1 WT or GST-SMURF1 S148A. Phosphorylated form of GST-SMURF1 was obtained by conducting AMPK phosphorylation assay described above. Samples were incubated with 0.7μg of E1, 1μg of UbcH5c (E2), 15μg of ubiquitin (Boston Biochem) in ubiquitination assay buffer (50mM Tris-HCl pH 8.0, 50mM NaCl, 1mM dithiothreitol, 5mM $MgCl_2$, 3mM ATP) for 15min at 30˚C and the reaction was terminated by the addition of Laemmli buffer before Western blotting with an anti-Ubiquitin antibody.

Streptozotocin treatment

Streptozotocin (Sigma) solution (5, 10 or 15mg/ml) was freshly prepared in 50mM citrate buffer (pH4.5). At E0.5, pregnant female mice following 6-hour fast received one IP injection of STZ at a dose of 50, 100 or 150mg/kg. Random feed glucose levels were monitored multiple time points during pregnancy and at the time of sacrifice to confirm development of hyperglycemia. Serum insulin levels of the pregnant females were measured at E18.5.

Immunohisochemistry

Immunohisochemistry of paraffin sections of bones of E18.5 embryos was carried out using rabbit

anti-type I Collagen (Rockland Immunochemicals Inc.), anti-type X Collagen (Thermo Fisher Scientific Inc.) and HRP-goat anti-Rabbit IgG Tyramide Signal Amplification kit (Life technologies) according to manufacture's protocol. Briefly, following deparaffinization and rehydration, 5μm paraffin sections of bones were subjected to Pepsin digestion (4mg/ml) at 37°C for 10 min and then incubated with a 1:200 dilution of primary antibody overnight at 4°C. The next day, following three times washing with 1XPBS, sections were incubated with a 1:100 dilution of anti- Rabbit-HRP conjugate secondary antibody for 1 hour at RT. Next, sections were rinsed three times with 1XPBS and then incubated with 100μL Alexa Fluor® 568 dye tyramide solution for 10 minutes at RT. After rinsed three times with 1XPBS, sections were mounted Fluoro-Gel with DAPI to counterstain nuclei (Electron Microscopy Sciences).

Chromatin Immunoprecipitation

Chromatin immunoprecipitation (ChIP) was performed on lysates from primary osteoblasts with the ChIP Assay Kit (Millipore, #17-295) and a ChIP grade anti-RUNX2 antibody (Santa Cruz Biotech). Binding of RUNX2 to the -811bp *Glut1* promoter region was detected by PCR using following primers: forward: 5' ACCTAGATGGGACATGGACTG 3' and reverse: 5' ATCAAACCCTGGGCTATGAGAA 3'. Negative control is a region that is at -4286bp of the *Glut1* promoter (forward: 5' GGTTTTGGTGGCTTGAGGTA 3' and reverse: 5' TGTCTAATGCATATTGGACTTCTGT 3').

DNA transfection and luciferase assay

Mouse *Glut1* promoter 1kb fragment was amplified by PCR, sequenced and subcloned upstream of the *Luciferase* gene in the pGL3 Luciferase vector (Promega). Conserved RUNX2 recognition site at -811bp “ACCACA” was mutated to “AGAACA” using standard site directed PCR mutagenesis protocol. *pcDNA-Runx2* and *pcDNA-Runx1* were generated previously (Ducy and Karsenty, 1995; Jiang et al., 2005). These plasmids were then co-transfected into COS-7 cells along with pCMV β-gal control plasmid using Lipofectamin 2000 according to manufacturer’s protocol (Invitrogen). Twenty-four hours post-transfection, luciferase activity was measured and normalized to beta-galactosidase levels as described previously (Ducy and Karsenty, 1995). Relative Luciferase activity was calculated with respect to cells transfected with pcDNA3.0 vector.

Statistics

All data are presented as mean ± standard error of mean. Statistical analyses were performed using unpaired, two-tailed Student’s *t* test for comparison between two groups, ANOVA test for experiments involving more than two groups. For all experiments, * denotes $P \leq 0.05$, # denotes $P \leq 0.001$ compared to control.

Results

Insulin-independent glucose uptake in osteoblasts

To determine what is/are the main nutrient(s) used by osteoblasts we measured their oxygen consumption rate (OCR) when incubated with individual nutrients. Like neurons and unlike myoblasts, osteoblasts had the highest OCR when cultured in the presence of glucose and the lowest when cultured in the presence of a representative fatty acid (Figure 1A). These results prompted us to measure through euglycemic hyperinsulinemic clamps the amount of glucose taken up by bone and the mechanism whereby it occurs in 3 month-old wild-type (WT) mice.

In the conditions of this assay bone takes up a fifth of the quantity of glucose taken up by skeletal muscle, the organ taking up the majority of glucose in the mouse (Ferrannini et al., 1988), and half of what is taken up by white adipose tissue (WAT) (Figure 1B). Unlike what is the case for skeletal muscle and WAT, glucose uptake in bone is not enhanced by insulin (Figure 1B). We also compared the uptake of 2-[U-^{14}C] deoxyglucose (2-DG) in osteoblasts and osteoclasts, to the one in myoblasts. Both bone cell types take up approximately a third of the quantity of 2-DG taken up by myoblasts and do so in an insulin-independent manner (Figure 1C). Consistent with these observations, *Glut1* that transports glucose in an insulin-independent manner, is expressed two orders of magnitude higher than any other class I glucose transporters in bone cells (Figure 1D). The rest of this study focuses on the functions of glucose in osteoblasts.–

To establish the biological importance of *Glut1* expression in these cells, we analyzed osteoblasts lacking or over-expressing modestly (1.75 fold) *Glut1* (Figure S1A-B). To do so, *Glut1fl/fl* osteoblasts

were infected with adenovirus expressing either empty vector (GFP) or the *Cre* recombinase to generate control or *Glut1* deficient osteoblasts. *Glut1-/-* osteoblasts took up 75% less and *α1(I)Col-Glut1* osteoblasts 20% more 2-DG than control osteoblasts (Figure 1E). Consequently, glycogen content was decreased 50% in *Glut1-/-* and increased 40% in *α1(I)Col-Glut1* osteoblasts compared to control ones (Figure S1C). Thus GLUT1 is responsible for the majority of glucose uptake in osteoblasts.

Glucose uptake is necessary for osteoblast differentiation during development

Next we analyzed *Glut1's* spatial and temporal pattern of expression during skeletogenesis by in situ hybridization and compared it to that of *α1(I) collagen* and *Runx2*, two marker genes of mesenchymal cells and osteoblasts; of *α1(II) Collagen,* a marker of non–hypertrophic chondrocytes; and of *α1(X) collagen* a marker of hypertrophic chondrocytes.

At E10.5 *Glut1* is highly expressed in *α1(I) Collagen*-expressing mesenchymal cells of the developing hindlimbs (Figure 1F panels a-j). *Runx2* begins to be expressed in *α1(I) Collagen/Glut1*-expressing cells at E12.5 and remains expressed in these cells throughout development (Figure1F, panels k-o). Prior to E12.5 another *Runx* gene, *Runx1*, is expressed in *α1(I) Collagen/Glut1*-expressing cells (Figure1F, panels p-t). The third *Runx* gene, *Runx3* is not expressed before E13.5 and its expression is predominant in *α1(II) Collagen*-expressing chondrocytes (Figure1F, panels u-y, z-b1). *Glut1* is virtually not expressed in chondrocytes (Figure 1F, panels a-e and z-e1). In view of this pattern of expression, we analyzed the function of *Glut1* during osteoblast differentiation by crossing mice harboring a floxed

allele of *Glut1* (Figure S2A) with mice expressing the *Cre* recombinase under the control of *Dermo1* (Yu et al., 2003) (*Glut1*$_{dermo1}$-/-) that delete genes starting at E12.5, or of *Osterix* regulatory elements (Rodda and McMahon, 2006) (*Glut1*$_{osx}$-/-) that delete genes starting at E14.5. We verified in each case that *Glut1* was efficiently deleted in the targeted cells but not in other cell types or tissues and that expression of other *Gluts* was not affected by the *Glut1* deletion (Figure S2B-E).

Using alcian blue/alizarin red staining of skeletal preparations to distinguish non-mineralized (blue) from mineralized ECM (red), *Glut1*$_{dermo1}$-/- and control embryos were indistinguishable until E13.5 (Figure S2F). E14.0 was the first time point when a delay in ECM mineralization in long bones and the jaws was seen in *Glut1*$_{dermo1}$-/- embryos (Figure 2A). This difference in ECM mineralization between control and *Glut1*$_{dermo1}$-/- embryos was verified histologically (Figure 2B). At E14.5 ECM mineralization was still absent in the mandibles of *Glut1*$_{dermo1}$-/- embryos (Figure 2A). Beyond E14.5 we also studied *Glut1*$_{osx}$-/- embryos. At E15.5 large area of mineralized ECM were present in the axial skeleton of controls but not of *Glut1*$_{osx}$-/- and *Glut1*$_{dermo1}$-/- embryos except in long bones (Figure 2C, S2F). Von Kossa staining of histological sections detected extensive ECM mineralization in skeletal elements of control embryos, while this mineralization was more restricted in *Glut1*$_{osx}$-/- embryos; alcian blue staining of these sections showed that the ECM in *Glut1*$_{osx}$-/- skeletal elements was mostly of cartilaginous nature (Figure 2D). Consistent with this observation, *α1(X) Collagen*-expressing hypertrophic chondrocytes covered a larger area in *Glut1*$_{osx}$-/- than in control skeletal elements and expression of *Osteocalcin*, was undetectable in *Glut1*$_{osx}$-/- skeletal elements (Figure 2E) indicating that

osteoblast differentiation was delayed in E15.5 *Glut1$_{osx}$-/-* embryos. Remarkably, despite these delays in osteoblast differentiation and bone formation, *Runx2* and *α1(I) Collagen* were normally expressed in E15.5 *Glut1$_{osx}$-/-* skeletal elements (Figure 2E).

At E18.5, the skull of *Glut1$_{osx}$-/-* embryos that ossifies mostly through an intramembranous process was poorly mineralized suggesting that osteoblast differentiation was delayed (Figure 2F). Von Kossa staining of histological sections showed numerous, long, and thick trabeculae in controls but not in *Glut1$_{osx}$-/-* long bones and an alcian blue staining showed many more cartilaginous remnants in *Glut1$_{osx}$-/-* than in control skeletal elements (Figure 2G). Accordingly, the area occupied by *α1(X) Collagen*-expressing hypertrophic chondrocytes remained larger in *Glut1$_{osx}$-/-* than in control skeletal elements and expression of *Osteocalcin* was still barely detectable (Figure 2H-J). This incomplete osteoblast differentiation in *Glut1$_{osx}$-/-* bones and osteoblasts was further illustrated by the decreased expression of *Bsp* (Figure 2I-J). This delay in osteoblast differentiation explains why E18.5 *Glut1$_{osx}$-/-* embryos had open fontanelles and hypoplastic clavicles (Figure 2F). Even though these two features are characteristic of CCD, a disease caused by a decrease in the function of RUNX2 (Lee et al., 1997a; Mundlos et al., 1997a), *Runx2* expression was normal in E18.5 *Glut1$_{osx}$-/-* bones. The same was true for *α1(I) Collagen* expression (Figure 2H-J).

Accounting for this delay in osteoblast differentiation and CCD phenotype, there was a 70% decrease in RUNX2 accumulation in E18.5 *Glut1$_{osx}$-/-* bones and *Glut1-/-* osteoblasts that were generated by infecting *Glut1fl/fl* osteoblasts with adenovirus expressing *Cre* recombinase (Figure 2K). This decrease

in RUNX2 accumulation was not observed for other transcription factors (Figure S2G). There was also a 70% decrease in Type I collagen accumulation in E18.5 *Glut1-/-* bones and osteoblasts because of a 60% decrease in the rate of collagen synthesis in *Glut1-/-* compared to control osteoblasts (Figure 2K-L). This latter finding explained the decreased bone formation in $Glut1_{osx}$-/- embryos. Of note, *Chrebp*, a transcriptional mediator of glucose signaling in other cell types (Yamashita et al., 2001), is not expressed and does not regulate glucose uptake in osteoblasts (Figure S2H-K).

Glucose uptake in osteoblasts is necessary for bone formation and whole-body glucose homeostasis post-natally

To study *Glut1* functions in osteoblasts post-natally, we crossed *Glut1fl/fl* mice with *Osteocalcin-Cre* mice ($Glut1_{ocn}$-/-) that do not initiate gene deletion before E18.5 (Zhang et al., 2002) and performed an inducible deletion of *Glut1* in osteoblasts in 6 week-old *Osx-Cre;Glut1fl/fl* mice ($Glut1_{Dox}$-/-). After verifying the specificity and efficiency of the gene deletions (Figure S3A-B), we examined both models of *Glut1-/-* mice at 3 months of age and included in this analysis *α1(I)Col-Glut1* mice that overexpress modestly (1.75-fold) *Glut1* in osteoblasts (Figure S2D).

$Glut1_{ocn}$-/- and $Glut1_{Dox}$-/- mice of either sex presented with a low bone mass in all bones analyzed whereas *α1(I)Col-Glut1* mice displayed a high bone mass. In these mouse models, only parameters of bone formation i.e., circulating levels of PINP, mineral apposition rate, bone formation rate and osteoblasts number were affected (Figure 3A-C, S3C-E). Expression of the cell cycle regulators *Ccnd2*, *Ccne1* and *Cdk4,* and osteoblast proliferation as measured by BrdU incorporation were decreased in

Glut1$_{ocn}$-/- and increased in *α1(I)Col-Glut1* bones (Figure 3D-E). Again the accumulation not the expression, of RUNX2 and Type I collagen was decreased in *Glut1$_{ocn}$-/-* and increased in *α1(I)Col-Glut1* bones (Figure 3F-G).

Following the fluctuation of RUNX2 accumulation, expression of *Osteocalcin,* a RUNX2 target gene*,* and circulating osteocalcin levels were low in *Glut1$_{ocn}$-/-* mice and high in *α1(I)Col-Glut1* compared to control mice (Figure 3F, S3F). As a result, insulin secretion after glucose stimulation, glucose tolerance measured by a glucose tolerance test, insulin sensitivity assessed by an insulin tolerance test and the steady-state glucose infusion rate during euglycemic-hyerpinsulinemic clamp, were suppressed in *Glut1$_{ocn}$-/-* mice and improved in *α1(I)Col-Glut1* compared to control mice (Figure 3H-N). In summary, glucose uptake in cells of the osteoblast lineage is necessary for osteoblast differentiation, bone formation, and whole-body glucose homeostasis.

Glucose uptake favors osteoblast differentiation and bone formation by inhibiting AMPK

To determine if the delay in osteoblast differentiation and the decrease in bone formation seen in *Glut1$_{osx}$-/-* embryos and mice were due to a decrease in protein synthesis that a poor glucose uptake triggers (Jeyapalan et al., 2007; Mayer et al., 2011), we measured AMP, ADP and ATP contents in *Glut1-/-* osteoblasts that were generated by infecting *Glut1fl/fl* osteoblasts with adenovirus expressing *Cre* recombinase.

Although AMP and ATP levels were not affected, there was a 3-fold increase in ADP content leading to a 3-fold increase in the ratio of ADP over ATP in *Glut1-/-* versus control osteoblasts that were

generated by infecting *Glut1fl/fl* osteoblasts with empty vector (Figure 4A, S4A). As a result, AMPK activity assessed by the phosphorylation of its *α* subunit at Thr172 and of its substrate ACC1 at Ser79 (Wilson et al., 1996; Woods et al., 1994) was increased (Figure 4B). Several lines of evidence indicated that the activity of the mTORC1 complex was decreased in *Glut1-/-* osteoblasts. Phosphorylation of the mTORC1 substrates p70S6K at Thr389, 4E-BP1 at Thr37 and eIF4G at Ser1108, was decreased (Bolster et al., 2002; Reiter et al., 2005) (Figure 4C), Raptor phosphorylation at Ser792 was increased and mTORC1 kinase activity was decreased in *Glut1-/-* osteoblasts (Figure 4B, D). Conversely, p70S6K phosphorylation and collagen accumulation were both decreased in *Raptor-/-* osteoblasts and knockdown of *Tsc1* and *Tsc2* not only restored mTORC1 activity as measured by p70S6K phosphorylation but also normalized collagen accumulation in *Glut1-/-* osteoblasts (Figure 4E, F).

To demonstrate that the decrease in mTORC1 activity and the phenotypes of the $Glut1_{osx}$*-/-* mice are caused by an increase in AMPK activity in osteoblasts we decreased the expression of *Ampk* in osteoblasts by generating *Glut1-/-* embryos or mice lacking in osteoblasts one allele of *Ampkα1*, the most highly expressed AMPK *α* subunit in these cells (Figure 4G). Phosphorylation of AMPK*α1* and p70S6K, ATP contents, RUNX2 and Type I collagen accumulations were similar in $Glut1_{osx}$*-/-;*$Ampka1_{osx}$*+/-* and control osteoblasts indicating that AMPK activity and therefore mTORC1 signaling had been restored in $Glut1_{osx}$*-/-;*$Ampka1_{osx}$*+/-* osteoblasts (Figure 4H, S4B-C). As a result, alcian blue/alizarin red staining of skeletal preparations, histological and in situ hybridization analyses

showed normal osteoblast differentiation and no evidence of CCD in *Glut1$_{osx}$-/-;Ampka1$_{osx}$+/-* embryos (Figure 4I-L). Bone formation parameters were also normal in *Glut1$_{ocn}$-/-;Ampka1$_{ocn}$+/-* mice (Figure 4M).

Two experiments showed that increasing AMPK activity in osteoblasts is deleterious for bone. Treating mouse osteoblasts with AICAR, an AMPK agonist, profoundly decreased Type I collagen and RUNX2 accumulations in these cells and, WT mice treated with AICAR from 6 to 14 weeks of age showed a significant decrease in bone formation parameters and bone mass (Figure 4N-O). Accordingly and as it is the case for *Glut1-/-* osteoblasts, WT osteoblasts deprived of glucose had higher levels of P-AMPK and lower levels of P-P70S6K and type I collagen than if cultured in the presence of glucose (Figure S4D).

Runx2 cannot induce osteoblast differentiation when glucose uptake is hampered

In the course of these experiments, we noticed that RUNX2 ubiquitination was increased in *Glut1-/-* osteoblasts generated by infecting *Glut1fl/fl* osteoblasts with adenovirus expressing *Cre* compared with control osteoblasts generated by infecting with adenoviral empty vector. RUNX2 accumulation was restored when *Glut1-/-* osteoblasts were treated with an inhibitor of proteasome degradation (Figure 5A). To add credence to this observation we analyzed *Glut1-/-;Ampka1+/-* and *Glut1-/-;Ampka1-/-* osteoblasts generated by infecting *Glut1fl/fl;Ampka1fl/+* and *Glut1fl/fl;Ampka1fl/fl,* osteoblasts with either empty vector or *Cre*-expressing adenovirus, respectively. RUNX2 ubiquitination is normal in *Glut1-/-;Ampka1+/-* and *Glut1-/-;Ampka1-/-* osteoblasts (Figure 5B) implicated AMPK in

RUNX2 polyubiquitination. Mass spectrometry and bioinformatics analyses identified a possible AMPK recognition site in SMURF1, an E3 ubiquitin ligase involved in RUNX2 degradation (Zhao et al., 2003) (Figure S5A-B). In vitro, AMPK phosphorylated SMURF1 at Ser148 and this phosphorylation event was needed for SMURF1-induced RUNX2 ubiquitination (Figure 5C-D). SMURF1 phosphorylation at Ser148 did not increase in *Ampka1-/-* osteoblasts and RUNX2 accumulation did not decrease in *Ampka1-/-* or *Smurf1-/-* osteoblasts cultured in the absence of glucose as it did in WT osteoblasts (Figure 5E-F). Moreover, an anti-phospho-SMURF1 antibody demonstrated AMPKα1 interaction with phospho-SMURF1 in *Glut1-/-* osteoblasts and that SMURF1 phosphorylation at S148 was higher in *Glut1-/-* than in control, *Glut1-/-;Ampka1+/-* and *Glut1-/-;Ampka1-/-* osteoblasts (Figure 5G-H). These results indicate that AMPK favors RUNX2 proteasomal degradation by phosphorylating SMURF1.

This unanticipated regulation of RUNX2 ubiquitination by AMPK allowed assessing selectively the ability of RUNX2 to induce osteoblast differentiation when glucose uptake is compromised. This was achieved by generating *Glut1$_{osx}$-/-* embryos and *Glut1$_{ocn}$-/-* mice lacking one allele of *Smurf1*. This manipulation normalized RUNX2 accumulation but did not restore mTORC1 signaling since p70S6K phosphorylation and Type I collagen synthesis remained low in *Glut1$_{osx}$-/-;Smurf1+/-* osteoblasts (Figure 5I-J). As a result and despite a normal accumulation of RUNX2, skeletal development was equally delayed in *Glut1$_{osx}$-/-;Smurf1+/-* and *Glut1$_{osx}$-/-* embryos at E15.5 and E18.5 (Figure 5K-L). The cartilaginous area and the zone of *α1(X)Col*-expressing cells were as enlarged in *Glut1$_{osx}$-/-;Smurf1+/-* as in *Glut1$_{osx}$-/-* embryos (Figure 5M-N). Hence, RUNX2 cannot induce proper osteoblast

differentiation during embryogenesis if glucose uptake is hampered because protein synthesis is decreased (Figure 5O). Likewise, *Glut1$_{ocn}$-/-;Smurf1+/-* mice were as osteopenic as *Glut1$_{ocn}$-/-* mice (Figure S5C).

Glucose can initiate bone formation in *Runx2*-deficient embryos

We next asked if conversely, raising the extracellular concentration of glucose was sufficient to initiate Type I collagen synthesis in *Runx2*-deficient osteoblasts. To that end *Runx2fl/fl* osteoblasts (Takarada et al., 2013) were infected with a *Cre*-expressing adenovirus (Figure S6A), these *Runx2-/-* osteoblasts were then cultured in a differentiation medium containing either 5 or 10mM glucose. In *Runx2-/-* osteoblasts cultured in the presence of 5mM glucose, GLUT1 accumulation and glucose consumption rate were decreased, phosphorylation of AMPKα1 was high, phosphorylation of p70S6K was low indicating that mTORC1 signaling was inhibited. As a result, ^{3}H-proline incorporation into collagen molecules and accumulation of Type I collagen were lower in *Runx2-/-* than in control osteoblasts (Figure 6A-C). In contrast, when the glucose concentration in the culture medium of *Runx2-/-* cells reached 10mM, the glucose consumption rate doubled, phosphorylation of AMPKα1 and p70S6K, incorporation rate of ^{3}H-proline into collagen molecules and the accumulation of Type I collagen were normalized in *Runx2-/-* cells, even though *Type I Collagen* gene expression was not changed (Figure 6A-D).

In view of these results we asked whether a chronic hyperglycemia would improve bone formation in *Runx2+/-* embryos. This was achieved by injecting streptozotocin (STZ, 150mg/kg) in

Runx2+/- female mice as soon as a vaginal plug was seen. By decreasing the number of β-cells and circulating insulin levels this manipulation caused a severe hyperglycemia in E18.5 embryos (Figure 6E). We focused our analysis on bones forming through intramembranous ossification because they are the ones in which osteoblast differentiation is hampered by *Runx2* haplo-insufficiency. While no difference was seen in WT embryos carried by STZ-treated mothers (Figure S6B), alcian blue/alizarin red staining of skeletal preparations showed that clavicles of E18.5 *Runx2*+/- embryos carried by STZ-treated mothers were twice as long as those of *Runx2*+/- embryos carried by vehicle-treated mothers (1.78±0.08 & 0.85±0.05 mm). Interparietal bones were also two-fold larger in *Runx2*+/- embryos carried by STZ-treated mothers (2.09±0.12 & 1.01±0.13 mm^2) than in those carried by control mothers and fontanelles of these embryos were less open than those of *Runx2*+/- embryos carried by vehicle-treated mothers (Figure 6F-G). Histological analyses showed the presence of mineralized bone trabeculae in the clavicles of E18.5 *Runx2*+/- embryos carried by STZ-treated mothers (Figure 6H-I). An immunohistochemistry analysis showed the presence of Type I collagen molecules in the clavicles of *Runx2*+/- embryos carried by STZ-treated mothers whereas only Type X collagen molecules were present in those of *Runx2*+/- embryos carried by vehicle-treated mothers (Figure 6J). Accumulation of Type I collagen was also increased in long bones of *Runx2*+/- embryos carried by STZ-treated mothers (Figure 6K-L). To further link the rescue of the bone phenotype in *Runx2*-deficient embryos to the increase in blood glucose levels, we repeated this experiment using lower doses of STZ (50 or 100mg/kg). One hundred mg/kg of STZ was toxic for β-cells since it decreased circulating

insulin levels nearly two-fold without raising blood glucose levels in mothers or embryos (Figure 6E). This STZ dose did not correct the delay in bone development of *Runx2*-deficient embryos (Figure 6F-G). Thus, raising blood glucose levels normalized collagen synthesis and enhanced bone formation in *Runx2+/-* osteoblasts and embryos.

Although Type I collagen accumulation was also normalized in skeletal elements obtained form *Runx2-/-* embryos carried by STZ-treated mothers (Figure 6M), alcian blue/alizarin red staining of skeletal preparations failed to show any ECM mineralization in the skeleton of E18.5 *Runx2-/-* embryos carried by STZ-treated mothers (Figure S6C). This is probably explained by the fact that RUNX2 regulates the expression of *Alkaline Phosphatase* (*Akp2*), a gene necessary for bone mineralization (Murshed et al., 2005) (Figure 6N, D).

A crosstalk between Runx2 and *Glut1* coordinates osteoblast differentiation and bone formation

The results presented above delineated the influence of glucose uptake on osteoblast differentiation and bone formation but did not explain how these two events are coordinated in vivo. In addressing this question we interpreted the fact that *Glut1* expression and glucose uptake were decreased in *Runx2+/-* bones (Figure 7A-B) as suggesting that RUNX2 regulates *Glut1* expression. *Runx1* expression in *Glut1/α1(I) Collagen*-expressing cells of the limb buds prompted us to test if Runx1 could trans-activate the *Glut1* promoter.

The *Glut1* promoter of the mouse and other vertebrate species has a canonical Runx binding

site at -811bp (Figure 7C). Chromatin immunoprecipitation assays verified that RUNX2 binds to this site (Figure 7D) and DNA co-transfection experiments performed in COS cells showed that *Runx2* or *Runx1* expression vectors could increase the activity of a *Glut1* promoter-luciferase reporter construct (p*Glut1-Luc)* only if this site was intact (Figure 7E). In agreement with these results, expression of *Glut1* was decreased in *Runx2-/-* and increased in *Schnurri-3-/-* osteoblasts (*Shn3-/-*) that display an increase in RUNX2 activity (Jones et al., 2006) (Figure 7F, S7A). These results explained why glucose uptake and mTORC1 activity were decreased in *Runx2-/-* and increased in *Shn3-/-* osteoblasts (Figure 7G, 6B).

If the feed-forward regulation between GLUT1-dependent glucose uptake and RUNX2 provides an explanation for the coordination of osteoblast differentiation and bone formation, $Glut1_{osx}$*+/-;Runx2+/-* embryos should display a delay in osteoblast differentiation similar to that of *Runx2-/-* embryos. Alcian blue/alizarin red staining of skeletal preparations showed that $Glut1_{osx}$*+/-;Runx2+/-* embryos were indistinguishable from *Runx2-/-* embryos up until E16.5 (Figure 7H, S7B). At E18.5, clavicles were barely detectable and most of the bones forming the skull were absent or severely hypoplastic in $Glut1_{osx}$*+/-;Runx2+/-* embryos (Figure 7I). Alcian blue staining of histological sections of long bones showed an enlargement of the area of hypertrophic chondrocytes and a cartilaginous ECM in E18.5 $Glut1_{osx}$*+/-;Runx2+/-* embryos (Figure 7J). *Osteocalcin* expression was undetectable in E18.5 $Glut1_{osx}$*+/-;Runx2+/-* skeletal elements, while it was present in single heterozygous embryos. Conversely, the area covered by *α1(X)Collagen*-expressing cells was greatly

enlarged in E18.5 *Glut1*$_{osx}$*+/-;Runx2+/-* embryos (Figure 7K). The extent of the delay in osteoblast differentiation in *Glut1*$_{osx}$*+/-;Runx2+/-* embryos and mice explained why they all died peri-natally. This cross-regulation between *Runx2* and *Glut1* also determined the extent of bone formation since 3-month-old *Glut1*$_{ocn}$*+/-;Runx2+/-* mice had a low bone mass not seen either in *Glut1*$_{ocn}$*+/-* or *Runx2+/-* mice (Figure 7L).

Accounting for this severe phenotype and in agreement with the feed forward loop between glucose uptake in osteoblasts and RUNX2, the accumulation of GLUT1, Type I collagen and RUNX2 was decreased more than 80% and phosphorylation of AMPK and SMURF1 was increased in *Glut1*$_{osx}$*+/-;Runx2+/-* compared to single heterozygous bones (Figure 7M). Hence, the cross-regulation of RUNX2 and *Glut1* is an amplification mechanism that determines the onset of osteoblast differentiation and the extent of bone formation throughout life. We also treated *Runx2+/-* mothers as soon as a vaginal plug was observed with STZ (150mg/kg). This dose of STZ raised blood glucose levels in mothers and embryos (Figure S7C), and increased bone formation in skeletal elements of the skull and in clavicles in *Glut1*$_{osx}$*+/-;Runx2+/-* embryos (Figure 7N).

Discussion

This study identifies glucose uptake in prospective osteoblasts as the earliest determinant of osteoblast differentiation and bone formation. It also shows that the coordination of osteoblast differentiation and bone formation throughout life is maintained by a feed-forward regulation between glucose uptake in osteoblasts and RUNX2 accumulation. In addition, glucose uptake in osteoblasts is necessary for whole-body glucose homeostasis.

The bases of the coordination between osteoblast differentiation and bone formation

A striking feature of bone biology that has never been explained is that the synthesis of the main constituent of the bone ECM, Type I collagen, precedes the expression of and is not regulated by RUNX2, the earliest transcriptional determinant of osteoblast differentiation. This apparent disconnect between osteoblast differentiation and Type I collagen synthesis in the bone could be explained by a single mechanism controlling both aspects of osteoblast biology and acting upstream of RUNX2. Our results suggest that this is the case and that this mechanism is glucose uptake in osteoblast progenitor cells. Glucose is the main nutrient of osteoblasts and is taken up by these cells in an insulin-independent manner through *Glut1* whose expression precedes the one of *Runx2*. Glucose uptake in osteoblasts favors osteoblast differentiation and bone formation through two distinct mechanisms. First, by inhibiting the activity of AMPK, glucose uptake enhances the activity of the mTORC1 pathway and therefore protein synthesis. Second and unexpectedly, glucose uptake inhibits another function of AMPK documented here, its ability to favor RUNX2 ubiquitination in part via

SMURF1. The two distinct functions of AMPK in osteoblasts revealed here explain why agonists of AMPK activity exert a deleterious influence on bone formation in vivo.

The *Glut1-Runx2* pathway described here could have clinical relevance. For instance, *Glut1*$_{osx}$*-/-* embryos develop a CCD, a disease most often caused by a decrease in RUNX2 expression. However, a significant number of CCD patients do not have any detectable mutations in *Runx2* (Puppin et al., 2005; Tessa et al., 2003). Conceivably in some of these patients, CCD may be caused by a decrease in glucose uptake or utilization in osteoblasts. If this was the case this would further support the notion that skeletal dysplasia may have a nutritional basis (Elefteriou et al., 2006)**.** Moreover, the predilection of osteoblasts for glucose demonstrated here provides a plausible explanation for why children fed chronically a ketogenic diet experience poor longitudinal growth (Groesbeck et al., 2006).

The respective functions of glucose uptake and Runx2 in osteoblasts

Remarkably, restoring RUNX2 accumulation in *Glut1-/-* cells did not translate into efficient bone formation in vivo simply because in osteoblasts unable to properly take up glucose, protein synthesis remains low regardless of the level of expression of *Runx2*. On the other hand, raising the extracellular concentration of glucose was sufficient to initiate bone formation even though osteoblasts were not fully differentiated in *Runx2+/-* embryos. Raising blood glucose levels in *Runx2-/-* embryos also increased collagen synthesis but that did not translate into the presence of a mineralized bone ECM because expression of *Akp2*, a gene necessary for bone ECM mineralization, is low in the absence of

Runx2. Thus RUNX2 is necessary for osteoblast differentiation and for bone ECM mineralization but, paradoxically, not for the synthesis of the main constituent of this ECM. In broader terms, the importance of glucose uptake in osteoblast differentiation described here raises the hypothesis that glucose uptake may be a more general determinant of cell differentiation during embryonic development. This may be particularly relevant for tissue like muscle that uptakes large amount of glucose.

Independently of its regulation of bone formation, glucose uptake in osteoblasts is necessary for another cardinal function of bone: the regulation of whole-body glucose metabolism. Indeed, through its regulation of RUNX2 accumulation, glucose favors expression of the hormone osteocalcin.

The synergistic functions of glucose uptake and Runx2 in osteoblasts

How are osteoblast differentiation and bone formation coordinated throughout life? The fact that *Runx2-/-* and *Glut1-/-* osteoblasts had a similar metabolic profile suggested that this coordination might be explained if *Glut1* was a target gene of RUNX2.

In support of this hypothesis, both molecular and genetic evidences identify RUNX2 as a major regulator of *Glut1* expression and glucose uptake in osteoblasts. As a result, *Runx2-/-* osteoblasts bear metabolic similarities with *Glut1-/-* osteoblasts, $Glut1_{osx}$*+/-;Runx2+/-* embryos are similar to *Runx2-/-* embryos and $Glut1_{ocn}$*+/-;Runx2+/-* mice display an osteopenia not seen in either *Runx2+/-* or $Glut1_{ocn}$*+/-* mice. Hence, the reciprocal regulation between GLUT1-mediated glucose uptake and

RUNX2 acts as an amplification chamber that determines the onset of osteoblast differentiation and the extent of bone formation throughout life. In addition, *Runx1* expression in the developing skeleton suggests that this Runx protein may regulate *Glut1* expression and thereby favors Type I collagen accumulation in prospective osteoblasts before E12.5.

In broader terms, results of this study cannot be separated from the recently described role of osteoblasts in maintaining glucose homeostasis in physiological and pathological situations (Ferron et al., 2010a; Lee et al., 2007; Wei et al., 2014e). The absolute necessity of glucose uptake for osteoblast differentiation, bone formation and glucose homeostasis documented here illustrates from the perspective of the osteoblast, the fundamental importance of the crosstalk between bone and glucose metabolism.

Acknowledgements

We thank Drs. P. Ducy, J. Wrana, J. Shim and L. Glimcher for critical reading of the manuscript and reagents. This work was supported by NIH grant R01AR045548 (G.K.), Columbia University Mandl Connective Tissue Research Fellowship (J. W.) and Honjo International Scholarship (J. S.).

Reference

Long, F. (2012). Building strong bones: molecular regulation of the osteoblast lineage. Nat Rev Mol Cell Biol *13*, 27-38.

Karsenty, G., Kronenberg, H.M., and Settembre, C. (2009). Genetic control of bone formation. Annu Rev Cell Dev Biol *25*, 629-648.

Vuorio, E., and de Crombrugghe, B. (1990). The family of collagen genes. Annu Rev Biochem *59*, 837-872.

Kern, B., Shen, J., Starbuck, M., and Karsenty, G. (2001). Cbfa1 contributes to the osteoblast-specific expression of type I collagen genes. J Biol Chem *276*, 7101-7107.

Lee, N.K., Sowa, H., Hinoi, E., Ferron, M.*, et al.* (2007). Endocrine regulation of energy metabolism by the skeleton. Cell *130*, 456-469.

Ferrannini, E., Simonson, D.C., Katz, L.D., Reichard, G., Jr.*, et al.* (1988). The disposal of an oral glucose load in patients with non-insulin-dependent diabetes. Metabolism *37*, 79-85.

Yu, K., Xu, J., Liu, Z., Sosic, D.*, et al.* (2003). Conditional inactivation of FGF receptor 2 reveals an essential role for FGF signaling in the regulation of osteoblast function and bone growth. Development *130*, 3063-3074.

Rodda, S.J., and McMahon, A.P. (2006). Distinct roles for Hedgehog and canonical Wnt signaling in specification, differentiation and maintenance of osteoblast progenitors. Development *133*, 3231-3244.

Mundlos, S., Otto, F., Mundlos, C., Mulliken, J.B.*, et al.* (1997). Mutations involving the transcription factor CBFA1 cause cleidocranial dysplasia. Cell *89*, 773-779.

Lee, B., Thirunavukkarasu, K., Zhou, L., Pastore, L.*, et al.* (1997). Missense mutations abolishing DNA binding of the osteoblast-specific transcription factor OSF2/CBFA1 in cleidocranial dysplasia. Nat Genet *16*, 307-310.

Yamashita, H., Takenoshita, M., Sakurai, M., Bruick, R.K.*, et al.* (2001). A glucose-responsive transcription factor that regulates carbohydrate metabolism in the liver. Proc Natl Acad Sci U S A *98*, 9116-9121.

Zhang, M., Xuan, S., Bouxsein, M.L., von Stechow, D.*, et al.* (2002). Osteoblast-specific knockout of the insulin-like growth factor (IGF) receptor gene reveals an essential role of IGF signaling in bone matrix mineralization. J Biol Chem *277*, 44005-44012.

Jeyapalan, A.S., Orellana, R.A., Suryawan, A., O'Connor, P.M.*, et al.* (2007). Glucose stimulates protein synthesis in skeletal muscle of neonatal pigs through an AMPK- and mTOR-independent process. Am J Physiol Endocrinol Metab *293*, E595-603.

Mayer, F.V., Heath, R., Underwood, E., Sanders, M.J.*, et al.* (2011). ADP regulates SNF1, the Saccharomyces cerevisiae homolog of AMP-activated protein kinase. Cell Metab *14*, 707-714.

Woods, A., Munday, M.R., Scott, J., Yang, X.*, et al.* (1994). Yeast SNF1 is functionally related to mammalian AMP-activated protein kinase and regulates acetyl-CoA carboxylase in vivo. J Biol Chem *269*, 19509-19515.

Wilson, W.A., Hawley, S.A., and Hardie, D.G. (1996). Glucose repression/derepression in budding

yeast: SNF1 protein kinase is activated by phosphorylation under derepressing conditions, and this correlates with a high AMP:ATP ratio. Curr Biol *6*, 1426-1434.

Bolster, D.R., Crozier, S.J., Kimball, S.R., and Jefferson, L.S. (2002). AMP-activated protein kinase suppresses protein synthesis in rat skeletal muscle through down-regulated mammalian target of rapamycin (mTOR) signaling. J Biol Chem *277*, 23977-23980.

Reiter, A.K., Bolster, D.R., Crozier, S.J., Kimball, S.R.*, et al.* (2005). Repression of protein synthesis and mTOR signaling in rat liver mediated by the AMPK activator aminoimidazole carboxamide ribonucleoside. Am J Physiol Endocrinol Metab *288*, E980-988.

Zhao, M., Qiao, M., Oyajobi, B.O., Mundy, G.R.*, et al.* (2003). E3 ubiquitin ligase Smurf1 mediates core-binding factor alpha1/Runx2 degradation and plays a specific role in osteoblast differentiation. J Biol Chem *278*, 27939-27944.

Takarada, T., Hinoi, E., Nakazato, R., Ochi, H.*, et al.* (2013). An analysis of skeletal development in osteoblast-specific and chondrocyte-specific runt-related transcription factor-2 (Runx2) knockout mice. J Bone Miner Res *28*, 2064-2069.

Murshed, M., Harmey, D., Millan, J.L., McKee, M.D.*, et al.* (2005). Unique coexpression in osteoblasts of broadly expressed genes accounts for the spatial restriction of ECM mineralization to bone. Genes Dev *19*, 1093-1104.

Jones, D.C., Wein, M.N., Oukka, M., Hofstaetter, J.G.*, et al.* (2006). Regulation of adult bone mass by the zinc finger adapter protein Schnurri-3. Science *312*, 1223-1227.

Puppin, C., Pellizzari, L., Fabbro, D., Fogolari, F.*, et al.* (2005). Functional analysis of a novel RUNX2 missense mutation found in a family with cleidocranial dysplasia. J Hum Genet *50*, 679-683.

Tessa, A., Salvi, S., Casali, C., Garavelli, L.*, et al.* (2003). Six novel mutations of the RUNX2 gene in Italian patients with cleidocranial dysplasia. Hum Mutat *22*, 104.

Elefteriou, F., Benson, M.D., Sowa, H., Starbuck, M.*, et al.* (2006). ATF4 mediation of NF1 functions in osteoblast reveals a nutritional basis for congenital skeletal dysplasiae. Cell Metab *4*, 441-451.

Groesbeck, D.K., Bluml, R.M., and Kossoff, E.H. (2006). Long-term use of the ketogenic diet in the treatment of epilepsy. Dev Med Child Neurol *48*, 978-981.

Ferron, M., Wei, J., Yoshizawa, T., Del Fattore, A.*, et al.* (2010). Insulin signaling in osteoblasts integrates bone remodeling and energy metabolism. Cell *142*, 296-308.

Wei, J., Hanna, T., Suda, N., Karsenty, G.*, et al.* (2014). Osteocalcin Promotes beta-Cell Proliferation During Development and Adulthood Through Gprc6a. Diabetes *63*, 1021-1031.

Nakada, D., Saunders, T.L., and Morrison, S.J. (2010). Lkb1 regulates cell cycle and energy metabolism in haematopoietic stem cells. Nature *468*, 653-658.

Narimatsu, M., Bose, R., Pye, M., Zhang, L.*, et al.* (2009). Regulation of planar cell polarity by Smurf ubiquitin ligases. Cell *137*, 295-307.

Ducy, P., and Karsenty, G. (1995). Two distinct osteoblast-specific cis-acting elements control expression of a mouse osteocalcin gene. Mol Cell Biol *15*, 1858-1869.

McLeod, M.J. (1980). Differential staining of cartilage and bone in whole mouse fetuses by alcian blue

and alizarin red S. Teratology *22*, 299-301.

Chappard, D., Palle, S., Alexandre, C., Vico, L.*, et al.* (1987). Bone embedding in pure methyl methacrylate at low temperature preserves enzyme activities. Acta Histochem *81*, 183-190.

Parfitt, A.M., Drezner, M.K., Glorieux, F.H., Kanis, J.A.*, et al.* (1987). Bone histomorphometry: standardization of nomenclature, symbols, and units. Report of the ASBMR Histomorphometry Nomenclature Committee. J Bone Miner Res *2*, 595-610.

Ducy, P., Zhang, R., Geoffroy, V., Ridall, A.L.*, et al.* (1997). Osf2/Cbfa1: a transcriptional activator of osteoblast differentiation. Cell *89*, 747-754.

Takeda, S., Bonnamy, J.P., Owen, M.J., Ducy, P.*, et al.* (2001). Continuous expression of Cbfa1 in nonhypertrophic chondrocytes uncovers its ability to induce hypertrophic chondrocyte differentiation and partially rescues Cbfa1-deficient mice. Genes Dev *15*, 467-481.

Figures

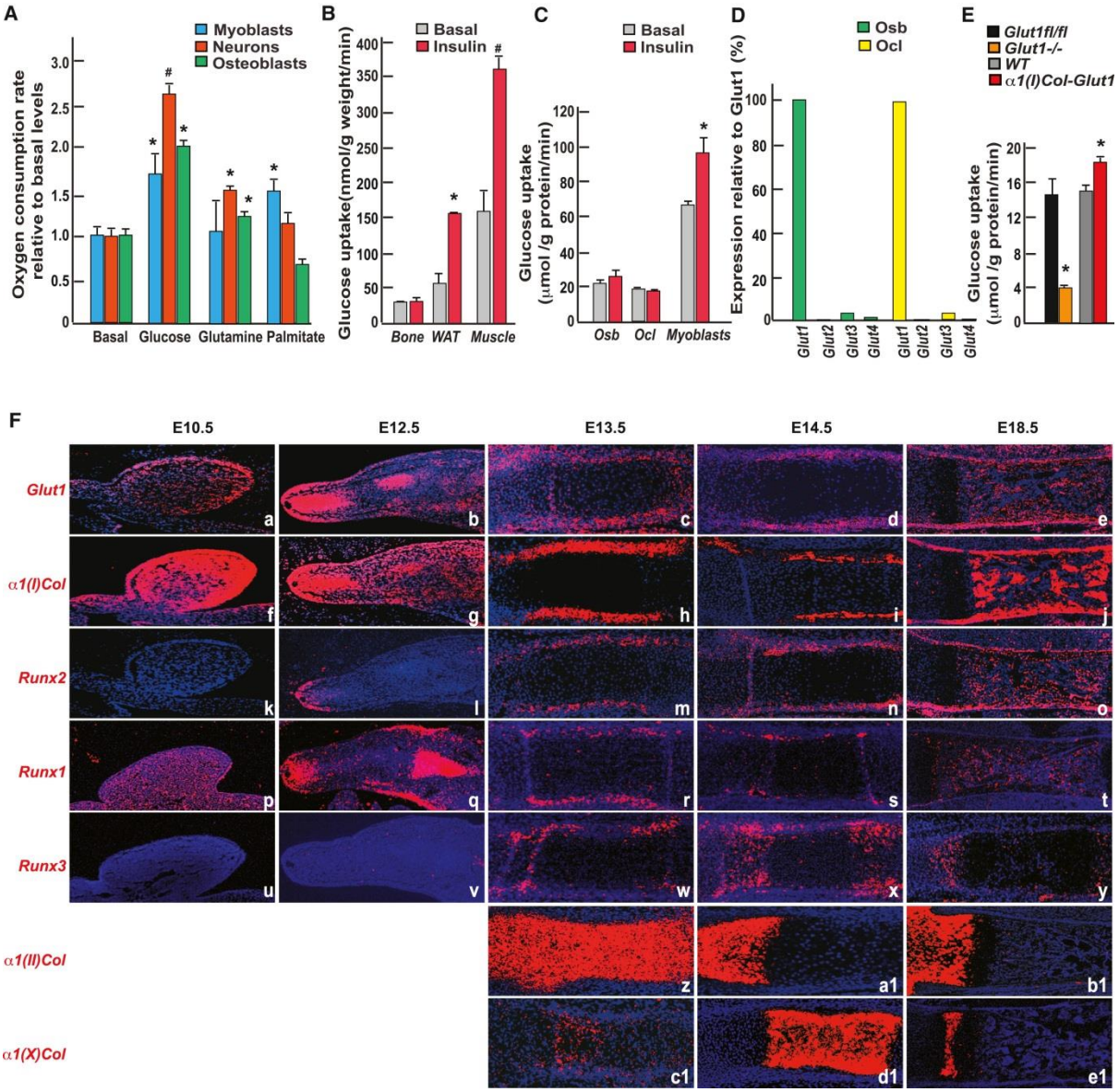

Figure 1. Insulin-independent glucose uptake in osteoblasts

A. Oxygen consumption rate (OCR) of osteoblasts, C2C12 myoblasts or hippocampal neurons incubated with vehicle, 10mM glucose, 2mM glutamine or 300μM palmitate in 1X KHB buffer for 2hrs (n=8).

B. Glucose uptake measured by euglycemic hyperinsulinemic clamps in femurs, white adipose tissue and gastrocnemius muscle of WT mice before or after insulin infusion (2.5 mU/kg/min) (n=4);

C. Uptake rate of 2-DG in osteoblasts (Osb), osteoclasts (Ocl) and myoblasts (n=3).

D. Expression of class I *Gluts* in osteoblasts and osteoclasts assayed by qPCR.

E. Uptake rate of 2-DG in *Glut1fl/fl*, *Glut1-/-*, WT and *α1(I)Col-Glut1* osteoblasts (n=6-8).

F. In situ hybridization analysis of *Glut1* (a-e)*, α1(I) Collagen* (f-j)*, Runx2* (k-o) *Runx1*(p-t), *Runx3* (u-v), *α1(II) Collagen* (z-b1) and *α1(X) Collagen* (c1-e1) in hind-limbs during embryonic development.

All error bars represent standard error of the mean. *denotes $p \leq 0.05$, and # denotes $p \leq 0.001$ compared to control when analyzed by Student's t tests.

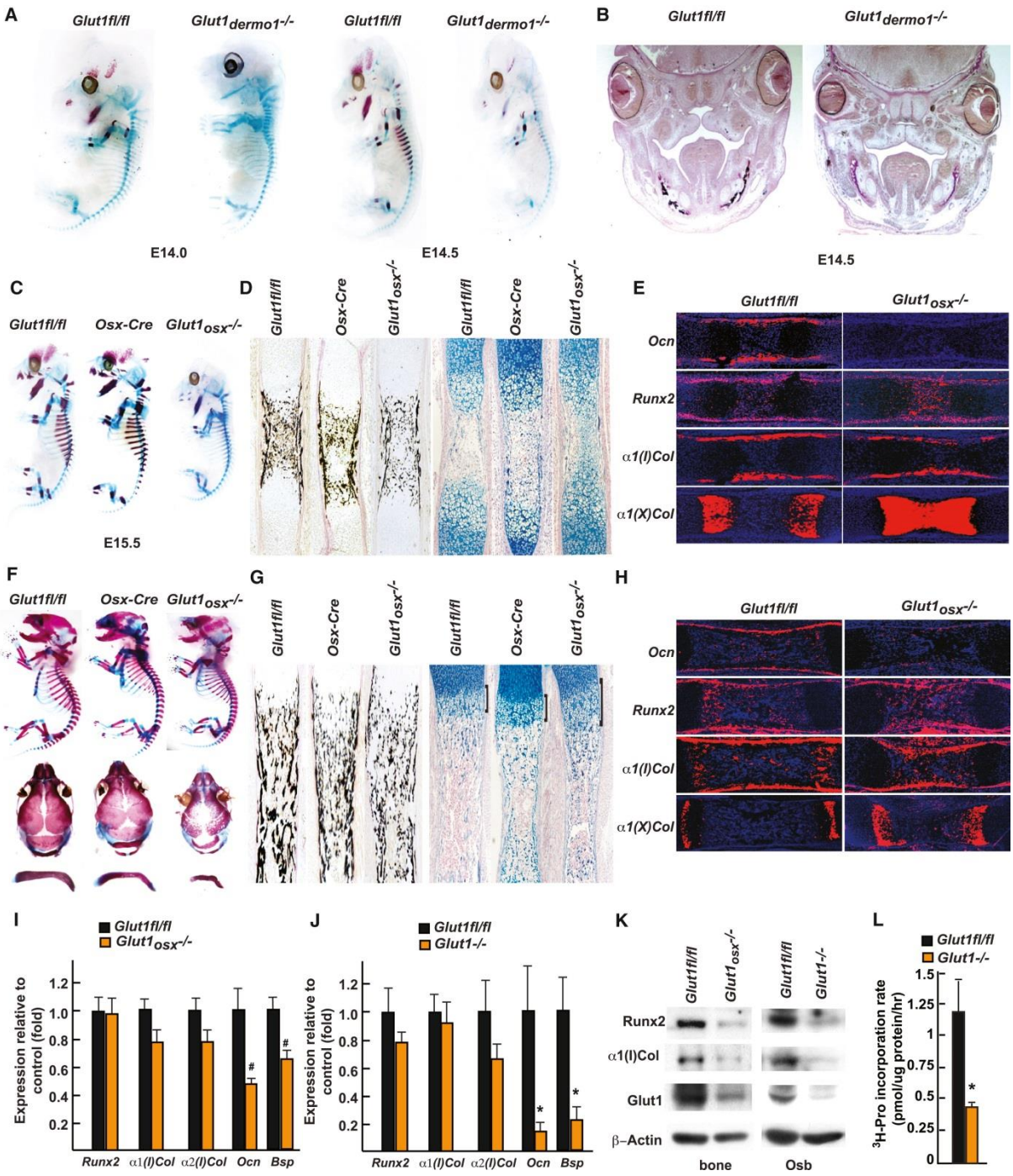

Figure 2. Glucose uptake is necessary for osteoblast differentiation during development

A. Alcian blue/alizarin red staining of skeletal preparations of E14.0 and 14.5 *Glut1$_{dermo1}$-/-* and *Glut1fl/fl* embryos.

B. Von Kossa staining of skull sections of E14.5 *Glut1$_{dermo1}$-/-* and *Glut1fl/fl* embryos.

C. Alcian blue/alizarin red staining of skeletal preparations of E15.5 *Glut1$_{osx}$-/-*, *Glut1fl/fl* and *Osx-cre*

embryos.

D. Von Kossa or alcian blue staining of femur from E15.5 *Glut1$_{osx}$-/-, Glut1fl/fl* and *Osx-cre* embryos.

E. In situ hybridization analysis of *Osteocalcin, α1(I), α1(X) Collagen* and *Runx2* expression in E15.5 *Glut1$_{osx}$-/-* and *Glut1fl/fl* femurs.

F. Alcian blue/alizarin red staining of skeletal preparations of E18.5 *Glut1$_{osx}$-/-*, *Glut1fl/fl* and *Osx-cre* embryos.

G. Von Kossa or alcian blue staining of femur from **E**18.5 *Glut1$_{osx}$-/-, Glut1fl/fl* and *Osx-cre* embryos.

H. In situ hybridization analysis of *Osteocalcin, α1(I), α1(X) Collagen* and *Runx2* expression in E18.5 *Glut1$_{osx}$-/-* and *Glut1fl/fl* femurs.

I. Expression of osteoblast markers in E18.5 *Glut1$_{osx}$-/-* and *Glut1fl/fl* femurs (n=9).

J. Expression of osteoblast marker genes in *Glut1fl/fl* and *Glut1-/-* osteoblasts. (n=6)

K. *α*1(I) Collagen and RUNX2 accumulations in E18.5 *Glut1$_{osx}$-/-* and *Glut1fl/fl* femurs and *Glut1fl/fl* and *Glut1-/-* osteoblasts.

L. ^{3}H-proline incorporation in collagen in *Glut1fl/fl* and *Glut1-/-* osteoblasts (n=6).

All error bars represent standard error of the mean. *denotes $p \leq 0.05$, and # denotes $p \leq 0.001$ compared to control when analyzed by Student's t tests.

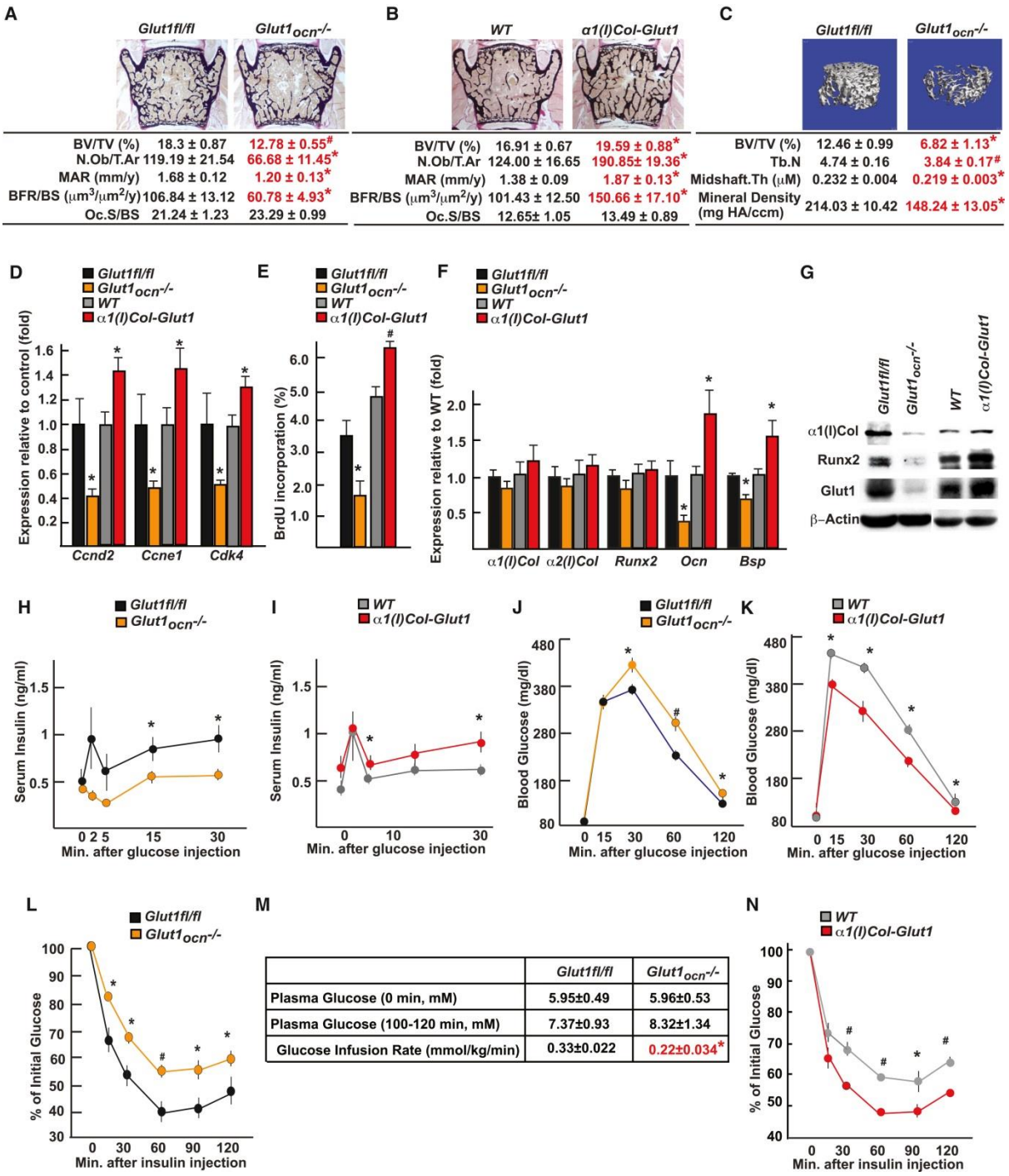

Figure 3. Glucose uptake in osteoblasts is necessary for bone formation and glucose homeostasis post-natally

A and **B.** Histomorphometric analysis of L4 vertebrae of 3 month-old *Glut1fl/fl*, *Glut1$_{ocn}$-/-*, WT and *α1(I)Col-Glut1* male mice (n=9-11).

C. μCT analysis of proximal femurs of *Glut1fl/fl* and *Glut1$_{ocn}$-/-* male mice (n=7).

D. Expression of *Ccnd2*, *Ccne1* and *Cdk4* in femurs of 3 month-old *Glut1fl/fl*, *Glut1$_{ocn}$-/-*, WT and *α1(I)Col-Glut1* mice (n=6).

E. BrdU incorporation in calvaria of P14 *Glut1fl/fl*, *Glut1$_{ocn}$-/-*, WT and *α1(I)Col-Glut1* mice (n=5-8).

F. Expression of osteoblast marker genes in femurs of 3 month-old *Glut1fl/fl*, *Glut1$_{ocn}$-/-,* WT and *α1(I)Col-Glut1* mice (n=8).

G. *α*1(I) Collagen and RUNX2 accumulations in femurs of 3 month-old *Glut1fl/fl*, *Glut1$_{ocn}$-/-*, WT and *α1(I)Col-Glut1* mice.

H-I. GSIS in 3 month-old *Glut1fl/fl*, *Glut1$_{ocn}$-/-*, WT and *α1(I)Col-Glut1* mice (n=10-11).

J-K. GTT in 3 month-old *Glut1fl/fl*, *Glut1$_{ocn}$-/-*, WT and *α1(I)Col-Glut1* mice (n=5-10).

L. ITT in 3 month-old *Glut1fl/fl* and *Glut1$_{ocn}$-/-*, WT mice (n=8-10).

M. Glucose infusion rate in 3 month-old *Glut1fl/fl* and *Glut1$_{ocn}$-/-* mice (n=6).

N. ITT in 3 month-old WT and *α1(I)Col-Glut1* mice (n=8-10).

All error bars represent standard error of the mean. *denotes $p \leq 0.05$, and # denotes $p \leq 0.001$ compared to control when analyzed Student's t tests.

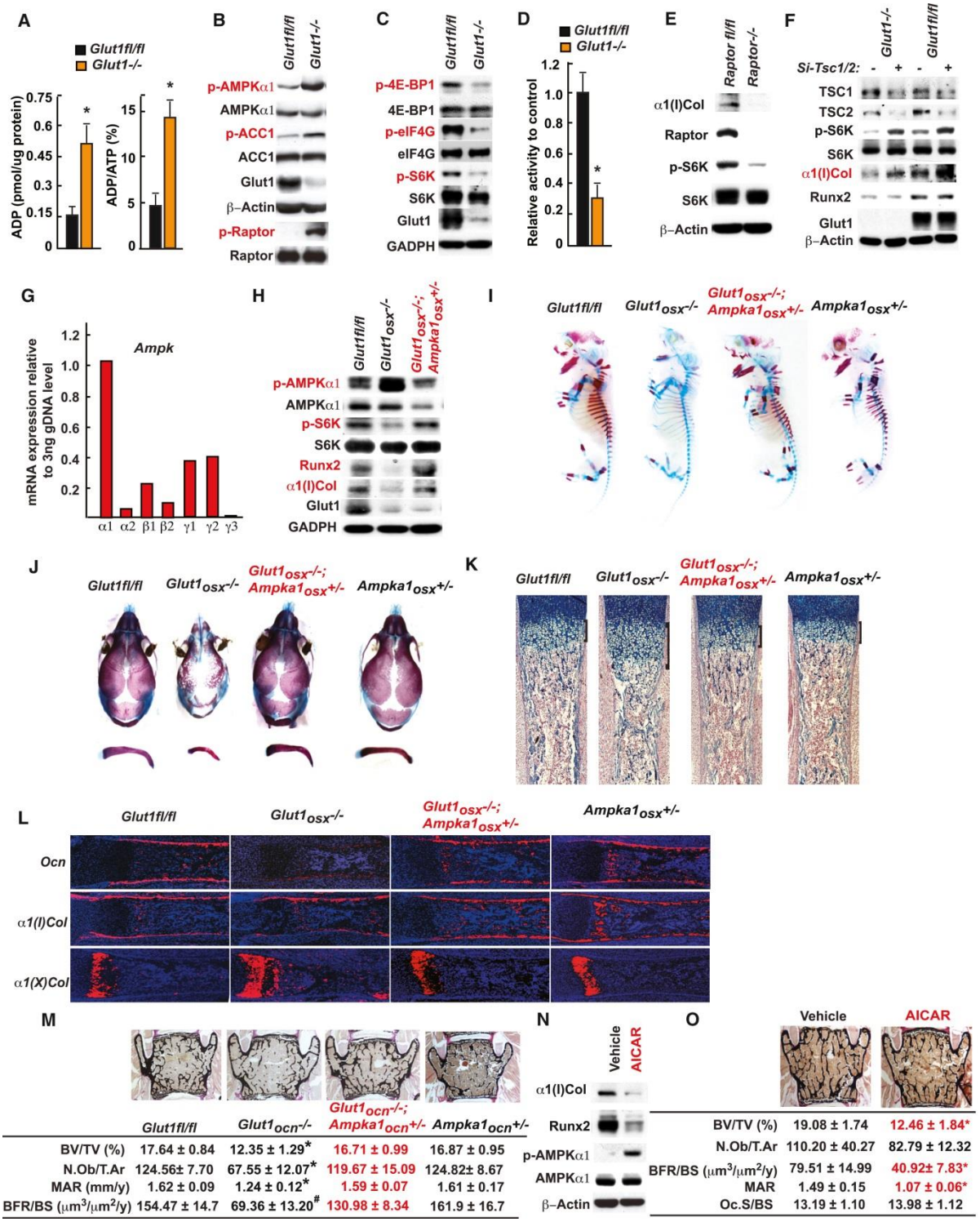

Figure 4. Glucose uptake favors osteoblast differentiation and bone formation by inhibiting AMPK

A. ADP content and ADP/ATP ratio in WT and *Glut1-/-* osteoblasts (n=6).

B-C. AMPK, ACC1, Raptor (B), p70S6K, 4E-BP1 and eIF4G phosphorylation in WT and *Glut1-/-* osteoblasts.

D. Kinase assay of immune-precipitated mTORC1 complex in WT and *Glut1-/-* osteoblasts (n=3).

E. Raptor, p70S6K phosphorylation and *α*1(I)Collagen accumulations in WT and *Raptor-/-* osteoblasts.

F. TSC1, TSC2, and p70S6K phosphorylation, *α*1(I)Collagen and RUNX2 accumulations in WT and *Glut1-/-* osteoblasts transfected with SiRNAs targeting *Tsc1* and *Tsc2* or scrambled SiRNA.

G. Expression of various AMPK subunits in osteoblasts.

H. AMPK and p70S6K phosphorylation, RUNX2 and *α*1(I)Collagen accumulations in *Glut1fl/fl,* *Glut1*$_{osx}$*-/-* and *Glut1*$_{osx}$*-/-;Ampka1*$_{osx}$+/- osteoblasts.

I-J. Alcian blue/alizarin red staining of skeletal preparations of E15.5 (I) and 18.5 (J) *Glut1fl/fl,* *Glut1*$_{osx}$*-/-, Ampka1*$_{osx}$+/- and *Glut1*$_{osx}$*-/-;Ampka1*$_{osx}$+/- embryos.

K. Alcian blue staining of histological sections of femurs of E18.5 *Glut1fl/fl, Glut1*$_{osx}$*-/-, Ampka1*$_{osx}$+/- and *Glut1*$_{osx}$*-/-;Ampka1*$_{osx}$+/- embryos.

L. In situ hybridization analysis of *Osteocalcin, α1(I), α1(II)* and *α1(X) Collagen* expression in femurs of E18.5 *Glut1fl/fl, Glut1*$_{osx}$*-/-, Ampka1*$_{osx}$+/- and *Glut1*$_{osx}$*-/-;Ampka1* $_{osx}$+/- embryos.

M. Histomorphometric analysis of L4 vertebrae of 3 month-old of *Glut1fl/fl*, *Glut1*$_{ocn}$*-/-*, *Ampka1*$_{ocn}$+/- and *Glut1*$_{ocn}$*-/-;Ampka1*$_{ocn}$+/- male mice (n=7-10).

N. AMPK phosphorylation, RUNX2 and *α*1(I)Collagen accumulations in osteoblasts treated with vehicle or AICAR (0.1mM) for 16 hrs.

O. Histomorphometric analysis of L4 vertebrae of 3 month-old of WT mice treated with vehicle or

AICAR (250mg/kg/day) for 8 weeks (n=6).

All error bars represent standard error of the mean. *denotes $p \leq 0.05$, and # denotes $p \leq 0.001$ compared to control when analyzed by Student's t tests.

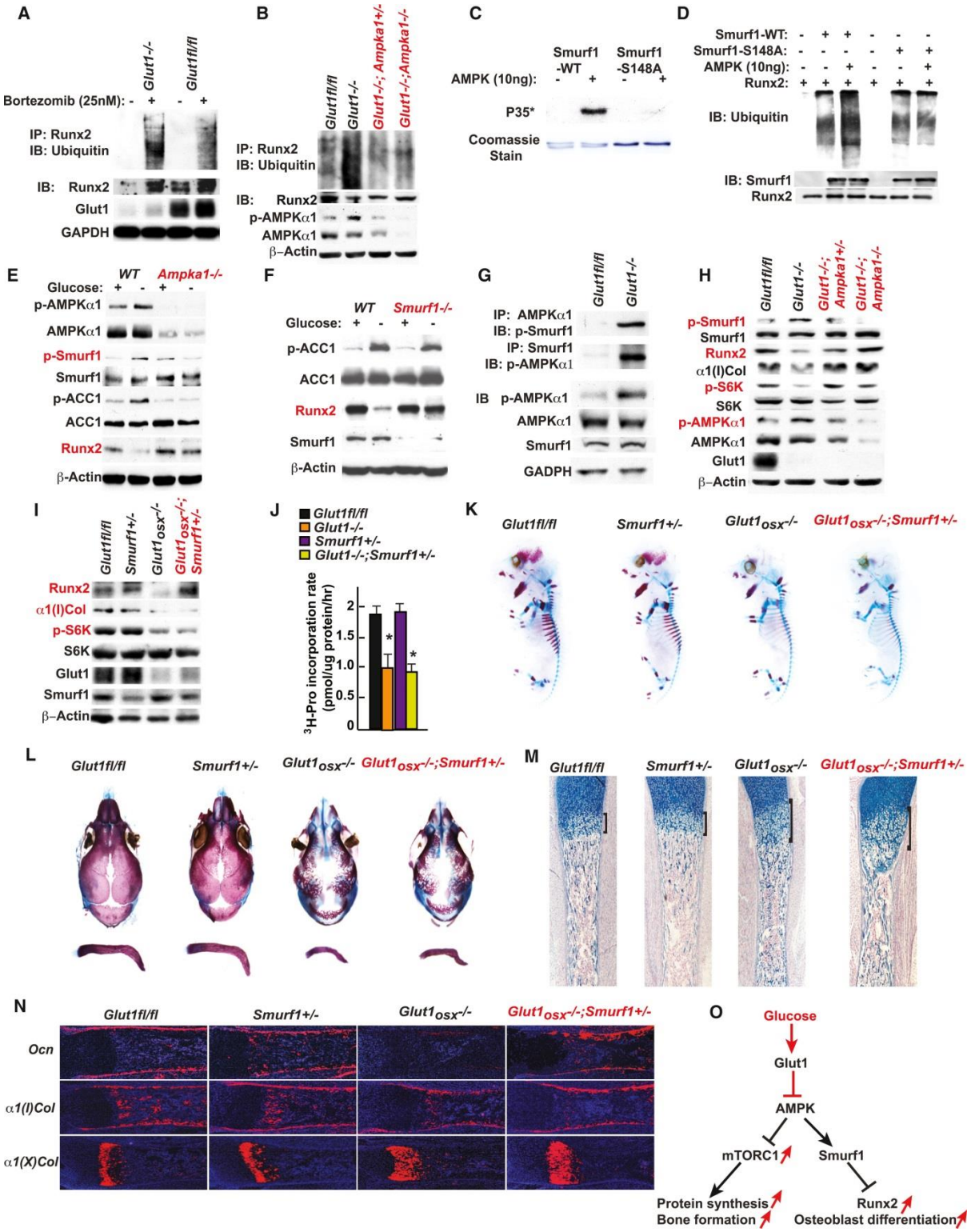

Figure 5. Runx2 cannot induce proper osteoblast differentiation if glucose uptake is hampered

A. Ubiquitination of immune-precipitated RUNX2 in WT and *Glut1-/-* osteoblasts treated with 25nM Bortezomib for 16hrs.

B. Ubiquitination of immune-precipitated RUNX2 in WT, *Glut1-/-*, *Glut1-/- Ampka1+/-* and *Glut1-/-*

Ampka1-/- osteoblasts treated with 25nM Bortezomib for 16hrs.

C. In vitro AMPK phosphorylation assay of SMURF1 and SMURF1-S148/A.

D. In vitro ubiquitination assay of SMURF1 and SMURF1-S148/A phosphorylated by AMPK.

E-F. RUNX2 and *α*1(I)Collagen accumulations, AMPK and SMURF1 phosphorylation in WT, *Smurf1-/-* (E) and *Ampka1-/-* (F) osteoblasts cultured with or without glucose for 16 hrs.

G. Co-immunoprecipitation of AMPK*α*1 and SMURF1 in WT and *Glut1-/-* osteoblasts.

H. RUNX2 and *α*1(I)Collagen accumulations, AMPK*α*1, p70S6K and SMURF1 phosphorylation in WT, *Glut1-/-*, *Glut1-/- Ampka1+/-* and *Glut1-/- Ampka1-/-* osteoblasts.

I. RUNX2 and *α*1(I)Collagen accumulations and p70S6K phosphorylation in *Glut1fl/fl*, $Glut1_{osx}$*-/-* and $Glut1_{osx}$*-/-;Smurf1+/-* osteoblasts.

J. ^{3}H-proline incorporation in collagen molecules in *Glut1fl/fl*, *Glut1-/-* and *Glut1-/-;Smurf1+/-* osteoblasts (n=6).

K-L. Alcian blue/alizarin red staining of skeletal preparations of E15.5 (G) and 18.5 (I) *Glut1fl/fl, Smurf1+/-,* $Glut1_{osx}$*-/-* and $Glut1_{osx}$*-/-;Smurf1+/-* embryos.

M. Alcian blue staining of sections of femurs of E18.5 *Glut1fl/fl*, $Glut1_{osx}$*-/-* and $Glut1_{osx}$ *-/-;Smurf1+/-* embryos.

N. In situ hybridization analysis of *Osteocalcin, α1(I)* and *α1(X) Collagens* expression, in femurs of E18.5 *Glut1fl/fl*, $Glut1_{osx}$*-/-* and $Glut1_{osx}$*-/-;Smurf1+/-* embryos.

O. Schematic representation of the pathways triggered by glucose uptake in osteoblasts.

All error bars represent standard error of the mean. *denotes $p \leq 0.05$, and # denotes $p \leq 0.001$ compared to control when analyzed by Student's t tests.

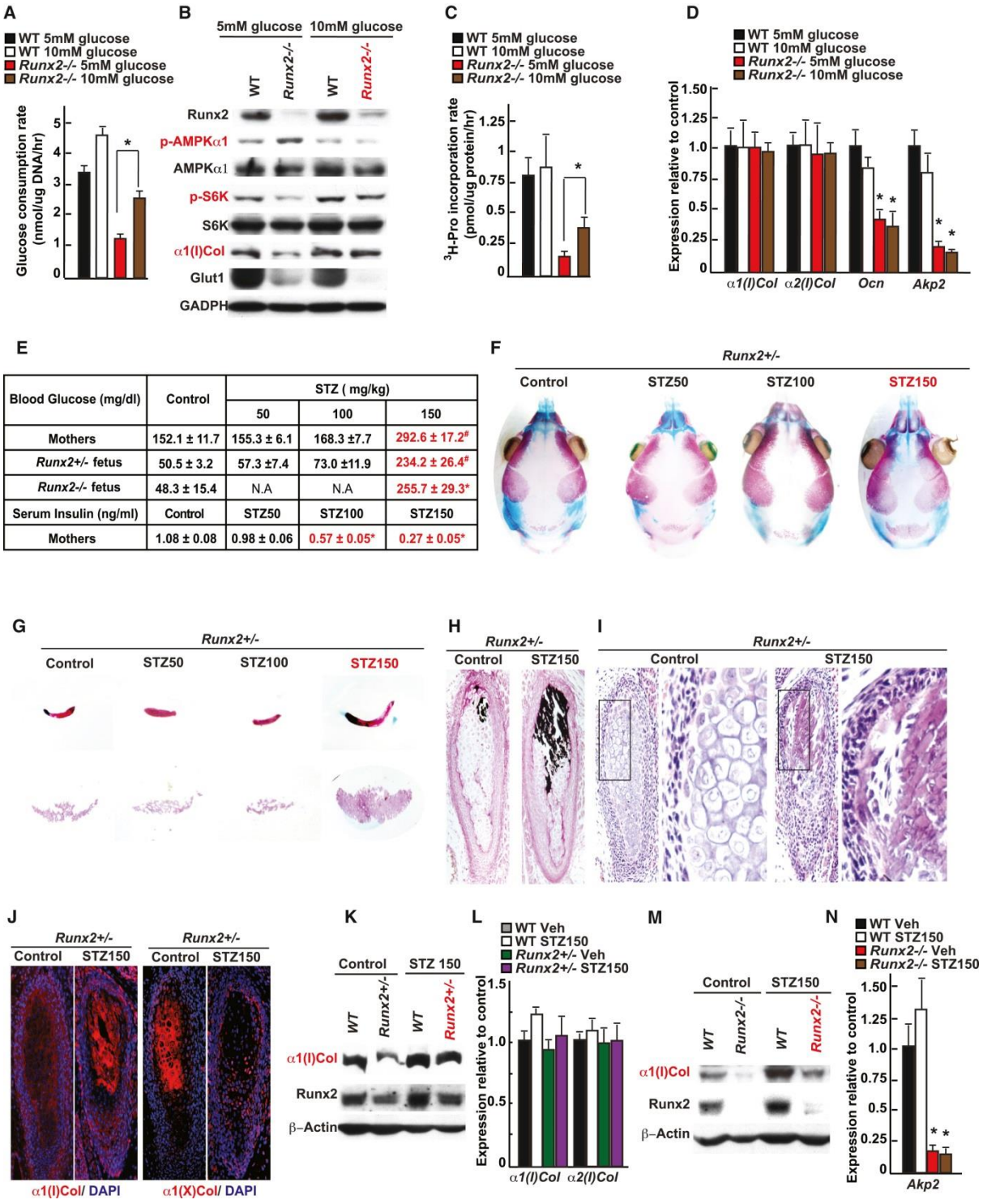

Blood Glucose (mg/dl)	Control	STZ (mg/kg)		
		50	100	150
Mothers	152.1 ± 11.7	155.3 ± 6.1	168.3 ±7.7	292.6 ± 17.2#
Runx2+/- fetus	50.5 ± 3.2	57.3 ±7.4	73.0 ±11.9	234.2 ± 26.4#
Runx2-/- fetus	48.3 ± 15.4	N.A	N.A	255.7 ± 29.3*
Serum Insulin (ng/ml)	Control	STZ50	STZ100	STZ150
Mothers	1.08 ± 0.08	0.98 ± 0.06	0.57 ± 0.05*	0.27 ± 0.05*

Figure 6. Glucose can initiate bone formation in *Runx2*-deficient embryos

A. Glucose consumption rate in WT and *Runx2-/-* osteoblasts cultured with 5 or 10mM glucose for 16hrs.

B. RUNX2, *α*1(I)Collagen and GLUT1 accumulations, AMPK*α*1 and p70S6K phosphorylation in WT

and *Runx2-/-* osteoblasts cultured with 5 or 10mM glucose for 14 days.

C. ^{3}H-proline incorporation in collagen molecules in WT and *Runx2-/-* osteoblasts cultured with 5 or 10mM glucose for 14 days (n=5).

D. qPCR analysis of osteoblast marker genes in WT and *Runx2-/-* osteoblasts cultured with 5 or 10mM glucose for 14 days (n=6).

E. Blood glucose and insulin levels in STZ (50, 100, 150mg/kg) and vehicle-treated *Runx2+/-* mothers and progenies at E18.5 (n=5-12).

F-G. Alcian blue/alizarin red staining of the skull (F), clavicles and interparietal bones (G) of E18.5 *Runx2+/-* embryos carried by STZ (50, 100, or 150mg/kg) and vehicle-treated mothers.

H-I. Von Kossa/van Gieson staining (H) and H&E staining (I) of clavicles of E18.5 *Runx2+/-* embryos carried by STZ- (150mg/kg) or vehicle-treated mothers.

J. Immunohistochemical detection of Type I and type X collagens in clavicles of E18.5 *Runx2+/-* embryos carried by STZ- (150mg/kg) or vehicle-treated mothers.

K. RUNX2 and *α*1(I)Collagen accumulations in femurs of E18.5 WT and *Runx2+/-* embryos carried by STZ- (150mg/kg) or vehicle-treated mothers.

L. *α1(I)* and *α2(I) Collagen* expression in femurs of E18.5 WT and *Runx2+/-* embryos carried by STZ- (150mg/kg) or vehicle-treated mothers (n=8).

M. RUNX2 and *α*1(I)Collagen accumulations in femurs of E18.5 WT and *Runx2-/-* embryos carried by STZ- (150mg/kg) or vehicle-treated mothers.

N. *Akp2* expression in femurs of E18.5 of WT and *Runx2-/-* embryos carried by STZ- (150mg/kg) or vehicle-treated mothers (n=6).

All error bars represent standard error of the mean. *denotes $p \leq 0.05$, and # denotes $p \leq 0.001$ compared to control when analyzed by Student's t tests.

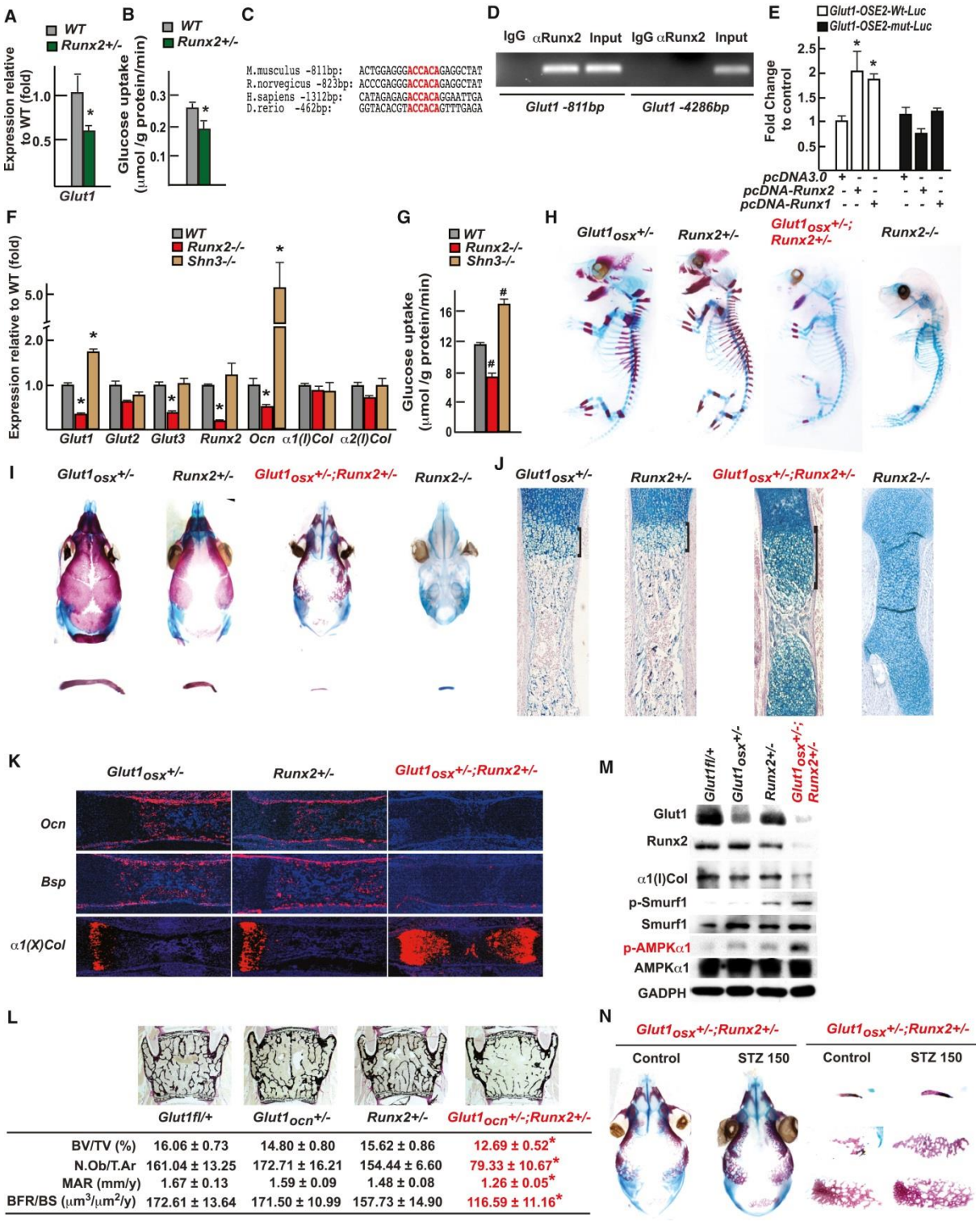

Figure 7. The reciprocal regulation between Runx2 and *Glut1* determines osteoblast differentiation and bone formation

A. *Glut1* expression in femurs of 3 month-old *Runx2*+/- mice (n=8).

B. Uptake rate of 2-DG in the calvaria of 6 week-old WT and *Runx2*+/- (n=4-5) mice.

C. Runx binding sites in the *Glut1* promoter of several species.

D. ChIP assay of RUNX2 binding to the promoter of mouse *Glut1.*

E. Luciferase assay of *pGlut1*-WT-*Luc* or *pGlut1-mut-Luc* in COS cells co-transfected with RUNX2 or Runx1 expression vector (n=6).

F. Expression of osteoblast marker genes in WT, *Runx2-/- and Shn3-/-* osteoblasts (n=6).

G. Glucose uptake in WT, *Runx2-/- and Shn3-/-* osteoblasts measured by the uptake rate of 2-DG (n=6).

H-I. Alcian blue/alizarin red staining of skeletal preparations of E16.5 (H) and 18.5 (I) *Glut1*$_{osx}$*+/-, Runx2+/-, Glut1*$_{osx}$*+/-;Runx2+/-* and *Runx2-/-* embryos.

J. Alcian blue staining of histological sections of femurs of E18.5 *Glut1*$_{osx}$*+/-, Runx2+/-, Glut1*$_{osx}$*+/-;Runx2+/-* and *Runx2-/-* embryos.

K. In situ hybridization analysis of *Osteocalcin, Bsp* and *α1(X) Collagen* expression, in E18.5 *Glut1*$_{osx}$*+/-, Runx2+/-* and *Glut1*$_{osx}$*+/-;Runx2+/-* femurs.

L. Bone histomorphometric analysis of L4 vertebrae of 3 month-old of *Glut1fl/+, Glut1*$_{ocn}$*+/-, Runx2+/-* and *Glut1*$_{ocn}$*+/-;Runx2+/-* female mice (n=9-12).

M. RUNX2 and *α*1(I)Collagen accumulations and AMPK*α*1 and SMURF1 phosphorylation in femurs of E18.5 *Glut1fl/+, Glut1*$_{osx}$*+/-, Runx2+/-,* and *Glut1*$_{osx}$*+/-; Runx2+/-* embryos.

N. Alcian blue/alizarin red staining of skeletal preparations of E18.5 *Glut1*$_{osx}$*+/-;Runx2+/-* embryos carried by mothers treated with STZ (150mg/kg) or vehicle.

All error bars represent standard error of the mean. *denotes $p \leq 0.05$, and # denotes $p \leq 0.001$ compared to control when analyzed by Student's t tests.

Supplemental Figures

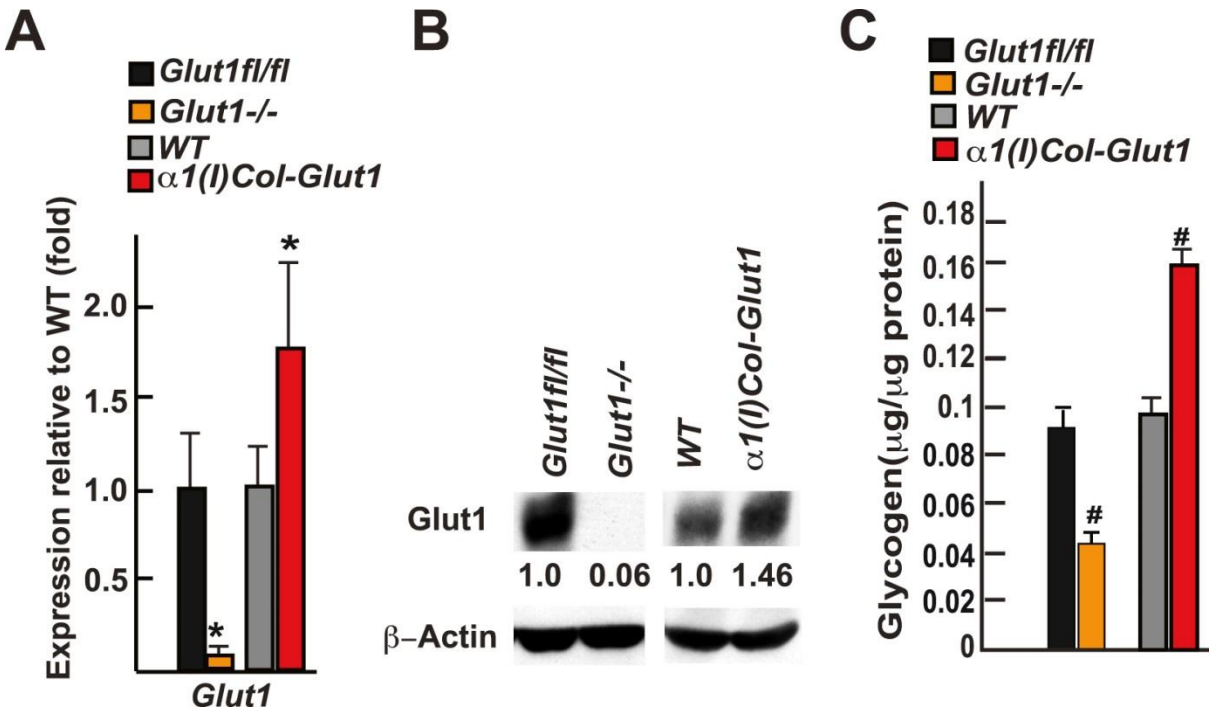

Figure S1. Insulin-independent glucose uptake in osteoblasts (related to Figure 1)

A. *Glut1* expression (qPCR) in *Glut1fl/fl* (n=7), *Glut1-/-* (n=9), WT (n=8) and *α1(I)Col-Glut1* (n=6) osteoblasts.

B. Western blot of Glut1 in *Glut1-/-* and *α1(I)Col-Glut1* osteoblasts.

C. Glycogen content in *Glut1fl/fl* (n=6), *Glut1-/-* (n=6) WT (n=6) and *α1(I)Col-Glut1* osteoblasts (n=6).

All error bars represent standard error of the mean. *denotes $p \leq 0.05$, and # denotes $p \leq 0.001$ compared to control when analyzed by Student's t tests.

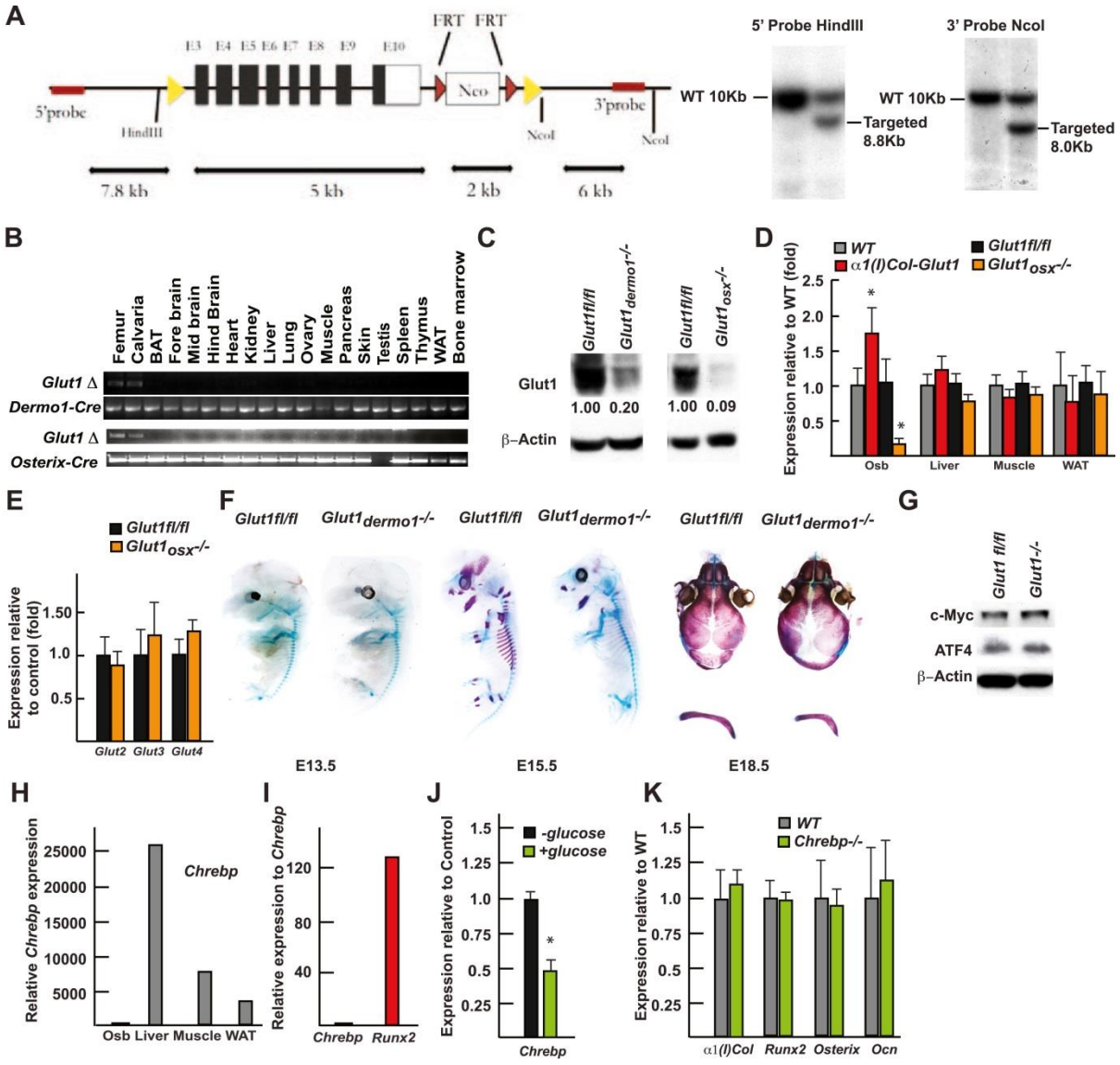

Figure S2. Glucose uptake is necessary for osteoblast differentiation during development (related to Figure 2)

A. Targeting strategy used to generate a floxed allele of *Glut1* and southern blots on WT and targeted ES cell DNA digested with HindIII and NcoI.

B. PCR analysis of *Glut1* deletion allele in various tissues in *Glut1*$_{demor1}$*-/-* and *Glut1*$_{osx}$*-/-* mice.

C. Western blot analysis of Glut1 accumulation in bones of E18.5 *Glut1*$_{demor1}$*-/-*, *Glut1*$_{osx}$*-/-* and *Glut1fl/fl* embryos.

D. qPCR analysis of *Glut1* expression in osteoblasts (osb), liver, muscle and WAT of *Glut1fl/fl* (n=6),

Glut1$_{osx}$-/- (n=7), WT (n=7) and *α1(I)Col-Glut1* (n=7) mice.

E. Expression of *Glut2, Glut3 and Glut4* (qPCR) in *Glut1fl/fl* (n=6) and *Glut1$_{osx}$-/-* (n=7) osteoblasts.

F. Alcian blue/alizarin red staining of skeletal preparations of E13.5, E15.5 and E18.5 *Glut1$_{dermo1}$-/-* and *Glut1fl/fl* embryos.

G. Western blot of ATF4 and c-Myc in *Glut1fl/fl* and *Glut1-/-* osteoblasts.

H. qPCR analysis of *Chrebp* expression in osteoblasts (Osb), liver, muscle and white adipose tissue (WAT).

I. qPCR analysis of *Chrebp* and *Runx2* expression in osteoblasts.

J. qPCR analysis of *Chrebp* expression in osteoblasts treated with or without glucose (n=4 of each samples).

K. qPCR analysis of *α1(I)Col1, Runx2, Osterix* and *Osteocalcin* expression in WT and *Chrebp-/-* osteoblasts (n=4 of each genotype).

All error bars represent standard error of the mean. *denotes $p \leq 0.05$, and # denotes $p \leq 0.001$ compared to control when analyzed by Student's t tests.

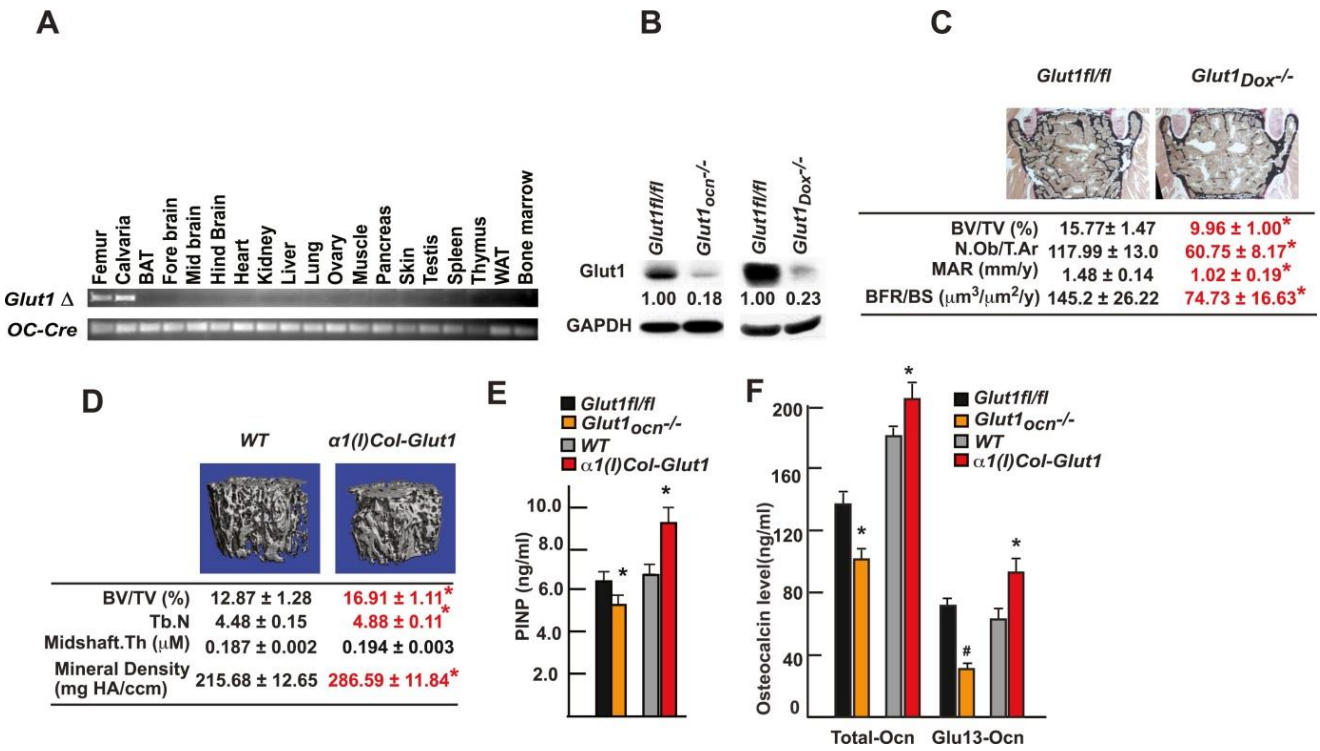

Figure S3. Glucose uptake in osteoblasts is necessary for bone formation and glucose homeostasis post-natally (related to Figure 3)

A. PCR analysis of *Glut1* deletion allele in various tissues in *Glut1*$_{ocn}$*-/-* mice.

B. Western blot analysis of Glut1 accumulation in bones of *Glut1fl/fl* and *Glut1*$_{ocn}$*-/-* mice and *Glut1*$_{Dox}$*-/-* mice, in which *Glut1* expression was inducibly deleted post-natally.

C. Bone histomorphometric analysis of L4 vertebrae of 3 month-old *Glut1fl/fl* females (n=6) and *Glut1*$_{Dox}$*-/-* (n=6) fed doxycycline diet (625mg/kg, TD.09651 Harlan) throughout pregnancy until 6 weeks old, and then fed with normal chow from week 6 to 12 weeks of age to induce *Glut1* deletion.

D. μCT analysis of proximal femurs of WT (n=8) and *α1(I)Col-Glut1* (n=8) male mice.

E. Serum levels of PINP of *Glut1fl/fl* (n=12), *Glut1*$_{ocn}$*-/-* (n=12), WT (n=8) and *α1(I)Col-Glut1* mice (n=8) mice at 3 month of age.

F. Serum levels of total and undercarboxylated forms of osteocalcin (Glu13-Ocn) in 3 month-old

Glut1fl/fl (n=10), *Glut1*$_{ocn}$*-/-* (n=10), WT (n=8) and *α1(I)Col-Glut1* mice (n=8) mice.

All error bars represent standard error of the mean. *denotes $p \leq 0.05$, and # denotes $p \leq 0.001$ compared to control when analyzed by Student's t tests.

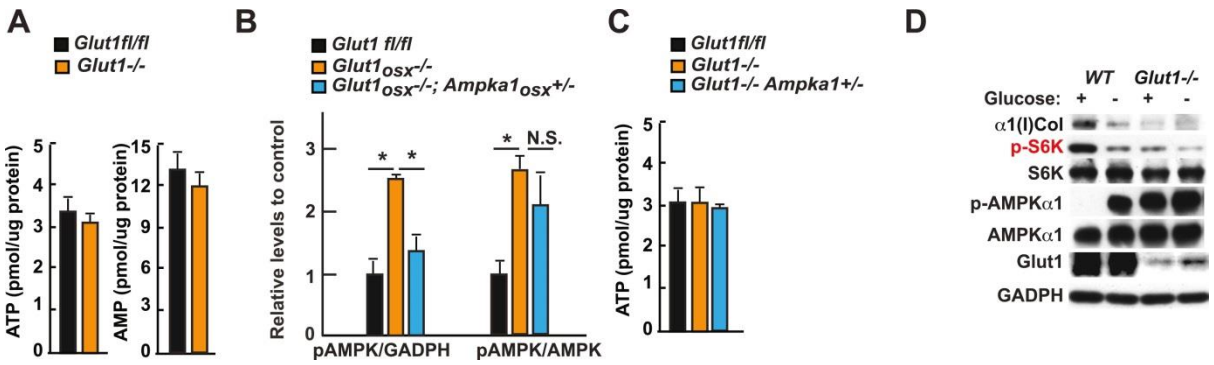

Figure S4. Glucose uptake favors osteoblast differentiation and bone formation by inhibiting AMPK (related to Figure 4)

A. ATP and AMP contents in *Glut1fl/fl* and *Glut1-/-* osteoblasts (n=6 of each group).

B. Quantification of levels of p-AMPK and p-AMPK/AMPK in *Glut1fl/fl,* $Glut1_{osx}$*-/-* and $Glut1_{osx}$*-/-;*$Ampka1_{osx}$*+/-* osteoblasts (n=6).

C. ATP content in *Glut1fl/fl, Glut1-/-* and *Glut1-/-;Ampka1+/-* osteoblasts (n=6 of each group).

D. *α*1(I)Collagen accumulation, AMPK and P70S6K phosphorylation in WT, and *Glut1-/-* osteoblasts cultured with or without 5mM glucose for 8 hrs.

All error bars represent standard error of the mean. *denotes p ≤ 0.05, and # denotes p ≤ 0.001 compared to control when analyzed by Student's t tests.

A

M.musculus	Ser148:	RIGGGGSVVDC
R.norvegicus	Ser148:	RIGGGGSVVDC
H.sapiens	Ser148:	RIGTGGSVVDC
P.troglodytes	Ser148:	RIGTGGSVVDC
B.taurus	Ser148:	RIGTGGSVVDC
G.gallus	Ser148:	RIGTGGSVVDC

B

	Score	Expectation	MD-score	Peptide Sequence
Ser148	80.25	0.0000011	37.47	R.IGTGGSVVDCR.G + Phospho (ST)

C

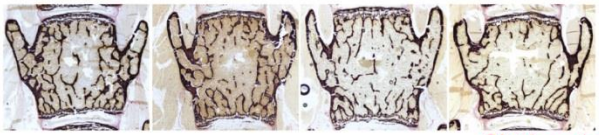

	Glut1fl/fl	*Smurf1+/-*	*Glut1$_{ocn}$-/-*	*Glut1$_{ocn}$-/-; Smurf1+/-*
BV/TV (%)	17.63 ± 0.62	16.76 ± 0.80	12.16 ± 0.76#	12.53 ± 0.88*
N.Ob/T.Ar	177.28 ± 8.29	150.82 ± 7.93	130.0 ± 6.95*	112.0± 5.67*
MAR (mm/y)	1.60 ± 0.05	1.64 ± 0.14	1.15± 0.09*	1.22 ± 0.13*
BFR/BS ($\mu m^3/\mu m^2/y$)	155.19 ± 17.40	143.17 ± 21.92	80.00 ± 10.27*	86.49 ± 10.0*

Figure S5. Runx2 cannot induce proper osteoblast differentiation if glucose uptake is hampered (related to Figure 5)

A. Putative AMPK phosphorylation site in Smurf1 of various species.

B. Mass spectrometric analysis of phosphorylation sites in Smurf1 phosphorylated by AMPK in vitro.

C. Bone histomorphometric analysis of L4 vertebrae of 3 month-old of *Glut1fl/fl* (n=10), *Smurf1+/-* (n=10), *Glut1$_{ocn}$-/-* (n=8) and *Glut1$_{ocn}$-/-;Smurf1+/-* (n=9) male mice.

All error bars represent standard error of the mean. *denotes $p \leq 0.05$, and # denotes $p \leq 0.001$ compared to control when analyzed by Student's t tests.

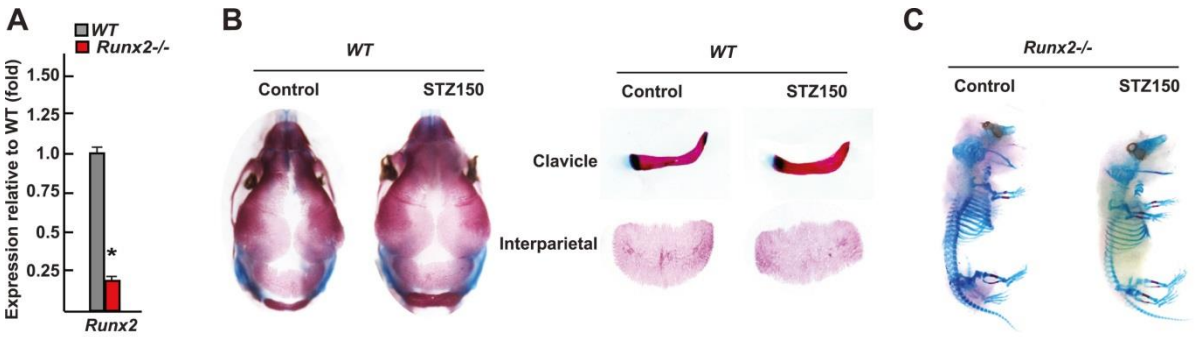

Figure S6. Glucose can initiate bone formation in *Runx2*-deficient embryos (related to Figure 6)

A. qPCR analysis of *Runx2* expression in *Runx2-/-* osteoblasts (n=6 of each group).

B. Alcian blue/alizarin red staining of skulls of E18.5 WT embryos carried by STZ (150mg/kg)-treated or vehicle-treated mothers.

C. Alcian blue/alizarin red staining of skeletal preparations of E18.5 *Runx2-/-* embryos carried by STZ(150mg/kg)-treated or vehicle-treated mothers.

All error bars represent standard error of the mean. *denotes $p \leq 0.05$, and # denotes $p \leq 0.001$ compared to control when analyzed by Student's t tests.

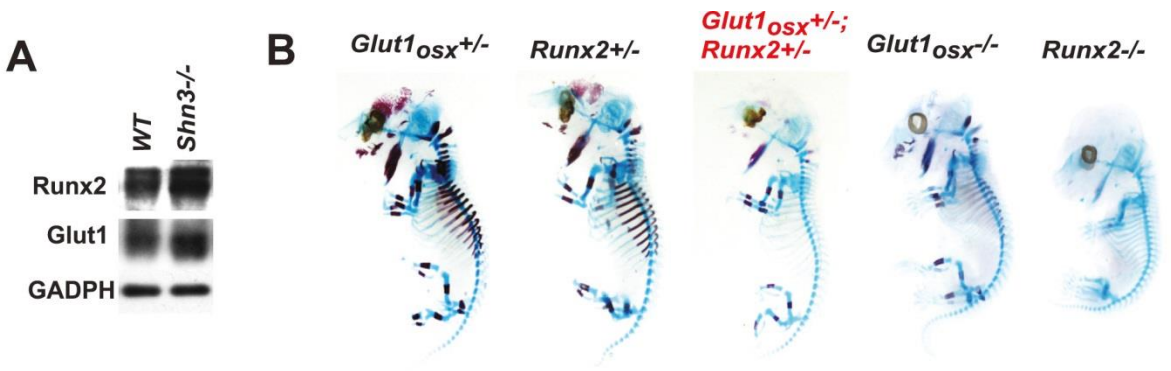

C

Blood Glucose (mg/dl)	Mothers	Fetus
Control	151.8 ± 7.57	45.0 ± 1.92
STZ (150 mg/kg)	349.6 ± 16.64*	233.7 ± 33.5*

Figure S7. The reciprocal regulation between Runx2 and *Glut1* determines bone formation (related to Figure 7)

A. Western blot analysis of RUNX2 and GLUT1 accumulation in WT and *Shn3-/-* osteoblasts.

B. Alcian blue/alizarin red staining of skeletal preparations of E15.5 *Glut1$_{osx}$+/-, Runx2+/-, Glut1$_{osx}$+/-;Runx2+/-, Glut1$_{osx}$-/-* and *Runx2-/-* embryos.

C. Blood glucose levels of STZ-treated mother and their E18.5 *Glut1$_{osx}$+/-;Runx2+/-* fetus (n=5 of each group).

All error bars represent standard error of the mean. *denotes p ≤ 0.05, and # denotes p ≤ 0.001 compared to control when analyzed by Student's t tests.

CHAPTER III: A single amino acid explains how Smurf1 regulate osteoblast differentiation, bone formation and glucose homeostasis

Junko Shimazu, Jianwen Wei, Gerard Karsenty. *Cell Reports 15*, 27-35 (2016).

Preface

The completion of this work is owed to the contribution of the people represented on the authorship list. I obtained generous help of others listed below. Dr. Jianwen Wei analyzed adult skeletal phenotype and critically read the manuscript. Dr. Chyuan-Sheng (Victor) Lin gave generous help to generate *Smurf1 S148A* knock-in mice. Dr. Patricia Ducy critically read this manuscript. *Smurf1*+/- mice were provided by Dr. Jeffrey L. Wrana. Under the instruction of Dr. Gerard Karsenty, I conceptualized and performed the rest of described experiments. The manuscript was written and edited by Dr. Karsenty and myself.

This work is supported by the RO1DK104727-A1 and PO1AG032959-06A1 (G.K.), Honjo International Scholarship (J.S.). The training program in Genetics and Development (J.S.) is supported by an NIH T32 training grant from the National Institute of General Medical Science.

A single amino acid explains Smurf1 ability to regulate osteoblast differentiation, bone formation, and glucose homeostasis

Junko Shimazu[1], Jianwen Wei[1], Gerard Karsenty[1*]

[1] Department of Genetics & Development, College of Physicians and Surgeons, Columbia University, New York, NY 10032, USA

*Address correspondence to: Gerard Karsenty, Department of Genetics and Development, 701W 168th Street, Room 1602A HHSC, New York, New York 10032, USA. Phone: 212.305.4011; Fax: 212.923.2090; E-mail: gk2172@columbia.edu.

Summary

The E3 ubiquitin ligase Smurf1 targets the master regulator of osteoblast differentiation Runx2, for degradation yet the function of Smurf1 if any during osteoblast differentiation in vivo is ill-defined. Here we show that Smurf1 prevents osteoblast differentiation by decreasing Runx2 accumulation in osteoblasts. Remarkably, mice harboring a substitution-mutation at serine 148 (S148) in Smurf1 that prevents its phosphorylation by AMPK (*Smurf1*$^{ki/ki}$) display an equally severe premature osteoblast differentiation phenotype as *Smurf1-/-* mice, a high bone mass and are also hyperinsulinemic and hypoglycemic. Consistent with the fact that Smurf1 targets the insulin receptor for degradation, there is in *Smurf1*$^{ki/ki}$ mice an increase in insulin signaling in osteoblasts that triggers a rise in the circulating levels of osteocalcin, a hormone that favors insulin secretion. These results identify Smurf1 as a determinant of osteoblast differentiation during development, of bone formation and glucose homeostasis post-natally and demonstrate the necessity of S148 for these functions.

Introduction

The transcription factor Runx2 has many attributes of a master regulator of osteoblast differentiation. In its absence, there are no osteoblasts anywhere in the skeleton and its haplo-insufficiency, by delaying osteoblast differentiation in bone forming through intramembranous ossification, results in a cleidocranial dysplasia (CCD), a disease characterized by open fontanelles and short clavicles (Ducy et al., 1997; Komori et al., 1997c; Lee et al., 1997d; Mundlos et al., 1997d; Otto et al., 1997a). Conversely, an increase in Runx2 activity as seen in mice and humans lacking one allele of *Twist*, results in craniosynostosis because of a premature osteoblast differentiation in the skull leading to early closure of the sutures (Bialek et al., 2004).

Not surprisingly given the paramount importance of this transcription factor for skeletogenesis, the mechanisms regulating the accumulation of Runx2 in cells of the osteoblast lineage have been intensively studied. Runx2 accumulation in osteoblast progenitor cells and differentiated osteoblasts is regulated in part by ubiquitination and several E3 ubiquitin ligases have been implicated in targeting Runx2 for degradation (Jones et al., 2006; Kaneki et al., 2006; Zhao et al., 2003). One of them Smurf1, interacts with Runx2 and other proteins regulating bone mass accrual such as Smad1, Smad5, MEKK2 and the insulin receptor (InsR) (Wei et al., 2014a; Yamashita et al., 2005; Zhu et al., 1999). Consistent with these biochemical findings, forced expression of *Smurf1* in osteoblasts inhibits, whereas deletion of *Smurf1* in all cells favors bone formation in adult mice (Yamashita et al., 2005; Zhao et al., 2004). It has been proposed that Smurf1 achieves these functions in part by targeting MEKK2 for degradation (Yamashita et al., 2005). Surprisingly given the biochemical

evidence indicating that Smurf1 favors the degradation of Runx2, no loss of function study has yet addressed the role of Smurf1 as a regulator of osteoblast differentiation in vivo.

A second important question regarding Smurf1 biology is to identify a domain if not a single amino acid that would confer to this protein the ability to target Runx2 for degradation in vivo. This question is even more relevant in view of the demonstration that in vitro, Smurf1 must be phosphorylated by AMPK on serine 148 (S148) in order to trigger the degradation of Runx2 (Wei et al., 2015e). This raises the question of the biological importance of this residue in the functions of Smurf1.

We have addressed the aforementioned questions by analyzing *Smurf1-/-* mice and mice harboring a mutated form of *Smurf1* in which S148 is mutated to alanine (*Smurf1*$^{ki/ki}$). We show here that *Smurf1* inhibits osteoblast differentiation through its ability to target Runx2 for degradation and that this function requires the presence of S148. Remarkably *Smurf1*$^{ki/ki}$ mice are also hypoglycemic and hyperinsulinemic because S148 is needed for Smurf1 ability to target the InsR for degradation. As a result, there is an accumulation of the InsR in bones of *Smurf1*$^{ki/ki}$ mice. This leads to an increase in the circulating levels of the bioactive form of the bone-derived hormone osteocalcin that favors insulin secretion and can cause hypoglycemia (Ferron et al., 2010a; Lee et al., 2007). These results define critical functions of Smurf1 in cells of the osteoblast lineage throughout life and highlight the importance of S148 for Smurf1 ability to target Runx2 and InsR for degradation.

Materials and Methods

Mice generation

To generate *Smurf1*$^{Ki/+}$ mice, a mutation was introduced into a BAC by recombineering using *galK* selection system (Warming et al., 2005). In the first step, the *galK* cassette was inserted into BAC by homologous recombination and clones were obtained through positive selection on minimal media plates in which galactose was the only carbon source. The successful recombination was validated by PCR analysis. In the second step, the *galK* cassette was substituted by double stranded oligonucleotides with the modified base-pair in the middle of the homology arms flanking the *galK* casette. This step was achieved by negatively selecting against the *galK* cassette by resistance to 2-deoxy-galactose (DOG) on plates with glycerol as the carbon source. Clones in which *galK* cassette is replaced by a mutation of interest were identified by PCR and sequencing. A *frt-neo-frt* (*FNF*) cassette was inserted upstream of the mutation and retrieved into pMCS-DTA by homologous recombination using standard protocol. The targeting vector that was verified by PCR, diagnostic digestions and sequencing, was electroporated into ES cells, positive ES cells were identified by PCR screening and sequencing. Selected ES cells were injected in 129Sv/EV blastocysts to generate chimeric mice. Chimeric mice were crossed to Gt(ROSA)26Sor$^{tm1(FLP1)Dym}$ to remove the neomycin resistance cassette.

Runx2+/- mice were generated previously (Otto et al., 1997a). *Smurf1*+/- mice were a generous gift of Dr. Jeff Wrana (U of Toronto, Canada) (Narimatsu et al., 2009). All mice strains were maintained on a C57/129 mixed background except for *Runx2*+/- mice, which are maintained on C57 background.

Littermates were used as controls in all experiments.

Cell culture

Primary mouse calvaria osteoblasts were cultured as described previously (Ducy and Karsenty, 1995). To determine formation of mineralized nodule, von Kossa staining was performed on osteoblasts cultured in differentiation medium supplemented with 5mM β-glycerophosphate and 100ug/mL ascorbic acid for 7 days. To detect the S148 phosphorylation in Smurf1, osteoblasts isolated from *Smurf1*$^{ki/ki}$ and WT pups were incubated overnight in glucose free KRH buffer (50mM HEPES pH7.4, 136mM NaCl, 4.7mM KCl, 1.25mM MgSO4, 1.25mM CaCl2 and 0.1% BSA) and followed by western blot analysis.

DNA transfection experiments

Myc-Smurf1 WT and *S148A* plasmids were constructed by inserting a full-length cDNA of mouse *Smurf1* WT or *S148A* into pcDNA^{TM} 3.1 /myc-His B vector (Invitrogen). *Myc-Smurf1* WT or *S148A* was co-transfected with *Flag-Runx2* or the human *InsR* cDNA expression constructs (Wei et al., 2014a; Wei et al., 2015e) in COS-7 cells. DNA transfection experiments were performed using Lipofectamin 2000 (Invitrogen) according to manufacturer's protocol.

Western blot analysis

Anti-Runx2 antibody (Santa Cruz Biotech Inc.), anti-β-ACTIN (Sigma), Anti-Smurf1 and Anti-Phospho-Ser148 Smurf1 (GenScript Inc.) were used. Others antibodies were obtained from Cell Signaling Technology. All western blot analyses were repeated at least three times, with different

samples.

Gene expression analysis

RNA samples were extracted using TRIZOL reagent (Invitrogen). Using two micrograms of total RNA, cDNA preparation was carried out following standard protocols. The cDNAs were used as templates for quantitative PCR analyses using CFX-Connect realtime PCR system (Bio-Rad). Expression levels of each gene analyzed by qPCR were normalized using *GAPDH* (*glyceraldehyde-3-phosphate dehydrogenase*) expression levels as an internal control. The sequences of specific primers used in this study were previously described (Obri et al., 2014).

Skeletal preparation and analysis

Alcian blue/alizarin red staining of the skeletal preparation was conducted according to standard protocols (McLeod, 1980). Littermate controls were analyzed in all experiments. Quantifications of the length of clavicles as well as the area of the opening of the skull were made using ImageJ.

Bone histomorphometry

This analysis was performed on L3 and L4 vertebrae of 2-month-old female mice as described previously (Chappard et al., 1987; Parfitt et al., 1987a). Mineralized bone volume over the total tissue volume (BV/TV), osteoblast number per tissue area (N.Ob/T.Ar) as well as trabecular number (Tb.N), and bone formation rate per bone surface (BFR/BS) were measured by conducting Von Kossa/ van Gieson staining, toluidine blue staining and calcein double-labeling, respectively. Osteoclasts parameters were measured by TRAP staining followed by counterstain with hematoxylin. Osteoclasts

were defined as multinucleated dark red cells along the bone surface. Histomorphometric analysis was performed using the Osteomeasure System (OsteoMetrics).

Biochemistry

ELISAs were performed according to manufacturer's instructions to measure mouse insulin (EZRMI-13K, Millipore) and undercarboxylated osteocalcin (Ferron et al., 2010m). For AMPK phosphorylation assay**,** GST-Smurf1 and GST-Runx2 constructs were generated and purified as previously described (Ferron et al., 2013; Wei, 2015). AMPK phosphorylation assay of GST-Smurf1 WT and S148A was performed using previously described method (Wei, 2015).

GST-Pulldown assay

GST-Smurf1 WT and GST-Smurf1S148A were bound to glutathione agarose beads (GE Healthcare) and blocked overnight at 4˚C in 5%BSA with end-over-end mixing. Beads were washed with AMPK assay buffer 5 times and AMPK phosphorylation assay was followed. Beads were washed with binding buffer (50mM Tris-Hcl pH 7.5, 100mM NaCl, 50mM β-glycerophosphate, 10% glycerol, 1% Tween-20, 1mM EDTA, 25mM NaF) 5 times. Cell lysates of transfected COS-7 cells were incubated with 25µg of GST for 2 hours at 4˚C with end-over-end mixing. This mixture was centrifuged and supernatants were mixed with GST-Smurf1 WT or S148A in 500µL of binding buffer for 2 hours at 4˚C with end-over-end mixing. The mixtures were washed 5 times and analyzed by SDS-PAGE followed by immunoblotting.

In situ hybridization

Tissues were fixed in 4% paraformaldehyde/PBS overnight at 4°C and then embedded in paraffin after

serial of dehydrations. Tissues were sectioned at 5μm. In situ hybridization was performed using ^{35}S-labeled riboprobe as described (Ducy et al., 1997). The *α1(I)Col, Bsp,* and *Osteocalcin* probes were prepared as previously described (Takeda et al., 2001a). Hybridizations were performed overnight at 55°C, and washes were performed at 63°C. Autoradiography were performed as previously described (Sundin et al., 1990) and nuclei were counterstained with DAPI.

Statistics

All data are presented as mean ± standard error of mean. In this paper, statistical analysis was performed by unpaired Student's t test. * denotes P ≤ 0.05, and # denotes P≤ 0.005 compared to control.

Results

Smurf1 regulates osteoblast differentiation

To determine whether *Smurf1* affects osteoblast differentiation in vivo, we analyzed in P4 and P10 *Smurf1-/-* mice two parameters that reflect the activity of Runx2 in cells of the osteoblast lineage during development: the closure of sutures in the skull and the length of clavicles.

Alcian blue/alizarin red staining of skeletal preparations showed that clavicles of *Smurf1-/-* mice were significantly longer than those of WT mice (Figure 1A) and sagittal sutures of *Smurf1-/-* skulls showed evidence of craniosynostosis (Figure 1B-C). Next, we analyzed by in situ hybridization the expression of *Bone sialoprotein* (*Bsp*), a biomarker of osteoblast differentiation (Bialek et al., 2004) in calvarial bones of E14.5 WT and *Smurf1-/-* embryos. The expression of *Bsp* was stronger in calvarial bones of E14.5 *Smurf1-/-* than in those of WT embryos (Figure 1D). The same was true for the expression of *Bsp* and *Osteocalcin* (*Ocn*), another osteoblast differentiation marker, in femurs of E14.5 *Smurf1-/-* embryos whether this was assayed by qPCR or in situ hybridization (Figure 1E-G). As a negative control in this experiment, we analyzed the expression of *α1(I) Collagen* (*α1(I)Col*), that is not regulated by Runx2 in vivo (Wei et al., 2015e).

To link this premature osteoblast differentiation to an increase in Runx2 accumulation, we analyzed the abundance of this transcription factor in the skulls of *Smurf1-/-* and WT littermates and observed that Runx2 was more abundant in *Smurf1-/-* than WT skulls (Figure 1H). This latter result explains the increase in the expression of *Ocn,* a target of Runx2 (Ducy et al., 1997) (Figure 1E, 1G and 1I). Taken together, these results established that Smurf1 is a negative regulator of osteoblast

differentiation in vivo, and suggested that this function occurs in part by targeting Runx2 for degradation.

Serine 148 is necessary for Smurf1 ability to inhibit osteoblast differentiation and bone formation

In vitro the phosphorylation of Smurf1 by AMPK at serine 148 (S148) is needed for its ability to target Runx2 for degradation (Wei et al., 2015e). Thus, we tested the importance of this residue for Smurf1 ability to inhibit osteoblast differentiation by analyzing mutant mice harboring a S148A mutation in *Smurf1* (*Smurf1*$^{ki/ki}$) (Figure S1A-S1C). A western blot analysis verified that the phosphorylation of Smurf1 at S148 was abolished in *Smurf1*$^{Ki/Ki}$ osteoblasts although Smurf1 accumulation was not affected (Figure 2A).

Alcian blue/alizarin red staining of skeletal preparations showed that clavicles were significantly longer and sagittal sutures of the skulls more closed in *Smurf1*$^{ki/ki}$ than in newborn WT mice (Figure 2B-D). Accordingly, osteoblasts isolated from *Smurf1-/-* or *Smurf1*$^{ki/ki}$ mice formed more mineralized nodules than WT osteoblasts (Figure S2A). In vivo, *Bsp* expression was stronger in calvarial bones of E14.5*Smurf1*$^{ki/ki}$ embryos than in those of WT embryos (Figure 2E). The expression of *Ocn* started earlier and the one of *Bsp* was stronger in femurs of *Smurf1*$^{ki/ki}$ than in those of E14.5 WT embryos indicating that osteoblast differentiation occurred earlier in *Smurf1*$^{ki/ki}$ embryos throughout the skeleton. In contrast, no overt difference in the expression of *α1(I)Col* between E14.5 WT and

Smurf1$^{ki/ki}$ embryos was noted (Figure 2F). The expression of *Ocn* and *Bsp* was also significantly higher in femurs of E14.5 *Smurf1*$^{ki/ki}$ embryos than in those of WT embryos when measured by qPCR (Figure 2G-H).

That *Bsp* and *Ocn* expression was higher in femurs of *Smurf1*$^{ki/ki}$ mice at P10 (Figure S2B-S2C) suggested that this S148A mutation in *Smurf1* may affect bone biology post-natally. Indeed, two month-old *Smurf1*$^{ki/ki}$ mice had a higher bone mass and higher trabeculae number than WT littermates because of an increase in their osteoblast number and bone formation rate (Figure 2I-L). These phenotypes could be traced in part to an increase in the accumulation of Runx2 in *Smurf1*$^{ki/ki}$ skulls (Figure 2M). To ascertain that the phosphorylation of Smurf1 at S148 is needed to target Runx2 for degradation, we performed a GST-Pull-down assay and observed that the interaction between Smurf1 and Runx2 that occurred upon phosphorylation of Smurf1 by AMPK was abrogated when S148 was mutated to alanine. Accordingly, forced expression of WT but not *S148A Smurf1* decreased the accumulation of Runx2 in COS-7 cells (Figure 2N-O). Taken collectively, these data establish the importance of S148 for Smurf1 ability to inhibit osteoblast differentiation and bone formation.

Smurf1 inhibits osteoblast differentiation by targeting Runx2 to degradation

If S148 is required for Smurf1 inhibition of osteoblast differentiation because it targets Runx2 for degradation, mutating S148 to alanine in Smurf1 should increase Runx2 accumulation and rescue in part, the CCD phenotype seen in *Runx2+/-* mice (Komori et al., 1997c; Otto et al., 1997a). To test this hypothesis, we analyzed *Runx2+/-;Smurf1*$^{ki/ki}$ mice.

Alcian blue/alizarin red staining of skeletal preparations showed a marked improvement of the CCD phenotype in *Runx2+/-;Smurf1*$^{ki/ki}$ compared to *Runx2+/-* mice (Figure 3A-C) while a western blot verified that Runx2 accumulation was increased in *Runx2+/-;Smurf1*$^{ki/ki}$ skulls (Figure 3D). This increase in Runx2 accumulation resulted in an improved osteoblast differentiation as shown by the increased *Ocn* expression in E15.5 *Runx2+/-;Smurf1*$^{ki/ki}$ compared to *Runx2+/-* embryos (Figure 3E). *Ocn* and *Bsp* expression was also significantly higher in bones of *Runx2+/-;Smurf1*$^{ki/ki}$ compared to those of *Runx2+/-* mice at P10 when measured by qPCR (Figure 3F-G).

Hence, the ability of Smurf1 to target Runx2 for degradation explains to a large extent why this E3 ubiquitin ligase inhibits osteoblast differentiation. That the rescue of the CCD phenotype was not complete in *Runx2+/-;Smurf1*$^{ki/ki}$ mice is consistent with the notion that Smurf1 also acts through additional mechanisms to prevent osteoblast differentiation such as targeting MEKK2, Smad1 and Smad5 for degradation (Yamashita et al., 2005; Zhu et al., 1999).

S148 is needed for Smurf1 ability to regulate glucose homeostasis

To determine if S148 is necessary for the interaction of Smurf1 with its other substrates, we focused on the insulin receptor (InsR) because both *Smurf1-/-* mice and *Smurf1*$^{ki/ki}$ mice were hypoglycemic and hyperinsulinemic (Figure 4A-C).

Following its phosphorylation by AMPK, WT but not S148A Smurf1 interacts readily with the InsR (Figure 4D) and forced expression of WT but not *S148A Smurf1* decreased the accumulation of InsR in COS-7 cells (Figure 4E). In vivo, the accumulation of the InsR was higher in *Smurf1-/-* and

Smurf1$^{ki/ki}$ than in WT bones. That the accumulation of the InsR was not affected in other insulin target tissues, such as liver, white adipose tissue (WAT), and muscle in *Smurf1-/-* and *Smurf1*$^{ki/ki}$ mice (Figure 4F) is explained in part by the fact that *Smurf1* expression is markedly higher in bone than in the liver, WAT and muscle (Figure 4G).

Given these observations, we tested whether the hypoglycemia seen in *Smurf1*$^{ki/ki}$ mice resulted in part, from an increase in insulin signaling in osteoblasts. Since insulin signaling in osteoblasts inhibits *Osteoprotegerin (Opg)* expression (Ferron et al., 2010a), we used the expression of this gene in *Smurf1*$^{ki/ki}$ femurs as a readout of insulin signaling in osteoblasts. In agreement with the increased accumulation of the InsR in bone (Figure 4F), *Opg* expression was decreased in *Smurf1*$^{ki/ki}$ compared to control femurs (Figure 4H) whereas *Rankl* expression was unchanged (Figure 4I). This decrease in *Opg* expression provides an explanation for the significant increase in the number of osteoclasts observed in the bones of adult *Smurf1*$^{ki/ki}$ mice (Figure 4J). This increase in bone resorption parameters was not of sufficient amplitude to compensate for the increase in bone formation parameters. As a result, *Smurf1*$^{ki/ki}$ mice had a high bone mass (Figure 2I-L).

Since bone resorption is the mechanism whereby osteocalcin, a hormone that favors insulin secretion, is activated by decarboxylation (Ferron et al., 2010a), we measured the circulating levels of undercarboxyated and bioactive osteocalcin in control and *Smurf1*$^{ki/ki}$ mice and observed that circulating undercarboxylated osteocalcin levels were approximately three-fold higher in *Smurf1*$^{ki/ki}$ than in control mice (Figure 4K). Such an increase in circulating osteocalcin levels should lead to a

hyperinsulinemia and hypoglycemia as seen in *Smurf1*$^{ki/ki}$ mice (Figure 4B-C). To demonstrate that this increase in osteocalcin activity contributes to the hypoglycemia observed in *Smurf1*$^{ki/ki}$ mice, we analyzed *Smurf1*$^{ki/ki}$ mice lacking one allele of *Osteocalcin* (*Smurf1*$^{ki/ki}$*;Ocn+/-).* As shown in Figure 4L blood glucose levels were normal in *Smurf1*$^{ki/ki}$*;Ocn+/-* mice. These results reveal the existence of a Smurf1-InsR-osteoprotegerin-osteocalcin pathway taking place in osteoblasts and contributing to glucose homeostasis.

Discussion

The mechanisms regulating Runx2 accumulation in osteoblast progenitor cells have been a topic of intense investigation. This has led to the identification mostly on biochemical grounds, of several E3 ubiquitin ligases that would trigger Runx2 for degradation. Given the number of E3 ubiquitin ligases known to interact with Runx2, one could fear that disrupting the interaction of only one of them with Runx2 would not significantly hamper osteoblast differentiation in vivo. Instead, our investigation shows that deleting a single E3 ubiquitin ligase implicated in Runx2 degradation *Smurf1*, results in an increase in Runx2 accumulation leading to a premature osteoblast differentiation during embryonic development and increased bone formation post-natally. We further show that the majority of this function of Smurf1 requires a single amino acid, S148, be phosphorylated by AMPK (Wei, 2015). These results highlight the importance of Smurf1 and of this particular residue in this molecule in targeting Runx2 for degradation in vivo and regulating osteoblast differentiation.

The functions of Smurf1 in osteoblasts extend beyond osteoblast differentiation and bone formation since by favoring the degradation of the InsR in osteoblasts, Smurf1 is a regulator of circulating osteocalcin levels. This explains the existence of hyperinsulinemia and hypoglycemia in *Smurf1*$^{ki/ki}$ mice. Indeed, Smurf1 regulates bone resorption and the production of the active form of osteocalcin, a hormone that favors insulin secretion (Lee et al., 2007). As it is the case for its ability to regulate osteoblast differentiation, this function of Smurf1 requires the presence of S148. Altogether, our results provide a deeper understanding of the molecular regulation of Runx2 accumulation and of the endocrine functions of bone.

Acknowledgements

We thank Dr. C.-S. Lin and F. Lee for generation of *Smurf1 S148A* knock-in mice, Drs. P. Ducy and J. Wrana for critical reading of the manuscript and for providing the *Smurf1*+/- mice, respectively. This work is supported by the RO1DK104727-A1 and PO1AG032959-06A1 (G.K.), Honjo International Scholarship (J.S.) and Mandl fellowship (J.W.). The training program in Genetics and Development (J.S.) is supported by an NIH T32 training grant from the National Institute of General Medical Science.

References

Ardley, H.C., and Robinson, P.A. (2005). E3 ubiquitin ligases. Essays Biochem *41*, 15-30.

Bar-Shavit, Z. (2007). The osteoclast: a multinucleated, hematopoietic-origin, bone-resorbing osteoimmune cell. J Cell Biochem *102*, 1130-1139.

Bialek, P., Kern, B., Yang, X., Schrock, M., Sosic, D., Hong, N., Wu, H., Yu, K., Ornitz, D.M., Olson, E.N.*, et al.* (2004). A twist code determines the onset of osteoblast differentiation. Dev Cell *6*, 423-435.

Blair, H.C., and Athanasou, N.A. (2004). Recent advances in osteoclast biology and pathological bone resorption. Histol Histopathol *19*, 189-199.

Bluher, M., Michael, M.D., Peroni, O.D., Ueki, K., Carter, N., Kahn, B.B., and Kahn, C.R. (2002). Adipose tissue selective insulin receptor knockout protects against obesity and obesity-related glucose intolerance. Dev Cell *3*, 25-38.

Bolster, D.R., Crozier, S.J., Kimball, S.R., and Jefferson, L.S. (2002). AMP-activated protein kinase suppresses protein synthesis in rat skeletal muscle through down-regulated mammalian target of rapamycin (mTOR) signaling. The Journal of biological chemistry *277*, 23977-23980.

Borle, A.B., Nichols, N., and Nichols, G., Jr. (1960). Metabolic studies of bone in vitro. I. Normal bone. The Journal of biological chemistry *235*, 1206-1210.

Boyce, B.F., and Xing, L. (2007). The RANKL/RANK/OPG pathway. Curr Osteoporos Rep *5*, 98-104.

Boyle, W.J., Simonet, W.S., and Lacey, D.L. (2003). Osteoclast differentiation and activation. Nature *423*, 337-342.

Bruning, J.C., Michael, M.D., Winnay, J.N., Hayashi, T., Horsch, D., Accili, D., Goodyear, L.J., and Kahn, C.R. (1998). A muscle-specific insulin receptor knockout exhibits features of the metabolic syndrome of NIDDM without altering glucose tolerance. Mol Cell *2*, 559-569.

Cao, Y., and Zhang, L. (2013). A Smurf1 tale: function and regulation of an ubiquitin ligase in multiple cellular networks. Cell Mol Life Sci *70*, 2305-2317.

Carvalho, K.C., Cunha, I.W., Rocha, R.M., Ayala, F.R., Cajaíba, M.M., Begnami, M.D., Vilela, R.S., Paiva, G.R., Andrade, R.G., and Soares, F.A. (2011). GLUT1 expression in malignant tumors and its use as an immunodiagnostic marker. Clinics *66*, 965-972.

Chappard, D., Palle, S., Alexandre, C., Vico, L., and Riffat, G. (1987). Bone embedding in pure methyl methacrylate at low temperature preserves enzyme activities. Acta Histochem *81*, 183-190.

Clarke, B. (2008). Normal bone anatomy and physiology. Clin J Am Soc Nephrol *3 Suppl 3*, S131-139.

Cohn, D.V., and Forscher, B.K. (1962). Aerobic metabolism of glucose by bone. The Journal of biological chemistry *237*, 615-618.

Copp, D.H., and Shim, S.S. (1963). The homeostatic function of bone as a mineral reservoir. Oral Surgery, Oral Medicine, Oral Pathology *16*, 738-744.

Deshaies, R.J., and Joazeiro, C.A. (2009). RING domain E3 ubiquitin ligases. Annu Rev Biochem *78*, 399-434.

Dessau, W., von der Mark, H., von der Mark, K., and Fischer, S. (1980). Changes in the patterns of collagens and fibronectin during limb-bud chondrogenesis. J Embryol Exp Morphol *57*, 51-60.

DiGirolamo, D.J., Clemens, T.L., and Kousteni, S. (2012). The skeleton as an endocrine organ. Nat Rev Rheumatol *8*, 674-683.

Dikic, I., Wakatsuki, S., and Walters, K.J. (2009). Ubiquitin-binding domains - from structures to functions. Nat Rev Mol Cell Biol *10*, 659-671.

Ducy, P., and Karsenty, G. (1995). Two distinct osteoblast-specific cis-acting elements control expression of a mouse osteocalcin gene. Mol Cell Biol *15*, 1858-1869.

Ducy, P., Starbuck, M., Priemel, M., Shen, J., Pinero, G., Geoffroy, V., Amling, M., and Karsenty, G. (1999). A Cbfa1-dependent genetic pathway controls bone formation beyond embryonic development. Genes Dev *13*, 1025-1036.

Ducy, P., Zhang, R., Geoffroy, V., Ridall, A.L., and Karsenty, G. (1997). Osf2/Cbfa1: a transcriptional activator of osteoblast differentiation. Cell *89*, 747-754.

Elefteriou, F., Benson, M.D., Sowa, H., Starbuck, M., Liu, X., Ron, D., Parada, L.F., and Karsenty, G. (2006). ATF4 mediation of NF1 functions in osteoblast reveals a nutritional basis for congenital skeletal dysplasiae. Cell metabolism *4*, 441-451.

Esen, E., and Long, F. (2014). Aerobic glycolysis in osteoblasts. Curr Osteoporos Rep *12*, 433-438.

Feng, X., and McDonald, J.M. (2011). Disorders of bone remodeling. Annu Rev Pathol *6*, 121-145.

Ferrannini, E., Simonson, D.C., Katz, L.D., Reichard, G., Jr., Bevilacqua, S., Barrett, E.J., Olsson, M., and DeFronzo, R.A. (1988). The disposal of an oral glucose load in patients with non-insulin-dependent diabetes. Metabolism: clinical and experimental *37*, 79-85.

Ferron, M., Hinoi, E., Karsenty, G., and Ducy, P. (2008). Osteocalcin differentially regulates beta cell and adipocyte gene expression and affects the development of metabolic diseases in wild-type mice. Proc Natl Acad Sci U S A *105*, 5266-5270.

Ferron, M., Lacombe, J., Germain, A., Oury, F., and Karsenty, G. (2015). GGCX and VKORC1 inhibit osteocalcin endocrine functions. J Cell Biol *208*, 761-776.

Ferron, M., Settembre, C., Shimazu, J., Lacombe, J., Kato, S., Rawlings, D.J., Ballabio, A., and Karsenty, G. (2013). A RANKL-PKCbeta-TFEB signaling cascade is necessary for lysosomal biogenesis in osteoclasts. Genes Dev *27*, 955-969.

Ferron, M., Wei, J., Yoshizawa, T., Del Fattore, A., DePinho, R.A., Teti, A., Ducy, P., and Karsenty, G. (2010a). Insulin signaling in osteoblasts integrates bone remodeling and energy metabolism. Cell *142*, 296-308.

Ferron, M., Wei, J., Yoshizawa, T., Ducy, P., and Karsenty, G. (2010m). An ELISA-based method to quantify osteocalcin carboxylation in mice. Biochem Biophys Res Commun *397*, 691-696.

Florencio-Silva, R., Sasso, G.R., Sasso-Cerri, E., Simoes, M.J., and Cerri, P.S. (2015). Biology of Bone Tissue: Structure, Function, and Factors That Influence Bone Cells. Biomed Res Int *2015*, 421746.

Friedman, J.M., and Halaas, J.L. (1998). Leptin and the regulation of body weight in mammals. Nature *395*, 763-770.

Fukumoto, S., and Martin, T.J. (2009). Bone as an endocrine organ. Trends Endocrinol Metab *20*, 230-236.

Gallagher, E., Gao, M., Liu, Y.C., and Karin, M. (2006). Activation of the E3 ubiquitin ligase Itch through a phosphorylation-induced conformational change. Proc Natl Acad Sci U S A *103*, 1717-1722.

Gao, M., Labuda, T., Xia, Y., Gallagher, E., Fang, D., Liu, Y.C., and Karin, M. (2004). Jun turnover is controlled through JNK-dependent phosphorylation of the E3 ligase Itch. Science *306*, 271-275.

Gould, G.W., and Holman, G.D. (1993). The glucose transporter family: structure, function and tissue-specific expression. Biochem J *295 (Pt 2)*, 329-341.

Groesbeck, D.K., Bluml, R.M., and Kossoff, E.H. (2006). Long-term use of the ketogenic diet in the treatment of epilepsy. Dev Med Child Neurol *48*, 978-981.

Gwinn, D.M., Shackelford, D.B., Egan, D.F., Mihaylova, M.M., Mery, A., Vasquez, D.S., Turk, B.E., and Shaw, R.J. (2008). AMPK phosphorylation of raptor mediates a metabolic checkpoint. Mol Cell *30*, 214-226.

Hardie, D.G. (2007). AMP-activated/SNF1 protein kinases: conserved guardians of cellular energy. Nat Rev Mol Cell Biol *8*, 774-785.

Hardie, D.G., Ross, F.A., and Hawley, S.A. (2012). AMPK: a nutrient and energy sensor that maintains energy homeostasis. Nat Rev Mol Cell Biol *13*, 251-262.

Hauschka, P.V., Lian, J.B., Cole, D.E., and Gundberg, C.M. (1989). Osteocalcin and matrix Gla protein: vitamin K-dependent proteins in bone. Physiological Reviews *69*, 990-1047.

Hayami, R., Sato, K., Wu, W., Nishikawa, T., Hiroi, J., Ohtani-Kaneko, R., Fukuda, M., and Ohta, T. (2005). Down-regulation of BRCA1-BARD1 ubiquitin ligase by CDK2. Cancer Res *65*, 6-10.

Hwang, Y.C., Jeong, I.K., Ahn, K.J., and Chung, H.Y. (2009). The uncarboxylated form of osteocalcin is associated with improved glucose tolerance and enhanced beta-cell function in middle-aged male subjects. Diabetes Metab Res Rev *25*, 768-772.

Inoki, K., Zhu, T., and Guan, K.L. (2003). TSC2 mediates cellular energy response to control cell growth and survival. Cell *115*, 577-590.

Inui, T., Ishibashi, O., Inaoka, T., Origane, Y., Kumegawa, M., Kokubo, T., and Yamamura, T. (1997). Cathepsin K antisense oligodeoxynucleotide inhibits osteoclastic bone resorption. The Journal of biological chemistry *272*, 8109-8112.

Itzstein, C., Coxon, F.P., and Rogers, M.J. (2011). The regulation of osteoclast function and bone resorption by small GTPases. Small GTPases *2*, 117-130.

Jeyapalan, A.S., Orellana, R.A., Suryawan, A., O'Connor, P.M., Nguyen, H.V., Escobar, J., Frank, J.W., and Davis, T.A. (2007). Glucose stimulates protein synthesis in skeletal muscle of neonatal pigs through an AMPK- and mTOR-independent process. American journal of physiology Endocrinology and metabolism *293*, E595-603.

Jiang, H., Zhang, F., Kurosu, T., and Peterlin, B.M. (2005). Runx1 binds positive transcription elongation factor b and represses transcriptional elongation by RNA polymerase II: possible mechanism of CD4 silencing. Molecular and cellular biology *25*, 10675-10683.

Jones, D.C., Wein, M.N., Oukka, M., Hofstaetter, J.G., Glimcher, M.J., and Glimcher, L.H. (2006). Regulation of adult bone mass by the zinc finger adapter protein Schnurri-3. Science *312*, 1223-1227.

Joost, H.G., Bell, G.I., Best, J.D., Birnbaum, M.J., Charron, M.J., Chen, Y.T., Doege, H., James, D.E., Lodish, H.F., Moley, K.H.*, et al.* (2002). Nomenclature of the GLUT/SLC2A family of sugar/polyol transport facilitators. Am J Physiol Endocrinol Metab *282*, E974-976.

Kanazawa, I., Yamaguchi, T., Yamamoto, M., Yamauchi, M., Kurioka, S., Yano, S., and Sugimoto, T. (2009). Serum osteocalcin level is associated with glucose metabolism and atherosclerosis parameters in type 2 diabetes mellitus. J Clin Endocrinol Metab *94*, 45-49.

Kaneki, H., Guo, R., Chen, D., Yao, Z., Schwarz, E.M., Zhang, Y.E., Boyce, B.F., and Xing, L. (2006). Tumor necrosis factor promotes Runx2 degradation through up-regulation of Smurf1 and Smurf2 in osteoblasts. The Journal of biological chemistry *281*, 4326-4333.

Karsenty, G. (2006). Convergence between bone and energy homeostases: leptin regulation of bone mass. Cell Metab *4*, 341-348.

Karsenty, G., and Ferron, M. (2012). The contribution of bone to whole-organism physiology. Nature *481*, 314-320.

Karsenty, G., Kronenberg, H.M., and Settembre, C. (2009). Genetic control of bone formation. Annu Rev Cell Dev Biol *25*, 629-648.

Karsenty, G., and Oury, F. (2012). Biology without walls: the novel endocrinology of bone. Annu Rev Physiol *74*, 87-105.

Karsenty, G., and Wagner, E.F. (2002). Reaching a genetic and molecular understanding of skeletal development. Dev Cell *2*, 389-406.

Kasuga, M., Fujita-Yamaguchi, Y., Blithe, D.L., White, M.F., and Kahn, C.R. (1983). Characterization of the insulin receptor kinase purified from human placental membranes. The Journal of biological chemistry *258*, 10973-10980.

Kern, B., Shen, J., Starbuck, M., and Karsenty, G. (2001). Cbfa1 contributes to the osteoblast-specific expression of type I collagen genes. The Journal of biological chemistry *276*, 7101-7107.

Khosla, S., Melton, L.J., 3rd, Atkinson, E.J., and O'Fallon, W.M. (2001). Relationship of serum sex steroid levels to longitudinal changes in bone density in young versus elderly men. J Clin Endocrinol Metab *86*, 3555-3561.

Komori, T., Yagi, H., Nomura, S., Yamaguchi, A., Sasaki, K., Deguchi, K., Shimizu, Y., Bronson, R.T., Gao, Y.H., Inada, M.*, et al.* (1997a). Targeted disruption of Cbfa1 results in a complete lack of bone formation owing to maturational arrest of osteoblasts. Cell *89*, 755-764.

Komori, T., Yagi, H., Nomura, S., Yamaguchi, A., Sasaki, K., Deguchi, K., Shimizu, Y., Bronson, R.T., Gao, Y.H., Inada, M.*, et al.* (1997c). Targeted disruption of Cbfa1 results in a complete lack of bone formation owing to maturational arrest of osteoblasts. Cell *89*, 755-764.

Kronenberg, H.M. (2003). Developmental regulation of the growth plate. Nature *423*, 332-336.

Laplante, M., and Sabatini, D.M. (2009). mTOR signaling at a glance. J Cell Sci *122*, 3589-3594.

Larsen, K.I., Falany, M., Wang, W., and Williams, J.P. (2005). Glucose is a key metabolic regulator of osteoclasts; glucose stimulated increases in ATP/ADP ratio and calmodulin kinase II activity. Biochem Cell Biol *83*, 667-673.

Lee, B., Thirunavukkarasu, K., Zhou, L., Pastore, L., Baldini, A., Hecht, J., Geoffroy, V., Ducy, P., and Karsenty, G. (1997a). Missense mutations abolishing DNA binding of the osteoblast-specific transcription factor OSF2/CBFA1 in cleidocranial dysplasia. Nature genetics *16*, 307-310.

Lee, B., Thirunavukkarasu, K., Zhou, L., Pastore, L., Baldini, A., Hecht, J., Geoffroy, V., Ducy, P., and Karsenty, G. (1997d). Missense mutations abolishing DNA binding of the osteoblast-specific transcription factor OSF2/CBFA1 in cleidocranial dysplasia. Nat Genet *16*, 307-310.

Lee, N.K., Sowa, H., Hinoi, E., Ferron, M., Ahn, J.D., Confavreux, C., Dacquin, R., Mee, P.J., McKee, M.D., Jung, D.Y*., et al.* (2007). Endocrine regulation of energy metabolism by the skeleton. Cell *130*, 456-469.

Lefebvre, V., and de Crombrugghe, B. (1998). Toward understanding SOX9 function in chondrocyte differentiation. Matrix Biol *16*, 529-540.

Lefebvre, V., Huang, W., Harley, V.R., Goodfellow, P.N., and de Crombrugghe, B. (1997). SOX9 is a potent activator of the chondrocyte-specific enhancer of the pro alpha1(II) collagen gene. Mol Cell Biol *17*, 2336-2346.

Liu, S., Tang, W., Zhou, J., Stubbs, J.R., Luo, Q., Pi, M., and Quarles, L.D. (2006). Fibroblast growth factor 23 is a counter-regulatory phosphaturic hormone for vitamin D. J Am Soc Nephrol *17*, 1305-1315.

Logothetis, C.J., and Lin, S.H. (2005). Osteoblasts in prostate cancer metastasis to bone. Nat Rev Cancer *5*, 21-28.

Long, F. (2012). Building strong bones: molecular regulation of the osteoblast lineage. Nat Rev Mol Cell Biol *13*, 27-38.

Lu, K., Yin, X., Weng, T., Xi, S., Li, L., Xing, G., Cheng, X., Yang, X., Zhang, L., and He, F. (2008). Targeting WW domains linker of HECT-type ubiquitin ligase Smurf1 for activation by CKIP-1. Nature cell biology *10*, 994-1002.

Luxenburg, C., Geblinger, D., Klein, E., Anderson, K., Hanein, D., Geiger, B., and Addadi, L. (2007). The architecture of the adhesive apparatus of cultured osteoclasts: from podosome formation to sealing zone assembly. PLoS One *2*, e179.

Mackie, E.J., Ahmed, Y.A., Tatarczuch, L., Chen, K.S., and Mirams, M. (2008). Endochondral ossification: how cartilage is converted into bone in the developing skeleton. Int J Biochem Cell Biol *40*, 46-62.

Mackie, E.J., Tatarczuch, L., and Mirams, M. (2011). The skeleton: a multi-functional complex organ: the growth plate chondrocyte and endochondral ossification. J Endocrinol *211*, 109-121.

Maes, C., Kobayashi, T., Selig, M.K., Torrekens, S., Roth, S.I., Mackem, S., Carmeliet, G., and Kronenberg, H.M. (2010). Osteoblast precursors, but not mature osteoblasts, move into developing and fractured bones along with invading blood vessels. Dev Cell *19*, 329-344.

Mahoney, S.J., Dempsey, J.M., and Blenis, J. (2009). Cell signaling in protein synthesis ribosome biogenesis and translation initiation and elongation. Prog Mol Biol Transl Sci *90*, 53-107.

Mayer, F.V., Heath, R., Underwood, E., Sanders, M.J., Carmena, D., McCartney, R.R., Leiper, F.C.,

Xiao, B., Jing, C., Walker, P.A., *et al.* (2011). ADP regulates SNF1, the Saccharomyces cerevisiae homolog of AMP-activated protein kinase. Cell metabolism *14*, 707-714.

McLeod, M.J. (1980). Differential staining of cartilage and bone in whole mouse fetuses by alcian blue and alizarin red S. Teratology *22*, 299-301.

Mobasheri, A. (2012). Glucose: an energy currency and structural precursor in articular cartilage and bone with emerging roles as an extracellular signaling molecule and metabolic regulator. Front Endocrinol (Lausanne) *3*, 153.

Morrison, S.J., and Scadden, D.T. (2014). The bone marrow niche for haematopoietic stem cells. Nature *505*, 327-334.

Mueckler, M., and Thorens, B. (2013). The SLC2 (GLUT) family of membrane transporters. Mol Aspects Med *34*, 121-138.

Mundlos, S., Otto, F., Mundlos, C., Mulliken, J.B., Aylsworth, A.S., Albright, S., Lindhout, D., Cole, W.G., Henn, W., Knoll, J.H., *et al.* (1997a). Mutations involving the transcription factor CBFA1 cause cleidocranial dysplasia. Cell *89*, 773-779.

Mundlos, S., Otto, F., Mundlos, C., Mulliken, J.B., Aylsworth, A.S., Albright, S., Lindhout, D., Cole, W.G., Henn, W., Knoll, J.H., *et al.* (1997d). Mutations involving the transcription factor CBFA1 cause cleidocranial dysplasia. Cell *89*, 773-779.

Murshed, M., Harmey, D., Millan, J.L., McKee, M.D., and Karsenty, G. (2005). Unique coexpression in osteoblasts of broadly expressed genes accounts for the spatial restriction of ECM mineralization to bone. Genes & development *19*, 1093-1104.

Nakada, D., Saunders, T.L., and Morrison, S.J. (2010). Lkb1 regulates cell cycle and energy metabolism in haematopoietic stem cells. Nature *468*, 653-658.

Nakamura, T., Imai, Y., Matsumoto, T., Sato, S., Takeuchi, K., Igarashi, K., Harada, Y., Azuma, Y., Krust, A., Yamamoto, Y., *et al.* (2007). Estrogen prevents bone loss via estrogen receptor alpha and induction of Fas ligand in osteoclasts. Cell *130*, 811-823.

Narimatsu, M., Bose, R., Pye, M., Zhang, L., Miller, B., Ching, P., Sakuma, R., Luga, V., Roncari, L., Attisano, L., *et al.* (2009). Regulation of planar cell polarity by Smurf ubiquitin ligases. Cell *137*, 295-307.

Nishio, Y., Dong, Y., Paris, M., O'Keefe, R.J., Schwarz, E.M., and Drissi, H. (2006). Runx2-mediated regulation of the zinc finger Osterix/Sp7 gene. Gene *372*, 62-70.

Obri, A., Makinistoglu, M.P., Zhang, H., and Karsenty, G. (2014). HDAC4 integrates PTH and sympathetic signaling in osteoblasts. J Cell Biol *205*, 771-780.

Ornitz, D.M., and Marie, P.J. (2002). FGF signaling pathways in endochondral and intramembranous bone development and human genetic disease. Genes Dev *16*, 1446-1465.

Otto, F., Lubbert, M., and Stock, M. (2003). Upstream and downstream targets of RUNX proteins. J Cell Biochem *89*, 9-18.

Otto, F., Thornell, A.P., Crompton, T., Denzel, A., Gilmour, K.C., Rosewell, I.R., Stamp, G.W., Beddington, R.S., Mundlos, S., Olsen, B.R., *et al.* (1997a). Cbfa1, a candidate gene for cleidocranial

dysplasia syndrome, is essential for osteoblast differentiation and bone development. Cell *89*, 765-771.

Otto, F., Thornell, A.P., Crompton, T., Denzel, A., Gilmour, K.C., Rosewell, I.R., Stamp, G.W., Beddington, R.S., Mundlos, S., Olsen, B.R.*, et al.* (1997d). Cbfa1, a candidate gene for cleidocranial dysplasia syndrome, is essential for osteoblast differentiation and bone development. Cell *89*, 765-771.

Oury, F., Ferron, M., Huizhen, W., Confavreux, C., Xu, L., Lacombe, J., Srinivas, P., Chamouni, A., Lugani, F., Lejeune, H.*, et al.* (2013a). Osteocalcin regulates murine and human fertility through a pancreas-bone-testis axis. J Clin Invest *123*, 2421-2433.

Oury, F., Khrimian, L., Denny, C.A., Gardin, A., Chamouni, A., Goeden, N., Huang, Y.Y., Lee, H., Srinivas, P., Gao, X.B.*, et al.* (2013c). Maternal and offspring pools of osteocalcin influence brain development and functions. Cell *155*, 228-241.

Oury, F., Sumara, G., Sumara, O., Ferron, M., Chang, H., Smith, C.E., Hermo, L., Suarez, S., Roth, B.L., Ducy, P.*, et al.* (2011). Endocrine regulation of male fertility by the skeleton. Cell *144*, 796-809.

Oury, F., Yadav, V.K., Wang, Y., Zhou, B., Liu, X.S., Guo, X.E., Tecott, L.H., Schutz, G., Means, A.R., and Karsenty, G. (2010). CREB mediates brain serotonin regulation of bone mass through its expression in ventromedial hypothalamic neurons. Genes Dev *24*, 2330-2342.

Parfitt, A.M., Drezner, M.K., Glorieux, F.H., Kanis, J.A., Malluche, H., Meunier, P.J., Ott, S.M., and Recker, R.R. (1987a). Bone Histomorphometry - Standardization of Nomenclature, Symbols, and Units. J Bone Miner Res *2*, 595-610.

Parfitt, A.M., Drezner, M.K., Glorieux, F.H., Kanis, J.A., Malluche, H., Meunier, P.J., Ott, S.M., and Recker, R.R. (1987b). Bone histomorphometry: standardization of nomenclature, symbols, and units. Report of the ASBMR Histomorphometry Nomenclature Committee. Journal of bone and mineral research : the official journal of the American Society for Bone and Mineral Research *2*, 595-610.

Peterson, T.R., Laplante, M., Thoreen, C.C., Sancak, Y., Kang, S.A., Kuehl, W.M., Gray, N.S., and Sabatini, D.M. (2009). DEPTOR is an mTOR inhibitor frequently overexpressed in multiple myeloma cells and required for their survival. Cell *137*, 873-886.

Pittas, A.G., Harris, S.S., Eliades, M., Stark, P., and Dawson-Hughes, B. (2009). Association between serum osteocalcin and markers of metabolic phenotype. J Clin Endocrinol Metab *94*, 827-832.

Pritchard, J.J. (1952). A cytological and histochemical study of bone and cartilage formation in the rat. J Anat *86*, 259-277.

Puppin, C., Pellizzari, L., Fabbro, D., Fogolari, F., Tell, G., Tessa, A., Santorelli, F.M., and Damante, G. (2005). Functional analysis of a novel RUNX2 missense mutation found in a family with cleidocranial dysplasia. Journal of human genetics *50*, 679-683.

Razzaque, M.S. (2011). Osteocalcin: a pivotal mediator or an innocent bystander in energy metabolism? Nephrology Dialysis Transplantation *26*, 42-45.

Reiter, A.K., Bolster, D.R., Crozier, S.J., Kimball, S.R., and Jefferson, L.S. (2005). Repression of protein synthesis and mTOR signaling in rat liver mediated by the AMPK activator aminoimidazole

carboxamide ribonucleoside. American journal of physiology Endocrinology and metabolism *288*, E980-988.

Rodda, S.J., and McMahon, A.P. (2006). Distinct roles for Hedgehog and canonical Wnt signaling in specification, differentiation and maintenance of osteoblast progenitors. Development *133*, 3231-3244.

Roodman, G.D. (1991). Osteoclast differentiation. Crit Rev Oral Biol Med *2*, 389-409.

Sabek, O.M., Nishimoto, S.K., Fraga, D., Tejpal, N., Ricordi, C., and Gaber, A.O. (2015). Osteocalcin Effect on Human beta-Cells Mass and Function. Endocrinology *156*, 3137-3146.

Sancak, Y., Thoreen, C.C., Peterson, T.R., Lindquist, R.A., Kang, S.A., Spooner, E., Carr, S.A., and Sabatini, D.M. (2007). PRAS40 is an insulin-regulated inhibitor of the mTORC1 protein kinase. Mol Cell *25*, 903-915.

Schlessinger, J. (2000). Cell signaling by receptor tyrosine kinases. Cell *103*, 211-225.

Schmelzle, T., and Hall, M.N. (2000). TOR, a central controller of cell growth. Cell *103*, 253-262.

Sekiya, I., Tsuji, K., Koopman, P., Watanabe, H., Yamada, Y., Shinomiya, K., Nifuji, A., and Noda, M. (2000). SOX9 Enhances Aggrecan Gene Promoter/Enhancer Activity and Is Up-regulated by Retinoic Acid in a Cartilage-derived Cell Line, TC6. Journal of Biological Chemistry *275*, 10738-10744.

Severe, N., Dieudonne, F.X., and Marie, P.J. (2013). E3 ubiquitin ligase-mediated regulation of bone formation and tumorigenesis. Cell Death Dis *4*, e463.

Shen, R., Wang, X., Drissi, H., Liu, F., O'Keefe, R.J., and Chen, D. (2006). Cyclin D1-cdk4 induce runx2 ubiquitination and degradation. The Journal of biological chemistry *281*, 16347-16353.

Shimada, T., Kakitani, M., Yamazaki, Y., Hasegawa, H., Takeuchi, Y., Fujita, T., Fukumoto, S., Tomizuka, K., and Yamashita, T. (2004). Targeted ablation of Fgf23 demonstrates an essential physiological role of FGF23 in phosphate and vitamin D metabolism. J Clin Invest *113*, 561-568.

Shimada, T., Mizutani, S., Muto, T., Yoneya, T., Hino, R., Takeda, S., Takeuchi, Y., Fujita, T., Fukumoto, S., and Yamashita, T. (2001). Cloning and characterization of FGF23 as a causative factor of tumor-induced osteomalacia. Proceedings of the National Academy of Sciences of the United States of America *98*, 6500-6505.

Shimazu, J., Wei, J., and Karsenty, G. (2016). Smurf1 Inhibits Osteoblast Differentiation, Bone Formation, and Glucose Homeostasis through Serine 148. Cell Rep *15*, 27-35.

Shu, L., Zhang, H., Boyce, B.F., and Xing, L. (2013). Ubiquitin E3 ligase Wwp1 negatively regulates osteoblast function by inhibiting osteoblast differentiation and migration. J Bone Miner Res *28*, 1925-1935.

Siddle, K. (2011). Signalling by insulin and IGF receptors: supporting acts and new players. J Mol Endocrinol *47*, R1-10.

Sundin, O.H., Busse, H.G., Rogers, M.B., Gudas, L.J., and Eichele, G. (1990). Region-specific expression in early chick and mouse embryos of Ghox-lab and Hox 1.6, vertebrate homeobox-containing genes related to Drosophila labial. Development *108*, 47-58.

Takarada, T., Hinoi, E., Nakazato, R., Ochi, H., Xu, C., Tsuchikane, A., Takeda, S., Karsenty, G., Abe, T., Kiyonari, H.*, et al.* (2013). An analysis of skeletal development in osteoblast-specific and

chondrocyte-specific runt-related transcription factor-2 (Runx2) knockout mice. Journal of bone and mineral research : the official journal of the American Society for Bone and Mineral Research *28*, 2064-2069.

Takeda, S., Bonnamy, J.P., Owen, M.J., Ducy, P., and Karsenty, G. (2001a). Continuous expression of Cbfa1 in nonhypertrophic chondrocytes uncovers its ability to induce hypertrophic chondrocyte differentiation and partially rescues Cbfa1-deficient mice. Genes Dev *15*, 467-481.

Takeda, S., Bonnamy, J.P., Owen, M.J., Ducy, P., and Karsenty, G. (2001b). Continuous expression of Cbfa1 in nonhypertrophic chondrocytes uncovers its ability to induce hypertrophic chondrocyte differentiation and partially rescues Cbfa1-deficient mice. Genes & development *15*, 467-481.

Takeda, S., Elefteriou, F., and Karsenty, G. (2003). Common endocrine control of body weight, reproduction, and bone mass. Annu Rev Nutr *23*, 403-411.

Takeda, S., Elefteriou, F., Levasseur, R., Liu, X., Zhao, L., Parker, K.L., Armstrong, D., Ducy, P., and Karsenty, G. (2002). Leptin regulates bone formation via the sympathetic nervous system. Cell *111*, 305-317.

Tessa, A., Salvi, S., Casali, C., Garavelli, L., Digilio, M.C., Dotti, M.T., Di Giandomenico, S., Valoppi, M., Grieco, G.S., Comanducci, G.*, et al.* (2003). Six novel mutations of the RUNX2 gene in Italian patients with cleidocranial dysplasia. Hum Mutat *22*, 104.

Thomas, D.M., Rogers, S.D., Ng, K.W., and Best, J.D. (1996). Dexamethasone modulates insulin receptor expression and subcellular distribution of the glucose transporter GLUT 1 in UMR 106-01, a clonal osteogenic sarcoma cell line. J Mol Endocrinol *17*, 7-17.

Thorens, B., and Mueckler, M. (2010). Glucose transporters in the 21st Century. Am J Physiol Endocrinol Metab *298*, E141-145.

Tintut, Y., Parhami, F., Le, V., Karsenty, G., and Demer, L.L. (1999). Inhibition of osteoblast-specific transcription factor Cbfa1 by the cAMP pathway in osteoblastic cells. Ubiquitin/proteasome-dependent regulation. The Journal of biological chemistry *274*, 28875-28879.

Vaananen, H.K., Zhao, H., Mulari, M., and Halleen, J.M. (2000). The cell biology of osteoclast function. J Cell Sci *113 (Pt 3)*, 377-381.

Vu, T.H., Shipley, J.M., Bergers, G., Berger, J.E., Helms, J.A., Hanahan, D., Shapiro, S.D., Senior, R.M., and Werb, Z. (1998). MMP-9/gelatinase B is a key regulator of growth plate angiogenesis and apoptosis of hypertrophic chondrocytes. Cell *93*, 411-422.

Vuorio, E., and de Crombrugghe, B. (1990). The family of collagen genes. Annu Rev Biochem *59*, 837-872.

Warming, S., Costantino, N., Court, D.L., Jenkins, N.A., and Copeland, N.G. (2005). Simple and highly efficient BAC recombineering using galK selection. Nucleic Acids Res *33*, e36.

Webster, D.F., and Harvey, W. (1979). A quantitative assay for collagen synthesis in microwell fibroblast cultures. Analytical biochemistry *96*, 220-224.

Wei, J., and Ducy, P. (2010). Co-dependence of bone and energy metabolisms. Arch Biochem Biophys *503*, 35-40.

Wei, J., Ferron, M., Clarke, C.J., Hannun, Y.A., Jiang, H., Blaner, W.S., and Karsenty, G. (2014a). Bone-specific insulin resistance disrupts whole-body glucose homeostasis via decreased osteocalcin activation. J Clin Invest *124*, 1-13.

Wei, J., Hanna, T., Suda, N., Karsenty, G., and Ducy, P. (2014e). Osteocalcin Promotes beta-Cell Proliferation During Development and Adulthood Through Gprc6a. Diabetes *63*, 1021-1031.

Wei, J., and Karsenty, G. (2015). An overview of the metabolic functions of osteocalcin. Rev Endocr Metab Disord *16*, 93-98.

Wei, J., Shimazu, J., Makinistoglu, M.P., Maurizi, A., Kajimura, D., Zong, H., Takarada, T., Iezaki, T., Pessin, J.E., Hinoi, E.*, et al.* (2015a). Glucose Uptake and Runx2 Synergize to Orchestrate Osteoblast Differentiation and Bone Formation. Cell *161*, 1576-1591.

Wei, J., Shimazu, J., Makinistoglu, M.P., Maurizi, A., Kajimura, D., Zong, H., Takarada, T., Lezaki, T., Pessin, J.E., Hinoi, E.*, et al.* (2015e). Glucose Uptake and Runx2 Synergize to Orchestrate Osteoblast Differentiation and Bone Formation. Cell *161*, 1576-1591.

Wei, J., Shimazu, J., Makinistoglu, P.M., Maurizi,A., Kajimura,D., Zong,H., Takarada,T., Iezaki,T., Pessin, E.J. , Hinoi,E., Karsenty,G. (2015). Glucose uptake and Runx2 synergize to orchestrate osteoblast differentiation and bone formation. Cell *In Press*.

White, K.E., Evans, W.E., O'Riordan, J.L.H., Speer, M.C., Econs, M.J., Lorenz-Depiereux, B., Grabowski, M., Meitinger, T., and Strom, T.M. (2000). Autosomal dominant hypophosphataemic rickets is associated with mutations in FGF23. Nature genetics *26*, 345-348.

Wilden, P.A., Siddle, K., Haring, E., Backer, J.M., White, M.F., and Kahn, C.R. (1992). The role of insulin receptor kinase domain autophosphorylation in receptor-mediated activities. Analysis with insulin and anti-receptor antibodies. The Journal of biological chemistry *267*, 13719-13727.

Williams, J.P., Blair, H.C., McDonald, J.M., McKenna, M.A., Jordan, S.E., Williford, J., and Hardy, R.W. (1997). Regulation of osteoclastic bone resorption by glucose. Biochem Biophys Res Commun *235*, 646-651.

Wilson, S.R., Peters, C., Saftig, P., and Bromme, D. (2009). Cathepsin K activity-dependent regulation of osteoclast actin ring formation and bone resorption. The Journal of biological chemistry *284*, 2584-2592.

Wilson, W.A., Hawley, S.A., and Hardie, D.G. (1996). Glucose repression/derepression in budding yeast: SNF1 protein kinase is activated by phosphorylation under derepressing conditions, and this correlates with a high AMP:ATP ratio. Current biology : CB *6*, 1426-1434.

Wood, I.S., and Trayhurn, P. (2003). Glucose transporters (GLUT and SGLT): expanded families of sugar transport proteins. Br J Nutr *89*, 3-9.

Woods, A., Munday, M.R., Scott, J., Yang, X., Carlson, M., and Carling, D. (1994). Yeast SNF1 is functionally related to mammalian AMP-activated protein kinase and regulates acetyl-CoA carboxylase in vivo. The Journal of biological chemistry *269*, 19509-19515.

Xing, L., Zhang, M., and Chen, D. (2010). Smurf control in bone cells. J Cell Biochem *110*, 554-563.

Yadav, V.K., Oury, F., Suda, N., Liu, Z.W., Gao, X.B., Confavreux, C., Klemenhagen, K.C., Tanaka, K.F.,

Gingrich, J.A., Guo, X.E.*, et al.* (2009). A serotonin-dependent mechanism explains the leptin regulation of bone mass, appetite, and energy expenditure. Cell *138*, 976-989.

Yamashita, H., Takenoshita, M., Sakurai, M., Bruick, R.K., Henzel, W.J., Shillinglaw, W., Arnot, D., and Uyeda, K. (2001). A glucose-responsive transcription factor that regulates carbohydrate metabolism in the liver. Proceedings of the National Academy of Sciences of the United States of America *98*, 9116-9121.

Yamashita, M., Ying, S.X., Zhang, G.M., Li, C., Cheng, S.Y., Deng, C.X., and Zhang, Y.E. (2005). Ubiquitin ligase Smurf1 controls osteoblast activity and bone homeostasis by targeting MEKK2 for degradation. Cell *121*, 101-113.

Yamashita, T., Takahashi, N., and Udagawa, N. (2012). New roles of osteoblasts involved in osteoclast differentiation. World J Orthop *3*, 175-181.

Yang, X., and Karsenty, G. (2002). Transcription factors in bone: developmental and pathological aspects. Trends Mol Med *8*, 340-345.

Yu, K., Xu, J., Liu, Z., Sosic, D., Shao, J., Olson, E.N., Towler, D.A., and Ornitz, D.M. (2003). Conditional inactivation of FGF receptor 2 reveals an essential role for FGF signaling in the regulation of osteoblast function and bone growth. Development *130*, 3063-3074.

Zhang, M., Xuan, S., Bouxsein, M.L., von Stechow, D., Akeno, N., Faugere, M.C., Malluche, H., Zhao, G., Rosen, C.J., Efstratiadis, A.*, et al.* (2002). Osteoblast-specific knockout of the insulin-like growth factor (IGF) receptor gene reveals an essential role of IGF signaling in bone matrix mineralization. The Journal of biological chemistry *277*, 44005-44012.

Zhao, M., Qiao, M., Harris, S.E., Oyajobi, B.O., Mundy, G.R., and Chen, D. (2004). Smurf1 inhibits osteoblast differentiation and bone formation in vitro and in vivo. The Journal of biological chemistry *279*, 12854-12859.

Zhao, M., Qiao, M., Oyajobi, B.O., Mundy, G.R., and Chen, D. (2003). E3 ubiquitin ligase Smurf1 mediates core-binding factor alpha1/Runx2 degradation and plays a specific role in osteoblast differentiation. The Journal of biological chemistry *278*, 27939-27944.

Zhu, H., Kavsak, P., Abdollah, S., Wrana, J.L., and Thomsen, G.H. (1999). A SMAD ubiquitin ligase targets the BMP pathway and affects embryonic pattern formation. Nature *400*, 687-693.

Zoidis, E., Ghirlanda-Keller, C., and Schmid, C. (2011). Stimulation of glucose transport in osteoblastic cells by parathyroid hormone and insulin-like growth factor I. Mol Cell Biochem *348*, 33-42.

Zong, H., Bastie, C.C., Xu, J., Fassler, R., Campbell, K.P., Kurland, I.J., and Pessin, J.E. (2009). Insulin resistance in striated muscle-specific integrin receptor beta1-deficient mice. The Journal of biological chemistry *284*, 4679-4688.

Figures

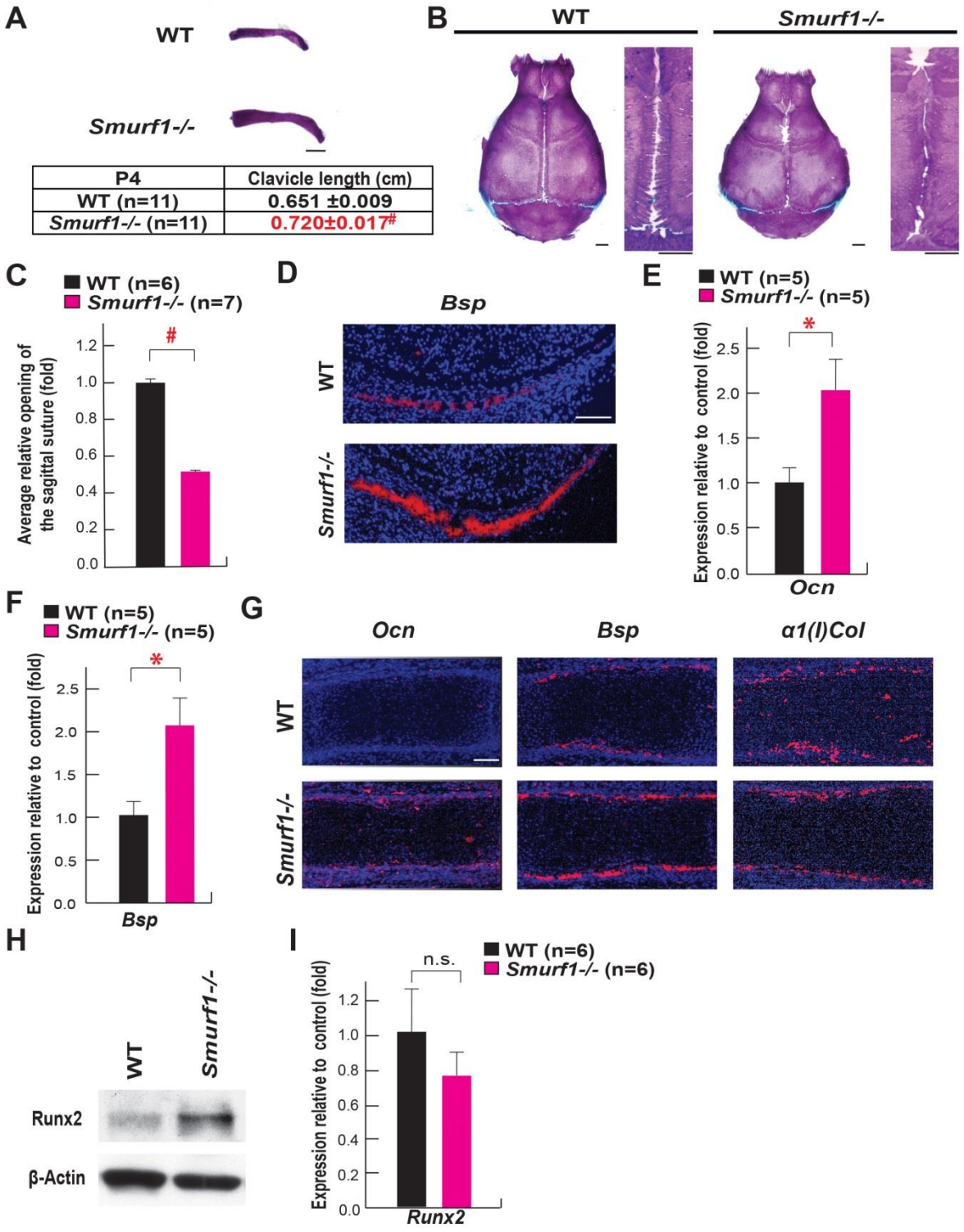

P4	Clavicle length (cm)
WT (n=11)	0.651 ±0.009
Smurf1-/- (n=11)	0.720±0.017#

Figure 1. Regulation of osteoblast differentiation by Smurf1 in vivo

A-B. Alcian blue/alizarin red staining of clavicles and skulls of P4 and P10 WT and *Smurf1-/-* mice, respectively.

C. Opening of sagittal sutures in P10 *Smurf1-/-* and WT mice.

D. In situ hybridization analysis of *Bsp* expression in calvarial bones of E14.5 *Smurf1-/-* and WT

embryos.

E to F. qPCR analysis of *Ocn* (**E**) and *Bsp* (**F**) expression in femurs of E14.5 WT and *Smurf1-/-* embryos (n=5).

G. In situ hybridization analysis of *Ocn, Bsp* and *α1(I)Col* expression in femurs of E14.5 *Smurf1-/-* and WT embryos.

H. Runx2 accumulation in skulls of P10 WT and *Smurf1-/-* mice.

I. Expression of *Runx2* in the femurs of P10 WT and *Smurf1-/-* mice (n=6). N.S., not significant.

Error bars indicate mean ± SEM. $^{*}p \leq 0.05$; $^{\#}p \leq 0.005$ (compared to control),when analyzed by Student's t tests.

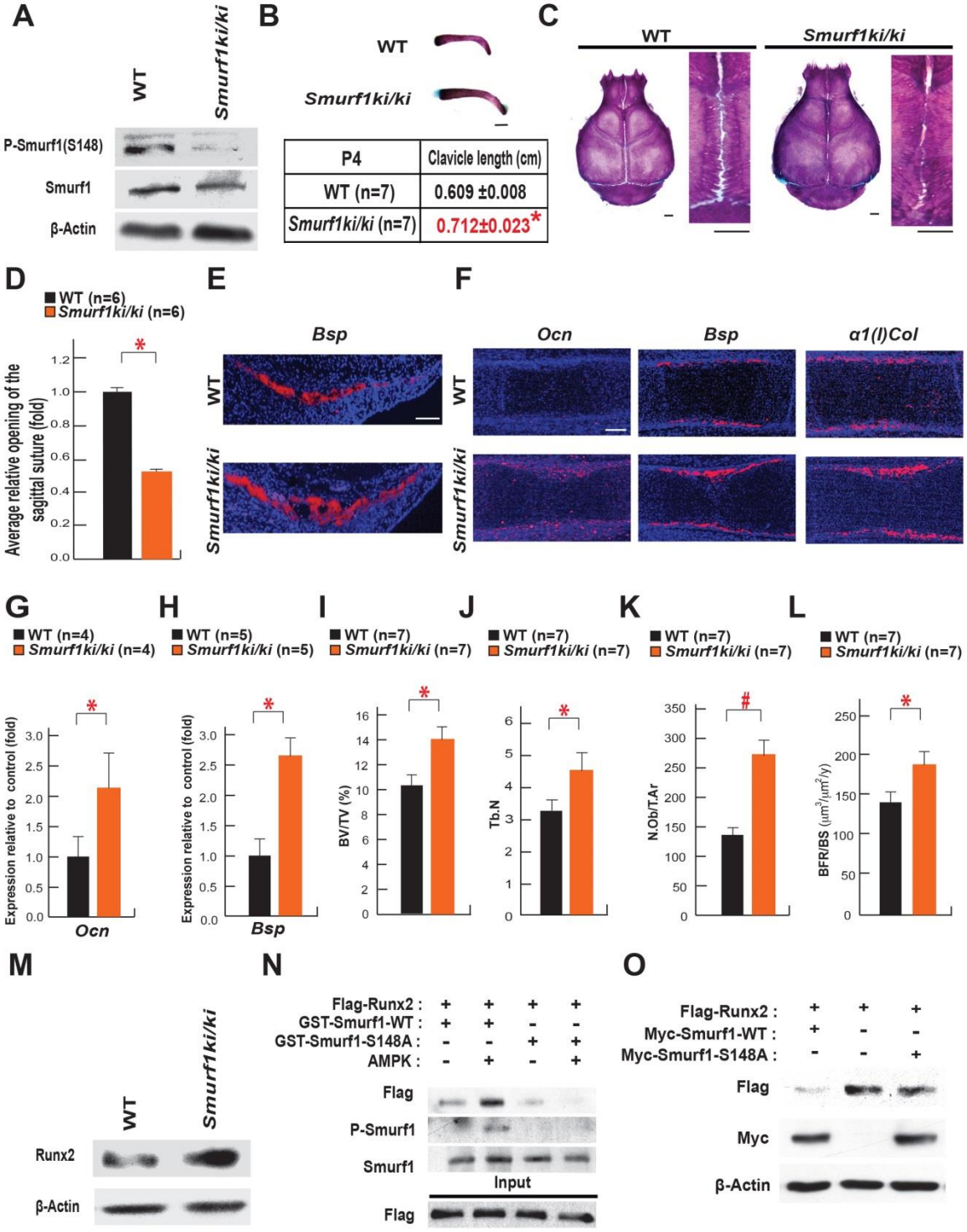

Figure 2. Phosphorylation of Smurf1 at S148 is necessary for Smurf1 ability to regulate osteoblast differentiation in vivo

A. Western blot analysis of S148 phosphorylation in Smurf1 in WT and *Smurf1*$^{ki/ki}$ osteoblasts.

B-C. Alcian blue/Alizarin red staining of clavicles and skulls of P4 and P10 WT and *Smurf1*$^{ki/ki}$ mice respectively.

A. Opening of sagittal sutures in P10 *Smurf1*$^{ki/ki}$ and WT mice.

E-F. In situ hybridization analysis of *Bsp* in calvarial bones (**E**) and of *Ocn, Bsp* and *α1(I)Col* expression in femurs (**F**) of E14.5 WT and *Smurf1*$^{ki/ki}$ embryos.

G to H. qPCR analysis of *Ocn* (**G**) and *Bsp* (**H**) expression in femurs of E14.5 WT and *Smurf1*$^{ki/ki}$ embryos (n=4-5).

I-L. Bone histomorphometric analysis of L3 and L4 vertebrae of 2 month-old WT and *Smurf1*$^{ki/ki}$ female mice (n=7). Mineralized bone volume per total volume (BV/TV) (**I**). Trabecular number (Tb.N) (**J**). Osteoblast number per tissue area (N.Ob/T.Ar) (**K**). The annual fractional volume of trabecular bone formed per unit trabecular surface area (BFR/BS) (**L**).

M. Runx2 accumulation in the skulls of P10 WT and *Smurf1*$^{ki/ki}$ mice.

N. GST-Pull down assay showing interaction of Flag-Runx2 with GST-Smurf1 WT or S148A after phosphorylation by AMPK.

O. Effect of the forced expression of WT or *S148A Smurf1* on the accumulation of Runx2 in COS-7 cells.

Error bars indicate mean ± SEM. $^{*}p \leq 0.05$; $^{\#}p \leq 0.005$ (compared to control), when analyzed by Student's t tests.

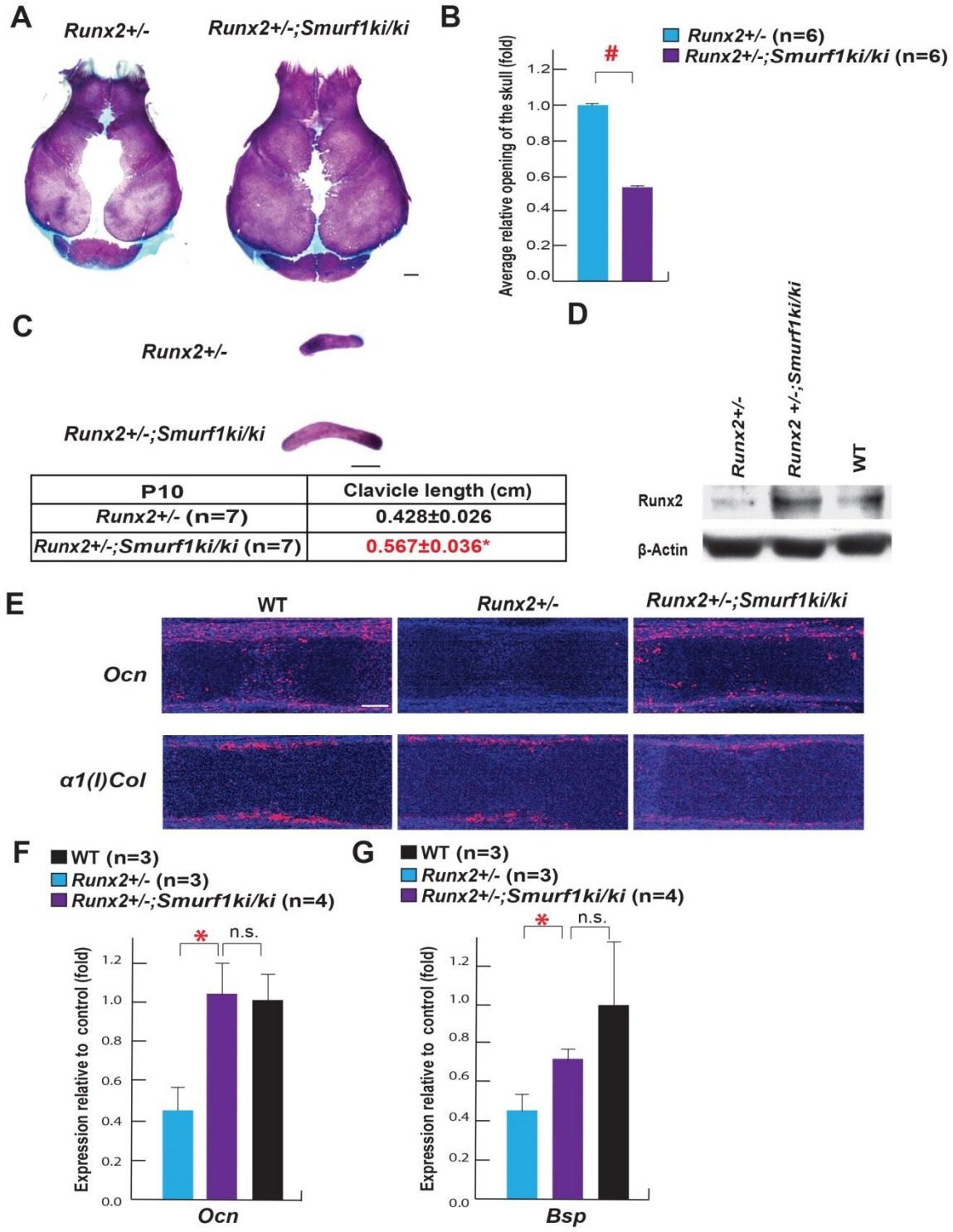

P10	Clavicle length (cm)
Runx2+/- (n=7)	0.428±0.026
Runx2+/-;Smurf1ki/ki (n=7)	0.567±0.036*

Figure 3. Smurf1 phosphorylation at S148 is necessary to regulate Runx2 in vivo

A. Alcian blue/alizarin red staining of skulls of P10 *Runx2+/-* and *Runx2+/-;Smurf1*$^{ki/ki}$ mice.

B. Area of the opening of skulls in P10 *Runx2+/-;Smurf1*$^{ki/ki}$ and *Runx2 +/-* mice.

C. Alcian blue/alizarin red staining of clavicles of P10 *Runx2+/-* and *Runx2+/-;Smurf1*$^{ki/ki}$ mice.

D. Runx2 accumulation in skulls of P10 *Runx2+/-, Runx2+/-;Smurf1*$^{ki/ki}$ and WT skulls.

E. In situ hybridization analysis of *Ocn* and *α1(I)Col* expression in E15.5 WT, *Runx2+/-* and

Runx2+/-;Smurf1$^{ki/ki}$ femurs.

F-G. qPCR analysis of *Ocn* (**F**) and *Bsp* (**G**) expression in femurs of P10 *WT*, *Runx2+/-* and *Runx2+/-;Smurf1*$^{ki/ki}$ mice (n=3-4).

Error bars indicate mean ± SEM. $^{*}p \leq 0.05$; $^{\#}p \leq 0.005$ (compared to control),when analyzed by Student's t tests.

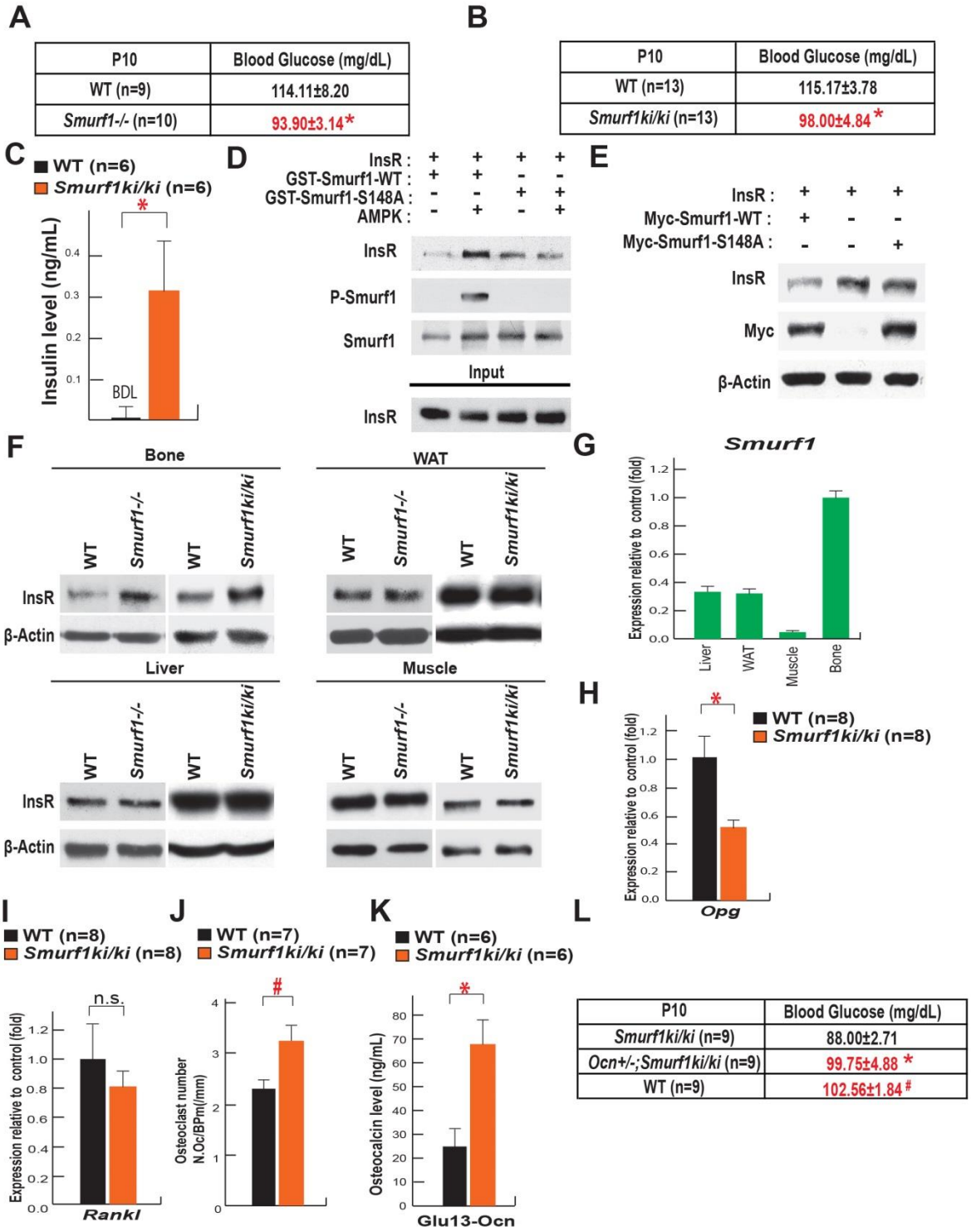

Figure 4. Phosphorylation of Smurf1 at S148 is necessary for Smurf1 activity to regulate InsR degradation

A-B. Blood glucose levels in P10 WT and *Smurf1-/-* mice (**A**), WT and *Smurf1*$^{ki/ki}$ mice (n=9-13 per group) (**B**).

C. Circulating insulin levels in P10 WT and *Smurf1*$^{ki/ki}$ mice (n=6). BDL: Below detection limit.

D. GST-Pull down assay showing interaction of InsR with GST-Smurf1 WT or GST-Smurf1 S148A

after AMPK phosphorylation.

E. Effect of the overexpression of WT or *S148A Smurf1* on the accumulation of InsR in COS-7 cells.

F. Accumulation of the InsR in skull, liver, WAT and muscle of P10 WT, *Smurf1-/-* and *Smurf1*$^{ki/ki}$ mice.

G. Expression of *Smurf1* in liver, WAT, muscle and skull of P10 WT mice.

H-I. Expression of *Osteoprotegerin* (*Opg*) (**H**) and *Rankl* (**I**) in the femur of P10 WT and *Smurf1*$^{ki/ki}$ mice (n=8).

J. Osteoclasts number (N.Oc/B.Pm (/mm)) in 2 month-old WT and *Smurf1*$^{ki/ki}$ female mice (n=7).

K. Serum levels of undercarboxylated osteocalcin in 2 month-old WT and *Smurf1*$^{ki/ki}$ mice (n=6).

L. Blood glucose levels in P10 WT, *Smurf1*$^{ki/ki}$ and *Ocn+/-;Smurf1*$^{ki/ki}$ mice (n=9).

Error bars indicate mean ± SEM. $^{*}p \leq 0.05$; $^{\#}p \leq 0.005$ (compared to control), when analyzed by Student's t tests.

Supplemental Figures

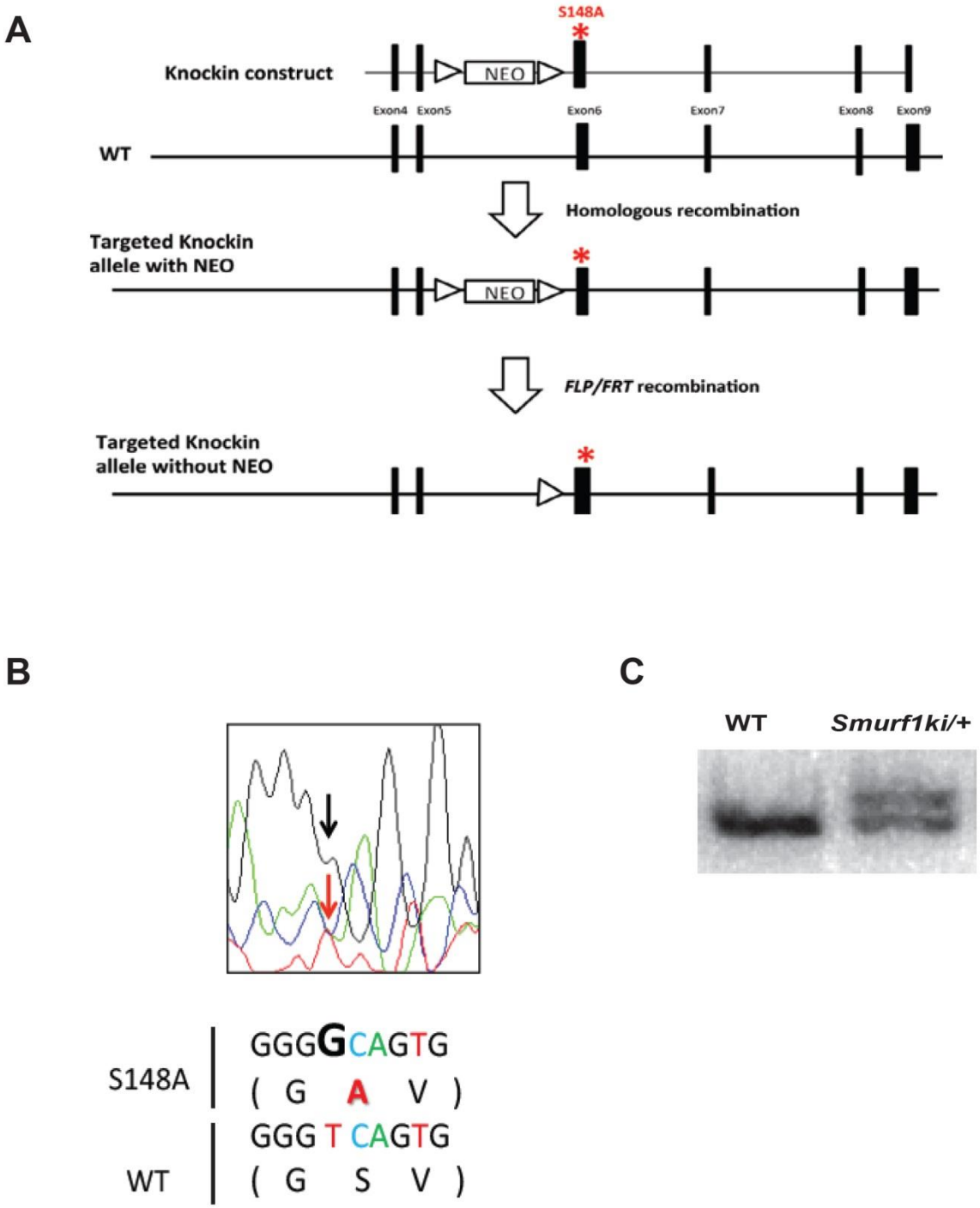

Figure S1. Generation of *Smurf1 S148A* knock-in mice (related to Figure 3-2)

A. Targeting strategy used to generate *Smurf1 S148A knock-in* allele.

B. DNA sequencing analysis showing the *Smurf1 S148A* mutation.

C. PCR analysis showing the *Smurf1 S148A knock-in* allele and WT allele after the targeting.

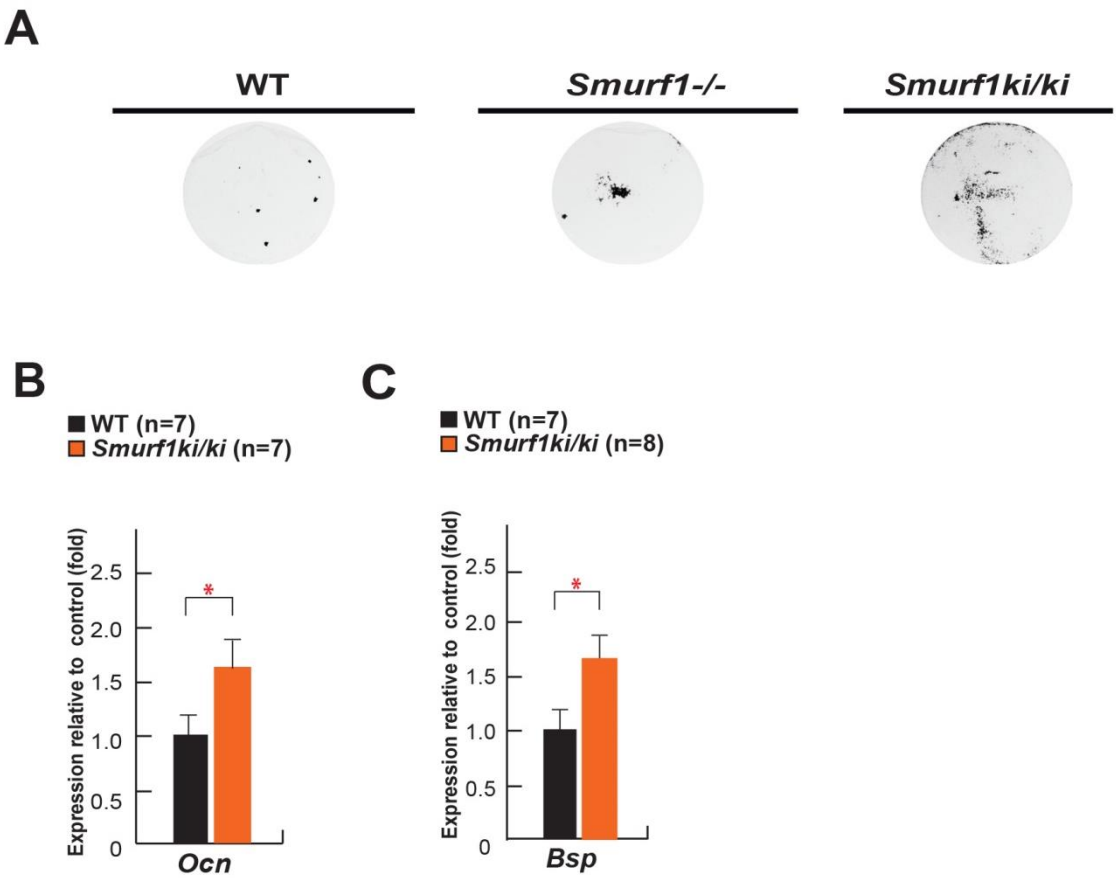

Figure S2. S148 in Smurf1 is necessary to inhibit osteoblast differentiation in vitro and in vivo (related to Figure2).

A. Formation of mineralized nodules in WT, *Smurf1-/-* and *Smurf1*$^{ki/ki}$ osteoblasts cultured for 7 days in differentiation medium followed by Von Kossa staining.

B to C. qPCR analysis of *Ocn* (**B**) and *Bsp* (**C**) expression in femurs of P10 WT and *Smurf1*$^{ki/ki}$ mice (n=7-8).

Error bars indicate mean ± SEM. $^{*}p \leq 0.05$; $^{\#}p \leq 0.005$ (compared to control),when analyzed by Student's t tests.

CHAPTER IV: General Discussion

General Conclusion: What is learned from my thesis

In conclusion, work I performed during my thesis has revealed the fundamental importance of GLUT1-dependent glucose uptake in osteoblasts as an earliest determinant of osteoblast differentiation, bone formation and whole-body glucose homeostasis. Moreover, I have also shown that AMPK integrates glucose signals to favor, in two distinct but synergistic manners, osteoblast differentiation and bone formation. Indeed glucose uptake by preventing AMPK activation prevents Runx2 ubiquitination thereby favoring osteoblast differentiation to occur. At the same time glucose uptake in cells of the osteoblast lineage enhances protein synthesis thereby favoring bone formation. Furthermore, I have uncovered a feedforward regulation between Runx2 and *Glut1* that acts as an amplification loop to initiate osteoblast differentiation during development and to regulate the extent of bone formation throughout life (Figure 1). Thus, these findings not only explain an apparent disconnect between the regulation of osteoblast differentiation and bone formation but also address in part the question of why bone acts as a regulator of whole-body glucose homeostasis by shedding light on the central importance of the intricate cross-talk between bone and glucose metabolism.

Moreover, the physiological importance of crosstalk between glucose homeostasis and the skeletal development and functions is further supported by the identification of the necessity of AMPK phosphorylation at S148 in Smurf1 to fulfill its functions of the regulation of osteoblast differentiation, bone formation and the osteocalcin-regulated whole-body glucose homeostasis by targeting both Runx2 and the InsR for degradation in osteoblasts (Figure 2).

Altogether, my thesis shows molecularly and genetically how the accumulation of a master

regulator of osteoblast differentiation, Runx2, is intimately linked to glucose homeostasis in osteoblasts and its physiological consequences that extend beyond osteoblast differentiation and bone formation to whole-body glucose homeostasis.

Future Directions: What would be interesting to study next?

Without doubts, there are several aspects described below that if further studied would strengthen the findings observed and expand the knowledge presented in this thesis.

First, it would be interesting to further study how *Glut1* expression is regulated before *Runx2* expression initiates in the early phase of osteoblast differentiation. This work has shown in vivo by in situ hybridization that the expression of *Runx1*, one of the members of the *Runx* family gene (Otto et al., 2003), is observed in cells expressing *α1(I) Collagen* and *Glut1* in hind limb during development from E10.5 (Wei et al., 2015a). In vitro, luciferase assay showed that *Runx1*, in addition to *Runx2*, promotes activity of a *Glut1* promoter as well (Wei et al., 2015a). Thus, further in vivo investigations of the initiation and regulation of the *Glut1* expression and the potential crosstalk between *Glut1* and *Runx1* in the early phage of osteoblast differentiation would be interesting to better delineate the mechanism of osteoblast differentiation.

Second, the identification of GLUT1-dependent glucose uptake as the determinant of osteoblast differentiation and functions leads to the question of whether there is/are an extracellular factor(s) that upregulates *Glut1* expression in osteoblasts and thereby favoring the function of osteoblasts. Specifically, this question was raised by the clinical observations that osteoblastic

(bone-forming) metastasis to bone is observed in patients with prostate cancer in which *Glut1* is robustly expressed (Carvalho et al., 2011; Logothetis and Lin, 2005). Thus, investigations of an extracellular factor(s) secreted by prostate cancer cells that promote *Glut1* expression in osteoblasts, may be beneficial for better understanding of the pathological principle of bone metastasis associated with prostate cancer.

Third, the extent of S148 phosphorylation-mediated regulation of Smurf1 activation would be interesting to study in vivo. Specifically, questions that remain to be addressed are whether AMPK-phosphorylation site S148 in Smurf1 is needed for the ability of AMPK to target additional Smurf1 substrates besides Runx2 and the InsR for degradation and whether there is/are another kinase(s) besides AMPK that phosphorylates S148 and activates Smurf1. Furthermore, identification of phosphatase is critical to better understand the S148 phosphorylation-mediated regulation of Smurf1 activation. It is known that Smurf1 functions extend beyond its regulation of the osteoblast differentiation and bone mass reported in this thesis. Smurf1 is involved in a number of mechanisms including cell growth, polarity, adhesion as well as viral autophagy and immune responses by targeting a variety of substrates (Cao and Zhang, 2013). Since the knowledge of the mechanism of Smurf1 activation is still limited, investigating the importance of Smurf1 phosphorylation at S148 may contribute to expand our understanding of the regulatory mechanism of Smurf1 activation.

Furthermore, the important question remained to be addressed is how structurally the phosphorylation of S148 in Smurf1 results in the activation of Smurf1. This thesis reports that S148

phosphorylation by AMPK enhances the interaction between Smurf1 and its substrates, Runx2 and the InsR in vitro. However, the biochemical evidence of the possible changes in the structural confirmation that leads to the enhancement of the affinity of Smurf1 to the substrates upon S148 phosphorylation by AMPK is missing. Thus, delineating structurally the mode of the AMPK-mediated activation of Smurf1 will also contribute to expand our knowledge about the regulation of the activation of Smurf1, this may also be beneficial of Smurf1 becomes as a therapeutic target for diseases such as osteoporosis and CCD.

Lastly, the identification of a novel function of AMPK to regulate protein accumulation by phosphorylating E3 ubiquitin ligase raises the question of whether AMPK targets other E3 ligases in vivo. Even in the context of bone biology, Smurf1 is not the only E3 ubiquitin ligase that regulates osteoblast biology. Thus, further investigations to search for the AMPK targets among E3 ubiquitin ligases are warranted as they may expand our knowledge on how cells integrate energy homeostasis and protein accumulations linked to developmental programs in vivo.

Figures

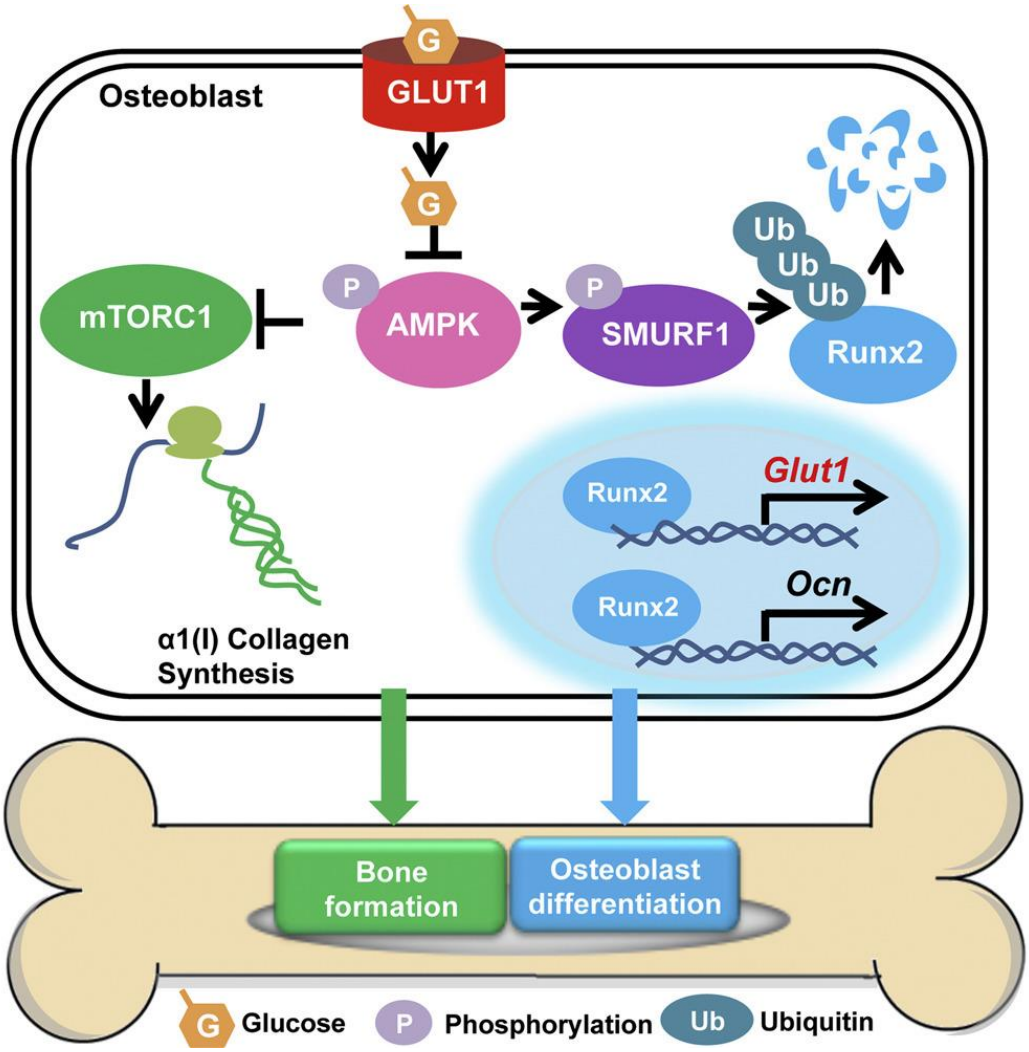

Figure 1. Glucose uptake and Runx2 synergize to orchestrate osteoblast differentiation and bone formation

Schematic view of the regulation of osteoblast differentiation and bone formation by crosstalk between GLUT1 dependent glucose uptake and Runx2 in osteoblasts. Taken from (Wei et al., 2015a).

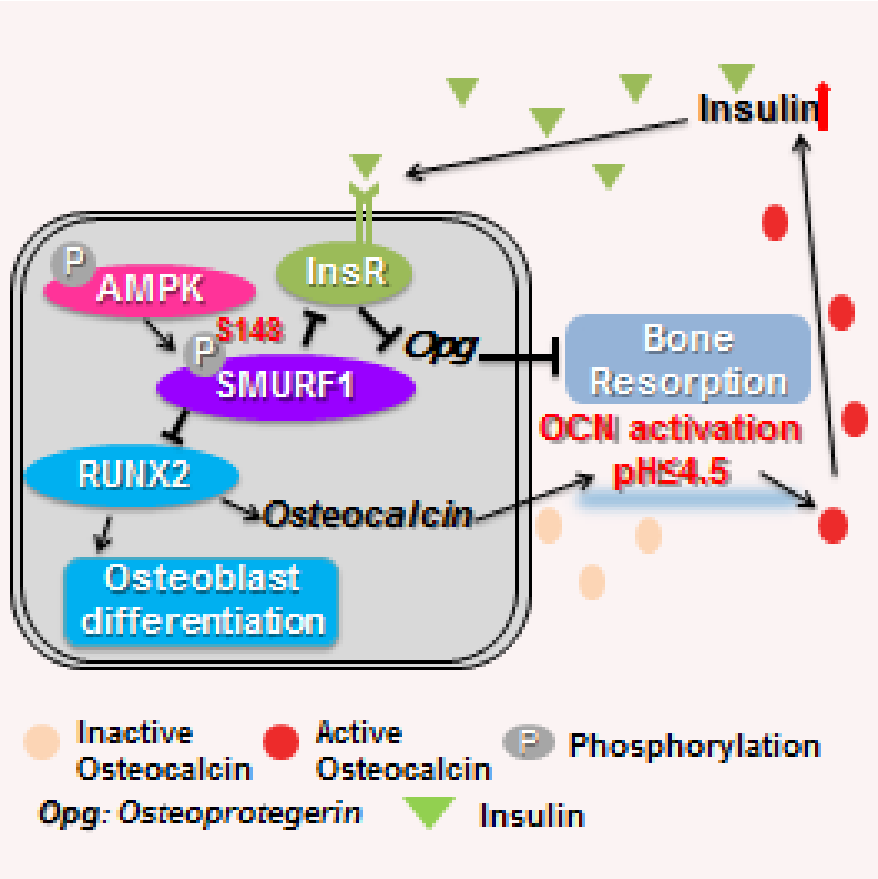

Figure 2. A single amino acid explains how Smurf1 regulate osteoblast differentiation, bone formation and glucose homeostasis

Schematic view of Smurf1 regulation of osteoblast differentiation, bone formation and glucose homeostasis and requirement of S148 in Smurf1 to fulfill those functions. Taken from (Shimazu et al., 2016).

References

Cao, Y., and Zhang, L. (2013). A Smurf1 tale: function and regulation of an ubiquitin ligase in multiple cellular networks. Cell Mol Life Sci *70*, 2305-2317.

Carvalho, K.C., Cunha, I.W., Rocha, R.M., Ayala, F.R., Cajaíba, M.M., Begnami, M.D., Vilela, R.S., Paiva, G.R., Andrade, R.G., and Soares, F.A. (2011). GLUT1 expression in malignant tumors and its use as an immunodiagnostic marker. Clinics *66*, 965-972.

Logothetis, C.J., and Lin, S.H. (2005). Osteoblasts in prostate cancer metastasis to bone. Nat Rev Cancer *5*, 21-28.

Otto, F., Lubbert, M., and Stock, M. (2003). Upstream and downstream targets of RUNX proteins. J Cell Biochem *89*, 9-18.

Shimazu, J., Wei, J., and Karsenty, G. (2016). Smurf1 Inhibits Osteoblast Differentiation, Bone Formation, and Glucose Homeostasis through Serine 148. Cell Rep *15*, 27-35.

Wei, J., Shimazu, J., Makinistoglu, M.P., Maurizi, A., Kajimura, D., Zong, H., Takarada, T., Iezaki, T., Pessin, J.E., Hinoi, E.*, et al.* (2015). Glucose Uptake and Runx2 Synergize to Orchestrate Osteoblast Differentiation and Bone Formation. Cell *161*, 1576-1591.